Sea Ice on the Southern Ocean

Stanley S. Jacobs

Lamont-Doherty Earth Observatory
of Columbia University
Palisades, NY 10964

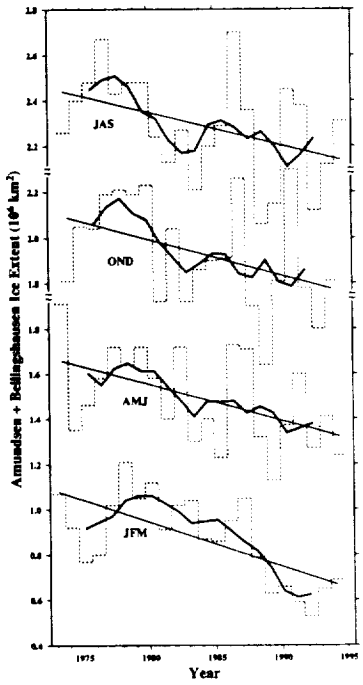

Final Technical Report
Grant # NAGW-3362

Polar Research Program
Office of Mission to Planet Earth
National Aeronautics and Space Administration

Sea Ice on the Southern Ocean

Stanley S. Jacobs

Lamont-Doherty Earth Observatory
of Columbia University
Palisades, NY 10964

Final Technical Report
Grant # NAGW-3362

Polar Research Program
Office of Mission to Planet Earth
National Aeronautics and Space Administration

March 1998

Table of Contents

Abstract 1

Project Description 1

Acknowledgments 2

Bibliography 3

Publications

A recent Sea-Ice Retreat west of the Antarctic Peninsula 5

Sea Ice Evolution in the Amundsen and Bellingshausen Seas 9

Late winter under the South Pacific Sea Ice 13

Cosmonaut Polynya in the Southern Ocean: Structure and Variability 15

Profiling the South Pacific Antarctic Continental Shelf 33

Climate Variability in the Amundsen and Bellingshausen Seas 37

Deep Coastal Oceanography from McMurdo Sound to Marguerite Bay 51

Thermohaline data and ocean circulation on the Ross Sea Continental Shelf 57

Interannual ocean and sea ice variability in the Ross Sea 81

Abstract

Year-round satellite records of sea ice distribution now extend over more than two decades, providing a valuable tool to investigate related characteristics and circulations in the Southern Ocean. We have studied a variety of features indicative of oceanic and atmospheric interactions with Antarctic sea ice. In the Amundsen & Bellingshausen Seas, sea ice extent was found to have decreased by ~20% from 1973 through the early 1990's. This change coincided with and probably contributed to recently warmer surface conditions on the west side of the Antarctic Peninsula, where air temperatures have increased by ~0.5°C/decade since the mid-1940's. The sea ice decline included multiyear cycles of several years in length superimposed on high interannual variability. The retreat was strongest in summer, and would have lowered the regional mean ice thickness, with attendant impacts upon vertical heat flux and the formation of snow ice and brine. The cause of the regional warming and loss of sea ice is believed to be linked to large-scale circulation changes in the atmosphere and ocean. At the eastern end of the Weddell Gyre, the Cosmonaut Polyna revealed greater activity since 1986, a recurrence pattern during recent winters and two possible modes of formation. Persistence in polynya location was noted off Cape Ann, where the coastal current can interact more strongly with the Antarctic Circumpolar Current. As a result of vorticity conservation, locally enhanced upwelling brings warmer deep water into the mixed layer, causing divergence and melting. In the Ross Sea, ice extent fluctuates over periods of several years, with summer minima and winter maxima roughly in phase. This leads to large interannual cycles of sea ice range, which correlate positively with meridinal winds, regional air temperatures and subsequent shelf water salinities. Deep shelf waters display considerable interannual variability, but have freshened by ~0.03/decade since the late 1950's. That could have slowed the thermohaline circulation beneath the Ross Ice Shelf and the properties or volume of local bottom water production.

Project Description

This report incorporates the main publications that have resulted from NASA support of the project, "Sea Ice on the Southern Ocean". Those and other products are listed in the accompanying bibliography. During the course of this work presentations were made in several forums, including meetings of the American Geophysical Union (AGU) in San Francisco and Brisbane, the Fifth International Symposium on Antarctic Glaciology in Cambridge (UK), and West Antarctic Ice Sheet workshops in Washington DC and Sterling VA. Most presentations evolved into the published material included here, and are thus not listed separately. Travel was also undertaken to attend the Radarsat Antarctic Mapping meeting in Columbus OH, and to confer with colleagues at the National Ice Center in Suitland, at a meeting of the American Meteorological Society in Dallas and at the Goddard Space Flight Center in Greenbelt.

During 1994 we carried out the first modern oceanographic surveys of the Antarctic continental shelf, slope and adjacent deep ocean sectors of the Amundsen and Bellingshausen Seas. While that field work was primarily supported by the National Science Foundation, it provided the observational data base for a study that has been initiated with J. Comiso on the Amundsen Sea Polynyas. These have been persistent

features of the ESMR, SMMR and SSMI satellite records, but appear to be accompanied by little or no shelf water formation. That situation could result from locally enhanced upwelling of deep water, misinterpretation of anomalous sea ice conditions depicted by algorithms currently in use, or from other factors. In addition, we obtained the first continuous temperature and salinity profiles beneath the winter sea ice in this sector, and in the Ross Sea. While these data have yet to be fully reduced and analyzed, they have revealed that thinner ice overlies the center of the Ross Sea gyre, that deep water temperatures in the Southeast Pacific appear to be warmer than at historical stations in the same region, and have confirmed that modified deep water intrudes year round deep onto the shelf in the Ross Sea.

In early 1996 work was started on volume 75 of the Antarctic Research Series, devoted to ocean circulation on and near the Antarctic continental shelf. To be published in 1998 by the American Geophysical Union, it will acknowledge partial NASA support of senior editor (SSJ), and will include several contributions that directly or indirectly related to ocean-sea ice interactions. SSJ also served as AGU's oversight Editor for volume 74 of the Antarctic Research Series, "Antarctic Sea Ice: Physical Processes, Interactions and Variability". That task included the editorship of contributed papers co-authored by volume editor M. Jeffries. NASA support of this "Sea Ice on the Southern Ocean" project provided much of the inspiration and justification for that effort.

A. Gordon was a co-investigator during the initial years of this project, and that led to the publication cited below by Comiso and Gordon. Other studies started with graduate students J. Albarracin and E. Lawson and described previously in progress reports remain incomplete, as those students left Columbia during the term of this project. However, both students were entrained into seagoing work in the study areas, helping to make it possible, e.g., to acquire thermohaline profiles beneath the winter sea ice. Gordon has continued his sea ice work under NSF support, collaborating on a paper for Antarctic Research Series volume 74, "Interannual Variability in Summer Sea Ice Minimum, Coastal Polynyas and Bottom Water Formation in the Weddell Sea".

Numerous reviews of manuscripts, proposals and other documents were undertaken during the course of this project. An essential element of this game, and as time consuming as editorial work, most reviews are soon interred in circular and other files. An occasional exception, such as "life in the Ice", cited below, may reach a wider audience.

Acknowledgments

We thank the National Aeronautics and Space Administration for support of this work under grant NAGW-3362. In particular, we are grateful to program manager Robert H. Thomas of the Polar Research Program for aiding and abetting our interest in the polar regions. We are also indebted to J. Comiso of the Goddard Space Flight Center for much good advice and fruitful collaboration. Some observational data used in conjunction with this work was obtained with the aid of field programs supported by the National Science Foundation, Office of Polar Programs. We have also been assisted by support provided by the Lamont-Doherty Earth Observatory of Columbia University.

Bibliography

Jacobs SS, Comiso JC, A Recent Sea Ice Retreat West of the Antarctic Peninsula, Geophys Res Lett, 20(12), 1171-1174, 1993.

Jacobs SS, Sea Ice Evolution in the Amundsen and Bellingshausen Seas, Antarct J of the US, 29(5), 111-113, 1994.

Hellmer HH, Jacobs SS, Rock SW, Belem AL, Late winter under the South Pacific Sea Ice, Antarct J of the US, 30(5), 114-115, 1995.

Jacobs SS, Life in the Ice, The Sciences, 36(1), 48, 1996.

Comiso JC, Gordon AL, Cosmonaut Polynya in the Southern Ocean: Structure and Variability, J Geophys Res, 101(C8), 18297-18313, 1996.

Jacobs SS, Some Implications of Decreasing Sea Ice in the SE Pacific Ocean, EOS Trans AGU, 77, 48, 1996.

Giulivi CG, Jacobs SS, Profiling the South Pacific Antarctic Continental Shelf, Antarct J of the US, 31(5), in press, 1996.

Jacobs SS, Comiso JC, Climate Variability in the Amundsen and Bellingshausen Seas, J of Climate, 10(4), 697-709, 1997.

Jacobs SS, Deep coastal oceanography from McMurdo Sound to Marguerite Bay. Antarct J of the US, in press, 1997.

Jacobs SS, Giulivi CG, Thermohaline Data and Ocean Circulation on the Ross Sea Continental Shelf, In: Oceanography of the Ross Sea, Antarctica, edited by G. Spezie and G. Manzella, Springer-Verlag, in press, 1998.

Jacobs SS, Weiss RF, (editors) Ocean, Ice and Atmosphere: Circulation and Interactions at the Antarctic Continental Margin, Ant Res Ser, vol 75, AGU, in press, 1998.

Jacobs, SS Giulivi CG, Interannual Ocean and Sea Ice Variability in the Ross Sea, In: Ant Res Ser, vol 75, AGU, in press, 1998.

GEOPHYSICAL RESEARCH LETTERS, VOL. 20, NO. 12, PAGES 1171-1174, JUNE 18, 1993

A RECENT SEA-ICE RETREAT WEST OF THE ANTARCTIC PENINSULA

S. S. Jacobs

Lamont-Doherty Earth Observatory of Columbia University, Palisades, NY

J. C. Comiso

NASA-Goddard Space Flight Center, Greenbelt, MD

Abstract. Satellite passive microwave data show a record decrease in sea ice extent in the Bellingshausen Sea from mid-1988 through early 1991. The change coincides with more southerly surface winds, increased cyclonic activity and rising surface air temperatures, which reached historic highs along the west coast of the Antarctic Peninsula in 1989. Preceded by high ice cover in 1986-87, the retreat was most evident during summer in the formerly perennial sea-ice field over the continental shelf. Ocean heat storage probably contributed to the persistence and coastal propagation of this anomaly.

Background

The Amundsen and Bellingshausen Seas (ABS) in the southeast Pacific sector of the Southern Ocean (Figure 1) are well known for their perennial sea ice and inaccessible coastlines. Indeed, the *Belgica* was beset there for a year in 1898-1899, the first "wintering over" in the Antarctic (Cook, 1900). Satellite passive microwave observations from 1973-1987 provided details of the spatial and temporal distribution of that sea-ice field (Zwally et al., 1983; Parkinson, 1992; Gloersen et al. in press). During this period, a low-amplitude seasonal cycle (Ackley, 1981; Enomoto and Ohmura, 1990) typically left a late summer (February-March) minimum ice cover over the continental shelf. That ice was exceeded in extent (area of ice and enclosed open water) only by the multi-year pack in the western Weddell Sea.

Ice extent west of the Antarctic Peninsula (AP) began to decrease in mid-1988, and a major retreat ensued during 1989 and early 1990. This would have lowered the regional albedo and ice export to other sectors. Greater solar heating of the more exposed ocean surface would have retarded sea ice formation. Enhanced air-sea interactions and deepened atmospheric depressions would have increased moisture transport onto the sea ice and continent. Ecosystems not accustomed to little sea ice or a 'warm' surface layer were likely impacted during the brief austral summers. The ice retreat was also associated with record high regional air temperatures, making it a potential analogue for future climate change.

Satellite Observations

Passive microwave measurements show the Bellingshausen Sea (62-100°W) ice retreat extended through all seasons, but was most obvious during the 1989-1991 summers. At those times monthly ice extents 30-60% below the 1973-1986 average eliminated most perennial ice (Figures 1 & 2a). The June 1989 northern ice edge retreated into Marguerite Bay (68°30' S&W), followed by a winter maximum 300 km south of average along some meridians. Temporal decreases of sea ice extent in one Southern Ocean sector are commonly balanced by increases elsewhere (Zwally et al., 1983), and small circumpolar decreases over the last two decades may or may not be significant (Jacka, 1990; Gloersen and Campbell, 1991; Chapman and Walsh, 1993). In this case, low ice extent in the ABS in early 1991 coincided with unusually heavy ice in the Weddell Sea (Figure 1), and circumpolar extent in 1988 and 1989 apparently exceeded a prior minimum in the mid-1970's.

Calculations of monthly ice extent west of the AP from the beginning of complete satellite coverage show no previous retreats of the same magnitude. Between 1973 and mid-1986, averages ranged from 0.41 to 1.25 x 10^6 km^2 in March and August, with little variability except during early winter (Figure 2a). Ice extent then rose more than 35% above the longer-term mean to a record 1.71 x 10^6 km^2 in September 1986, and highs persisted well into 1987. Intermittent lows in late 1987 and early 1988 presaged the record retreat to a summer minimum of 0.15 x 10^6 km^2 in March 1989, followed by a winter maximum of 0.89 x 10^6 km^2. The similar ice extent cycles indicate little change in growth and decay rates at the extrema. Occasional new monthly-record lows continued into 1991, and ice cover was generally below-average in the ABS during 1992 (NNJIC, 1991-92).

Atmospheric Connections

Minimum ice extent west of the AP coincided with the 1989 high surface air temperature at Rothera Station (Figure 2b). Temperature fluctuations are higher during winter (Sansom, 1989), and the Rothera record exceeded the 35-year mean by 3.5°C mainly due to July and August means 8-9°C above average. This area lagged the mean surface temperature for the entire south polar region (60-90°S), where a 30-year maximum in 1988 preceded a relative minimum in 1989 (Boden et al., 1990). The west AP warming extended ~3 years beyond the early winter of 1988, shorter but more intense than another warm episode in the 1970's. Summer ice at that earlier time was less extensive than during 1979-87 in the ABS (62-130°W; Parkinson, 1992). In this larger region, a record annual sea-ice minimum in 1988 was 20% below the mean of 13 years with full data, similar to changes in the Weddell and Ross Seas in 1976 and 1980.

Strong depressions commonly enter the Bellingshausen Sea

Paper number 93GL01200
0094-8534/93/93GL-01200$03.00

in association with short-term blocking highs around the Drake Passage (Schwerdtfeger, 1984). Rothera Station data show very low minimum atmospheric pressures during several 1989 months, in comparison with previous years. Greater storminess is consistent with higher temperatures and lower ice extent for several reasons. Warmer air will be imported from the northwest and the winds will generate local convergence and divergence in the sea ice field and along shorelines. Greater shear and ridging in convergence regions will effectively reduce the ice cover. Ice divergence will enlarge open water areas, increase sensible and latent heat flux from the ocean and intensify cyclonic activity (Ackley and Keliher, 1976).

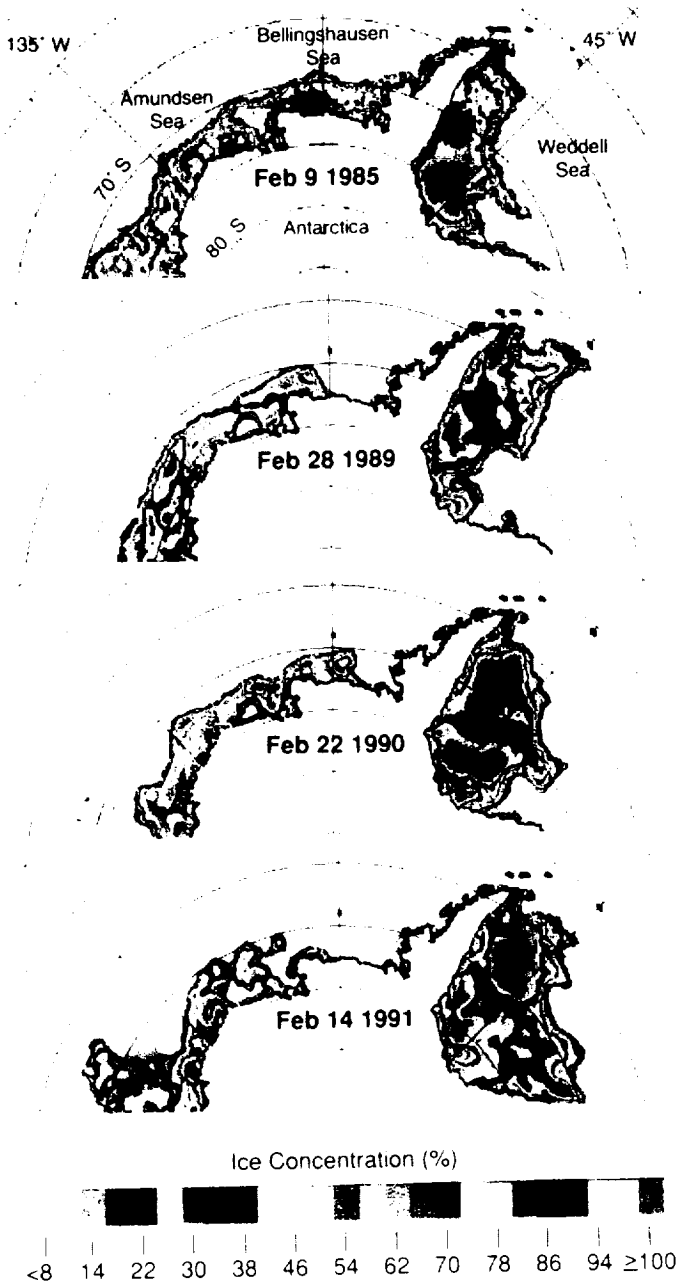

Fig. 1. Color-coded sea-ice concentrations derived from satellite passive microwave data at the summer minimum in the Bellingshausen Sea (62-100°W) for 1985, a year with ice cover close to the 1973-86 average in Figure 2a, and for years with record low ice cover (1989-91). We used the algorithm in Comiso and Sullivan (1986), which gives ice concentrations typically several percent higher than in Gloersen et al. (in press, 1979-87 data), but temporal changes are similar.

The sea-ice retreat is also compatible with regional wind patterns, which would have retarded winter expansion of the pack in 1989. Northwest winds occur ~90% of the time in this region, where annual northward components ranged from -0.4 m s^{-1} in 1986 to -3.7 m s^{-1} in 1989 (Figure 2c). Particularly strong southward flow was recorded during August 1989, and circumpolar westerlies exceeded the 1977-89 mean of +5.0 m s^{-1} by 25% that year. A divergence around 67°S separates these winds from the typically weaker continental easterlies, which averaged -3.2 m s^{-1} over the same period. These relative strengths were reversed during 1980, a cold year (Figure 2b) indicative of greater continental influence. These atmospheric variables have a large impact on sea-ice extent, but the persistence and behavior of this low-ice anomaly reveals the importance of ocean thermal inertia and heat transport.

Ocean Circulation

The ocean contributes to sea-ice change in several ways. For example, an ice retreat may signal melting by surface waters warmed by increased vertical convection. Historical observations in the deep Bellingshausen Sea reveal a stable pycnocline that would normally limit vertical heat flux to the ice. However, greater ice divergence and vertical mixing caused by the higher storm frequency would likely have increased heat flux from the Circumpolar Deep Water (CDW). Or low-ice and surface-water anomalies could have been advected into the region. The Amundsen Sea experienced a record low ice extent in 1988, and its deeper northern regions lie upstream of the AP. The large heat capacitance of the ocean, increased mixing and a lower regional albedo would strengthen initial perturbations. The water column would eventually be stabilized by excessive melting, precipitation, surface heating or a weaker atmospheric circulation (e.g., Manabe et al., 1991).

The ocean regime on the continental shelves of the ABS differs substantially from that found elsewhere around Antarctica. Here slightly modified 'warm' CDW invades the subsurface Bellingshausen Sea (Talbot, 1988). Stronger upwelling of this water would reduce ice thickness and increase the area or frequency of coastal leads and polynyas. Seasonal heating of the exposed surface water would lead to later ice formation in the fall (Jacobs and Comiso, 1989). Moderate northeast currents would have advected this anomaly along the AP, leading to the low-ice conditions observed there through the winter of 1989. Weaker currents west of ~75°W, inferred from the lengthy *Belgica* drift, imply a longer surface water residence time on the more southern shelf. Westward coastal flow from that region would have propagated the anomaly slowly downstream along the Amundsen shelf, where low summer ice extents continued beyond 1991.

We hypothesize that excessive flooding also conspired to lower the ice extent. Southward air flow and accompanying warmer temperatures west of the AP typically promote regionally high precipitation both on the continent and sea ice

(Schwerdtfeger, 1984; Kozlovskii and Romanov, 1989; Jeffries et al., 1992). Snow deposition lowers sea-ice freeboards, leading to snow-ice formation (Lange et al., 1990). However, when air temperatures are anomalously warm and a thicker blanket of snow adds insulation, the ice will be warmer and the rate of flooding may exceed the rate of snow-ice production. Even in the much colder Weddell Sea, slush has been observed at the snow-ice interface in late winter (Lytle et al., 1990). Surface temperatures as warm as those in Figure 2b would result in basal melting of the ice for oceanic heat fluxes higher than 10-20 W m^{-2} (Lange et al., 1990). Multi-year ice fields on each side of the Antarctic Peninsula have different microwave signatures (Zwally et al., 1983), quite likely because the west-side ice field is warmer and wetter. Available AVHRR imagery supports the ice extents derived from satellite passive microwave data.

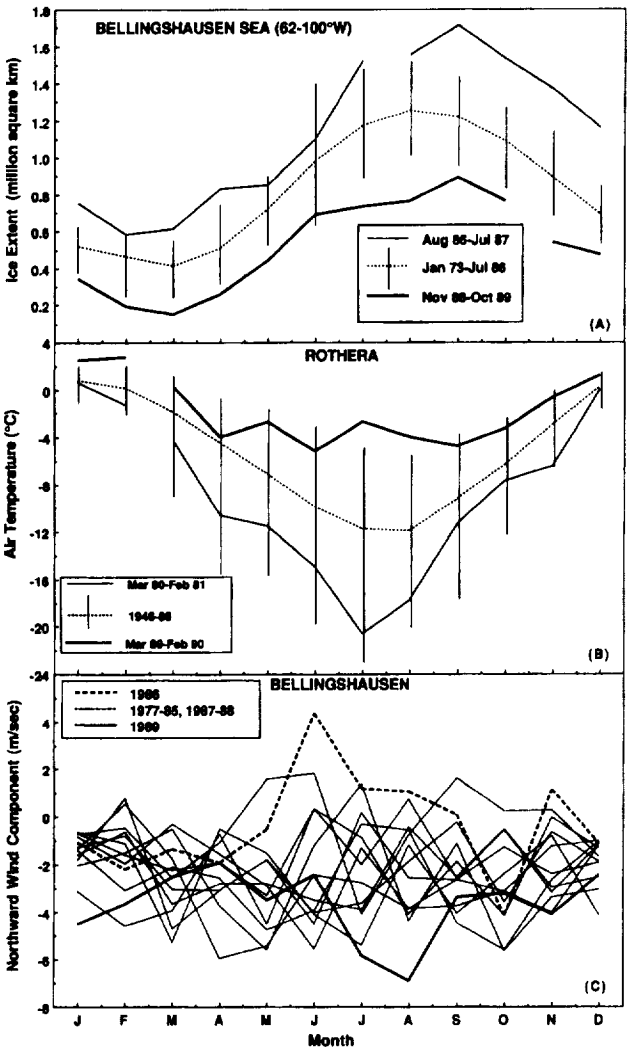

Fig. 2a. Monthly-average ice extent (ice concentration > 15%) in the Bellingshausen Sea during years with unusually high and low ice cover, compared with the mean and observed ranges for 1973-86. Satellite sea ice measurements and data reduction methods using different algorithms for 1973-87 appear in Zwally et al. (1983) and Gloersen et al. (in press). Ice extent from the DMSP Special Sensor Microwave Imager (SSM/I; Cavalieri, 1992) after mid-1987 may be offset slightly from earlier data due to the different coordinate grids and continent masks employed.

Fig. 2b. The annual march of surface air temperature at Rothera Station, 67°34'S on the west coast of the Antarctic Peninsula, and the ranges for 1946-86. The warmest and coldest annual cycles during the satellite sea-ice era occurred in 1989-90 and 1980-81. Data from Jones and Limbert (1987) and the British Antarctic Survey (BAS, unpublished).

Fig. 2c. Monthly wind components between 60-76°S and 65-100°W in the Bellingshausen Sea from 1977-1989. Southward components were strongest when the ice extent was low (1989) and weakest when the ice extent was high (1986). From Australian Bureau of Meteorology data.

Discussion

We have documented a major decrease in sea-ice extent in the Bellingshausen Sea from late 1988 through early 1991. In August 1989, ice extent dropped 0.25 to 0.50 x 10^6 km^2 below its previous low-to-average conditions, comparable to the 0.20-0.35 x 10^6 km^2 Weddell Polynya events of the mid-1970's (Gordon and Comiso, 1988). The 1989-91 minima receded to 1/3 of the 1973-86 average during summer, a critical time for Southern Ocean ecosystems dependent upon the presence or absence of sea ice (Fraser et al., 1992). The greater ice-free areas imply a smaller 'marginal ice zone', regionally deeper wind mixing and increased exposure to UV radiation, factors that would reduce primary productivity.

A remarkable feature of this Bellingshausen sea-ice anomaly is its relation to regional warming throughout the west AP area. Regression analysis of merged annual air temperatures for more than 4 decades at Rothera and Faraday Stations displays a trend of +0.5°K/decade with a standard deviation of 1.4°K (Figure 3). Sea-ice records are available for less than

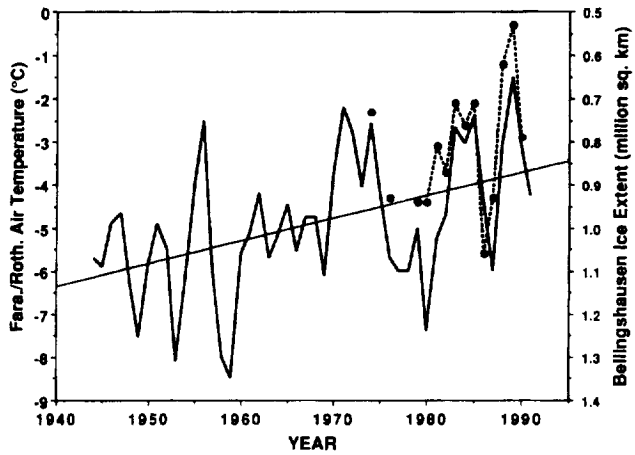

Fig. 3. *Left axis:* Annual-average surface air temperature (heavy line) and least squares regression (lighter line), from a composite of Rothera (Figure 2b) and Faraday Station (65°15'S, 64°16'W) records on the west side of the Antarctic Peninsula (Jones and Limbert, 1987; Smith, 1991; BAS, unpublished). Because Rothera Station is ~300 km south of Faraday and 0.95°C colder, on average, temperatures have been adjusted by -0.5°C for 13 years with only Faraday data. *Right axis:* Annual-average ice extent in the Bellingshausen Sea (dots and dashed line) for years with 12 months of fully processed satellite passive microwave data. The ice-extent scale is inverted to better illustrate the correlation (0.77) between low ice extent and high air temperature.

half that time, but correlate strongly and negatively (0.77) with air temperature. Circumpolar data through 1987 showed the strongest cross correlations between concurrent anomalies of these parameters near the AP in winter (Weatherly et al., 1991). For 1973-89, Jacka and Budd (1991) found that circumpolar sea ice extent decreased ~ 0.19°lat./decade while coastal Antarctic temperatures increased ~ 0.13°K/decade. Even the longer Antarctic temperature records are relatively brief, however, and display high interannual variability. As a result, statistical analyses of a 30-yr subset of the Faraday data did not reveal a significant trend (Sansom, 1989). Although based on only two decades of data, these findings in the ABS nonetheless appear inconsistent with projections of a fresher surface layer and thicker sea ice on the Southern Ocean in a warmer climate (Manabe et al., 1991). Rather, the close correspondence between this recent sea ice breakout and record-high air temperature suggests a regional threshhold, beyond which a perennial ice cover cannot be maintained.

Acknowledgments. We thank R. Allegrino, S. Brower and B. Huber for data processing and figures; A. Jenkins, J. King and J. Richman for British Antarctic Survey and Australian Bureau of Meteorology data; D. Ainley, B. Huber, M. Jeffries, S. Smith and others for helpful comments on the manuscript. Lamont-Doherty Earth Observatory Contribution # 5076, supported by the NASA Polar Research Program.

References

Ackley, S. F. and T. E. Keliher, Antarctic sea ice dynamics and its possible climatic effects, *AIDJEX Bull., 33*, 53-76, 1976.

Ackley, S. F., A Review of sea-ice weather relationships in the Southern Hemisphere, in *Sea Level, Ice and Climatic Change*, Edited by I. Allison, pp. 127-159, Int'l. Assoc. Scient. Hydrol., 131, Washington DC, 1981.

Boden, T. A., P. Kanciruk and M. P. Farrell (Eds.), *Trends '90, A Compendium of Data on Global Change,* 263 pp., U.S. Dept. of Energy, Oak Ridge, 1990.

Cavalieri, D. J. (Ed.) NASA sea ice validation program for the DMSP/SSMI: Final Report, *NASA TM 104559,* 107 pp., Goddard Space Flight Center, Greenbelt MD, 1992.

Comiso, J. C. and C. W. Sullivan, Satellite microwave and in situ observations of the Weddell Sea ice cover and its marginal ice zone, *J. Geophys. Res., 91(C8),* 9663-9681, 1986.

Cook, F. A., *Through the First Antarctic Night,* 413 pp., Heinemann, London, 1900.

Enomoto, H. and A. Ohmura, Influences of atmosheric half-yearly cycle on the sea ice extent in the Antarctic, *J. Geophys. Res., 95(C6),* 9497-9511, 1990.

Fraser, W. R., W. Z. Trivelpiece, D. G. Ainley and S. G. Trivelpiece, Increases in Antarctic penguin populations: reduced competition with whales or a loss of sea ice due to environmental warming?, *Polar Biol., 11*, 525-531, 1992.

Gloersen, P. and W. J. Campbell, Recent variations in Arctic and Antarctic sea-ice covers, *Nature, 352*, 33-36, 1991.

Gloersen, P., W. J. Campbell, D. J. Cavalieri, J. C. Comiso, C. L. Parkinson, and H. J. Zwally, *Arctic and Antarctic Sea Ice, 1978-1987: Satellite passive microwave observations and analysis*, NASA SP-511, in press.

Gordon, A. L. and J. C. Comiso, Polynyas in the Southern Ocean, *Sci. Amer., 258(6)*, 90-97, 1988.

Jacka, T. H. and W. F. Budd, Detection of temperature and sea ice extent changes in the Antarctic and Southern Ocean, in *Proc. Int'l Conf. on the Role of the Polar Regions in Global Change*, Edited by G. Weller, C. L. Wilson and B. A. B. Severin, Univ. Alaska, Fairbanks, 1, 63-70, 1991.

Jacobs, S. S. and J. C. Comiso, Sea ice and oceanic processes on the Ross Sea continental shelf, *J. Geophys. Res., 94(C12)*, 18195-18211, 1989.

Jeffries, M. O., A. Danielson, K. Morris, and R. A. Shaw, Turbulent environments, multiple growth mechanisms and sea ice development in the Pacific sector of the Southern Ocean, *Eos Trans. AGU, 73*, Supplement, 283, 1992.

Jones, P. D. and D. W. S. Limbert, A data bank of Antarctic surface temperature and pressure data, *DOE/ER/60397-H2*, 52 pp., U.S. Dept. of Energy, 1987.

Kozlovskii, A. M. and A. A. Romanov, Snow covered ice in the Pacific ice massif, *Sovietskais Antarkt. Eksped. Inform. Biull., 112*, in Russian with English abstract, 84-87, 1989.

Lange, M. A., P. Schlosser, S. F. Ackley, P. Wadhams and G. S. Dieckmann, ^{18}O concentrations in sea ice of the Weddell Sea, Antarctica, *J. Glaciol., 36(124)*, 315-323, 1990.

Lytle, V. I., K. C. Jezek, S. Gogineni, R. K. Moore and S. F. Ackley, Radar backscatter measurements during the winter Weddell gyre study, *Ant. J. of the U.S., 25(5)*, 123-125, 1990.

Manabe, S., R. J. Stouffer, M. J. Spelman and K. Bryan, Transient response of a coupled ocean-atmosphere model to gradual changes of atmospheric CO_2, Part 1, Annual mean response, *J. Climate, 4*, 785-818, 1991.

NNJIC, Antarctic Ice Charts, 1991-92, *Navy-NOAA Joint Ice Center,* Suitland MD, in press.

Parkinson, C. L., Interannual variability of monthly Southern Ocean sea ice distributions, *J. Geophys. Res., 97(C4)*, 5349-5363, 1992.

Sansom, J., Antarctic surface temperature time series, *J. Climate, 2*, 1164-1172, 1989.

Schwerdtfeger, W., *Weather and Climate of the Antarctic* , Developments in Atmospheric Science, 15, 261 pp., Elsevier, NY, 1984.

Smith, S. R., Antarctic climate anomalies associated with the minimum of the Southern Oscillation Index, M.S. Thesis, 121 pp., Univ. of Wisconsin, Madison, 1991.

Talbot, M. H., Oceanic environment of George VI Ice Shelf, Antarctic Peninsula, *Ann. Glaciol., 11*, 161-164, 1988.

Weatherly, J. W., J. E. Walsh and H. J. Zwally, Antarctic sea ice variations and seasonal air temperature relationships, *J. Geophys. Res., 96(C8)*, 15119-15130, 1991.

Zwally, H. J., J. C. Comiso, C. L. Parkinson, W. J. Campbell, F. D. Carsey, and P. Gloersen, *Antarctic Sea Ice, 1973-1976: Satellite Passive-Microwave Observations,* NASA SP-459, 206 pp., 1983.

Joey Comiso, Code 971, NASA Goddard Space Flight Center, Greenbelt, MD 20771; Stan Jacobs, Lamont-Doherty Earth Observatory, Palisades, NY 10964

Received: March 18, 1993
Accepted: April 14, 1993

Sea-ice evolution in the Amundsen and Bellingshausen Seas

STANLEY S. JACOBS, *Lamont-Doherty Earth Observatory of Columbia University, Palisades, New York 10964*

Satellite passive microwave data revealed a record decrease in sea-ice extent in the Bellingshausen Sea (62–100°W) through all seasons from mid-1988 through early 1991 (Jacobs and Comiso 1993). Following a relatively high ice cover in 1986–1987, this retreat removed most of the typically perennial icefield in the 1989–1991 summers, when monthly ice extents were 30–60 percent below the 1973–1986 average. The sea-ice changes were inversely correlated with annual average surface temperatures along the west coast of the Antarctic Peninsula (see also Weatherly, Walsh, and Zwally 1991); temperatures reached a historic high in 1989 (figure 1). A minimum ice extent in 1989 also coincided with greater cyclonic activity and stronger southward winds, whereas the maximum extent in 1986 corresponded to more northward winds, particularly during the winter months (figure 2).

This sea-ice retreat was one factor that led to the February and March 1994 Amundsen and Bellingshausen Seas cruise on the *Nathaniel B. Palmer*. Underway observations of ice extent and type were made by several groups aboard the *Palmer*. Satellite imagery was obtained through the Antarctic Support Associates (Wood 1993), assisted by individuals at the National Aeronautics and Space Administration/Goddard Space Flight Center in Greenbelt, Maryland, the National Ice Center in Suitland, Maryland, and the Antarctic Research Center in La Jolla, California. Cryologists on the *Polarstern* and at O'Higgins Station concurrently obtained ERS-1/SAR (European Research Satellite/synthetic aperture radar) data and a number of sea-ice cores in the Amundsen and Bellingshausen Seas region (Haas and Vielhoff 1994). The ice and ocean data sets have yet to be fully reduced, but in the inter-

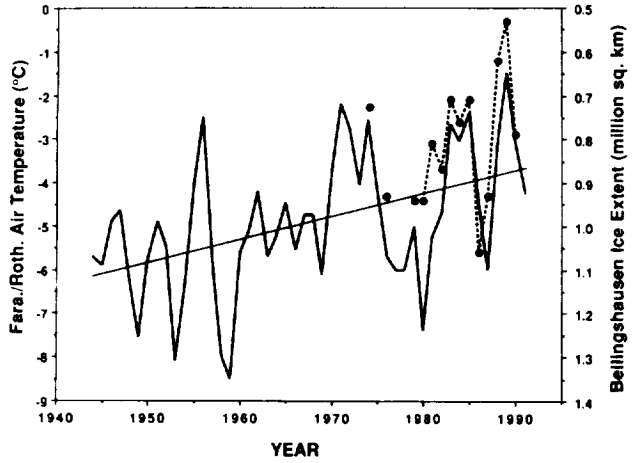

Figure 1. *Left axis:* Annual-average surface air temperature (heavy line) and least squares regression (lighter line), from a composite of Rothera and Faraday Station records on the west side of the Antarctic Peninsula. *Inverted right axis:* Annual-average ice extent (in square kilometrs) in the Bellingshausen Sea (dots with dashed line) for full years of passive microwave data through 1990. From Jacobs and Comiso (1993); update in preparation.

im, we can compare the early 1994 sea-ice cover with that of previous years.

Antarctic sea-ice records have been available from several satellite sources since the beginning of 1973. Passive microwave data, relatively little perturbed by clouds and darkness, have provided the most quantitative information. Substantial gaps exist between microwave sensor flight times, however, and lengthy data processing has limited access to very recent data. The National Ice Center's weekly Northern Ice Limit charts offer a reasonable alternative. Based on a combination of microwave, AVHRR (advance very-high-resolution radiometer), and other data, these maps provide a more continuous and current perspective on the evolving sea-ice cover. One important aspect of these records is the northern ice edge, a feature that is potentially sensitive to climate change and that has been used by Jacka and Budd (1991, pp. 63–70) to calculate a decrease in the circumpolar ice extent from 1973 to 1989. Evaluations over shorter periods, using discrete microwave data sets and ice coverage exceeding a specified percentage of the sea surface (e.g., Gloersen and Campbell 1991), have not revealed significant temporal changes in the total sea-ice extent of the southern oceans.

We extended through early 1994 a portion of the Jacka data set, which comprises the mid-month northern ice edge at 10° longitude intervals. This subset spans 65–135°W, encompasses most of the Amundsen and Bellingshausen Seas, and uses all weekly values, for which a full-year comparison with the abbreviated Jacka compilation showed no substantial differences. The 21 years of data prior to 1994 were divided into septennials of average latitude for each month (figure 3). It is readily apparent from this index that the northern ice edge has moved southward in the Amundsen and Bellingshausen Seas during the satellite era. In all months but June, the ice edge was farthest south in the most-recent 7-

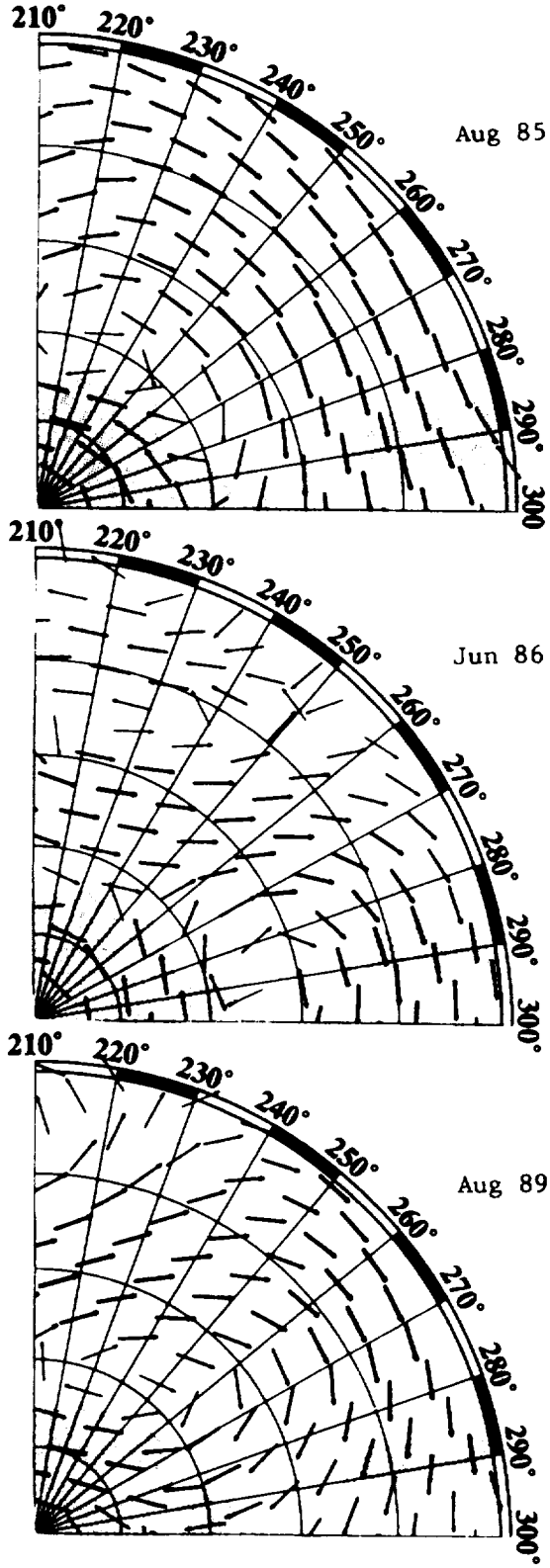

Figure 2. Southern Hemisphere (40–90°S) vector winds during months for years with average (1985), high (1986), and low (198 ice extents in the Bellingshausen Sea (260–300°E). From unpub B. Huber analyses of Australian Bureau of Meteorology compila Latitude arcs at 10° intervals; vector thickness proportional to strength.

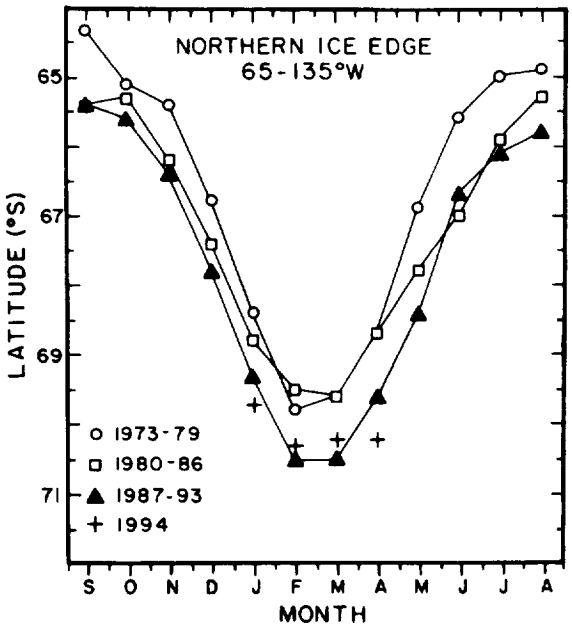

Figure 3. Annual cycles of the latitude of the northern ice edge in the Amundsen and Bellingshausen Seas (225–295°E) averaged over septennials. Based on a compilation reported in Jacka and Budd (1991) and extended through early 1994 from the weekly Northern Ice Limit charts of the National Ice Center.

year period. The 1994 summer ice edge did not attain the high latitude of the recent record minima but remained below the 21-year average. In both January and April 1994, the ice edge was farther south than during 18 of 21 prior years. Our relatively easy access to the Amundsen and Bellingshausen Seas coastlines suggests that the apparent northern ice-edge retreat was not simply caused by stronger southward winds compacting the sea-ice cover.

This work is supported by grants NAGW-3362 from the National Aeronautics and Space Administration and OPP 92-20009 from the National Science Foundation.

References

Gloersen, P., and W.J. Campbell. 1991. Recent variations in arctic and antarctic sea-ice covers. *Nature*, 352, 33–36.

Haas, C., and T. Vielhoff. 1994. Sea ice conditions in the Bellingshausen/Amundsen Sea: Shipboard observations and satellite imagery during ANT XI/3. *Berichte aus dem Fachbereich Physik* (report 51). Alfred-Wegener-Institut.

Jacka, T.H., and W.F. Budd. 1991. Detection of temperature and sea ice extent changes in the antarctic and southern ocean. In G. Weller, C.L. Wilson, and B.A.B. Severin (Eds.), *Proceedings of an International Conference on the Role of the Polar Regions in Global Change* (Vol 1). Fairbanks: University of Alaska.

Jacobs, S.S., and J.C. Comiso. 1993. A recent sea-ice retreat west of the Antarctic Peninsula. *Geophysical Research Letters*, 20(12), 1171–1174.

Weatherly, J.W., J.E. Walsh, and H.J. Zwally. 1991. Antarctic sea ice variations and seasonal air temperature relationships. *Journal of Geophysical Research*, 96(C8), 15119–15130.

Wood, K. 1993. New data collection network improves USAP ship operations. *Antarctic Journal of the U.S.*, 28(4), 4–6.

Carbon dioxide partial pressure in surface waters in the Pacific sector of the southern oceans during austral summers 1992 and 1994

STEPHANY RUBIN, JOHN GODDARD, DAVID CHIPMAN *and* TARO TAKAHASHI, *Lamont-Doherty Earth Observatory of Columbia University, Palisades, New York 10964*

In the austral summers (February and March) of 1992 and 1994, the partial pressure of carbon dioxide (pCO_2) and concentration of total carbon dioxide (TCO_2) dissolved in sea water were determined for surface and deep waters along the two cruise tracks (WOCE S-4 in 1992, *NBP*94-02 in 1994) in the Pacific sector of the southern oceans. These expeditions included sections across the continental shelf areas of the Bellingshausen and Amundsen Seas. The station locations are shown in figure 1. Most of this area has not been previously studied for carbon dioxide and nutrients such as nitrate (NO_3^-), phosphate ($PO_4^{\equiv}$), and silicate ($SiO_3^=$). During the two cruises, discrete surface-water samples were analyzed for carbon dioxide and nutrients at approximately 260 sites. The pCO_2 and TCO_2 contents of discrete sea-water samples were measured using a gas chromatograph and coulometer, respectively (Chipman, Marra, and Takahashi 1993). Atmospheric CO_2 concentrations in dry air were obtained with an infrared CO_2 analyzer. The dissolved nitrate, phosphate, and silicate were measured using standard colorimetric methods, by personnel of the Ocean Data Facility of the Scripps Institution of Oceanography.

The direction and amount of net transfer of CO_2 are determined by the difference between the pCO_2 in surface water and the overlying atmosphere (ΔpCO_2). Variations in the global CO_2 fluxes are primarily attributed to changes in the surface ocean pCO_2, since the atmospheric pCO_2 is relatively uniform. Several factors control the pCO_2 in ocean water. Sea water exhibits a large temperature effect on the pCO_2 of 4.2 percent per degree Celsius under isochemical conditions: a 16°C increase will double the pCO_2. If photosynthesis lowers the TCO_2 concentration in the water by 40 micromoles per kilogram (μmol/kg), corresponding to the

Late winter under the South Pacific sea ice

H.H. HELLMER, S.S. JACOBS, *and* S.W. ROCK, *Lamont-Doherty Earth Observatory of Columbia University, Palisades, New York 10964*
A.L. BELEM, *Department of Physics, University of Rio Grande, Rio Grande, Brazil 96201-900*

Cruise 94–5 of the icebreaker *Nathaniel B. Palmer* (*NBP*), a study of sea-ice properties in the Pacific sector of the southern ocean (Jeffries et al. 1995), provided an opportunity to observe the late winter/early spring transition in the upper water column of the Amundsen Sea and northern Ross Sea. This work complemented late summer/early fall observations made to the south of this region 6 months earlier (Jacobs et al. 1994), revealing seasonal extremes in the upper ocean related to the growth and decay of sea ice. The continental shelf and slope were inaccessible because of heavy sea ice, but 16 deep stations of cruise *NBP*94-2 and World Ocean Circulation Experiment lines S4 and P19S were reoccupied.

At 50 locations (figure 1), 109 conductivity and temperature vs. depth (CTD) casts were taken with a Seabird SBE 911*plus* system to depths of from 1,000 meters (m) to more than 4,000 m. Sea water was sampled with a 24-bottle General Oceanics rosette for analyses of salinity, dissolved oxygen, total carbon dioxide (CO_2), and partial pressure of CO_2, nutrients, chlorophyll, chlorofluorocarbons, and oxygen isotopes. On four stations, multiple samples were drawn for an intercalibration experiment between two automated oxygen titrators. No systematic differences were found between Scripps' photometric and Lamont's amperometric titrators (Langdon and Bitte in preparation).

During daily stops of several hours for work on the sea ice, profiling of the upper 1,000 m provided information on the temporal variability of the pycnocline. This region of higher vertical density gradients separates the surface mixed layer from the deep-water temperature and salinity maxima. Acoustic doppler current profiles were recorded to depths of 200 m, and expendable bathythermograph (XBT) temperature profiles were made in the Bellingshausen Sea and across the Antarctic Circumpolar Current (ACC) west of 170°W (figure 1). XBT casting while a ship is underway through the pack ice can require more than the usual data editing, because the fine wire frequently catches on ice floes. Nonetheless, the resulting XBT transect in the northern Bellingshausen Sea, tied to CTD casts at each end, shows several consistent features (figure 2). The transect across the ACC without supporting

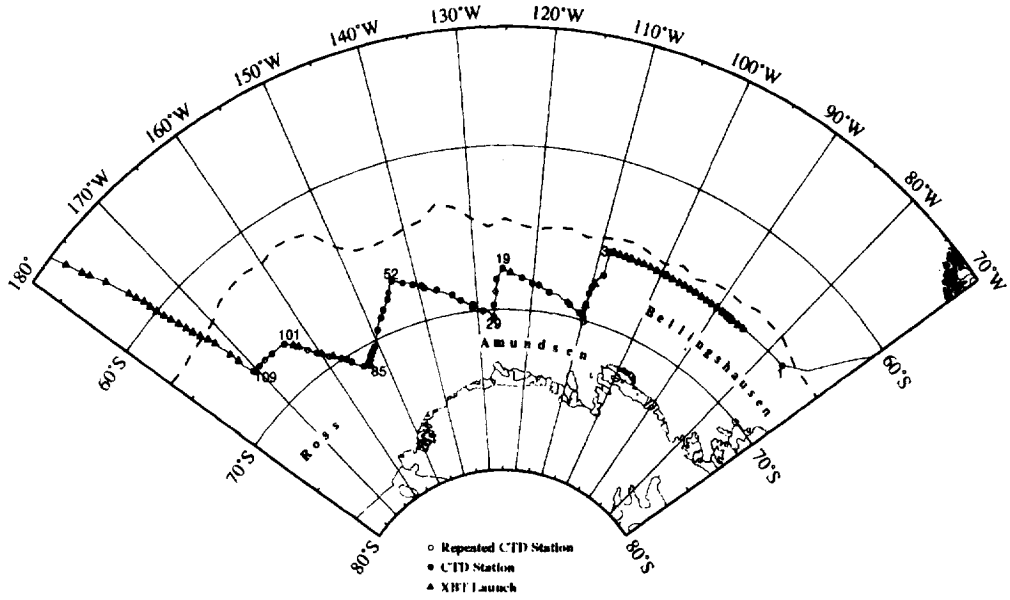

Figure 1. Track of cruise NBP94–5 in the Bellingshausen, Amundsen and Ross Seas from 14 September to 16 October 1994. The position of the sea ice edge (dashed line) from weekly National Ice Center charts, reached an annual maximum about 2 weeks after this section was made. That location exceeded a two-decade average in the Amundsen and Bellingshausen sector, following several years of lower ice extent (Jacobs 1994).

CTD casts requires a more detailed analysis and will be discussed in a later report.

The thermocline near 200 m in figure 2 deepens slightly toward the west and is overlain by a highly variable mixed layer. Temperatures in this layer are typically warmer than the surface freezing point (below −1.85°C), often by several tenths of a degree, indicating melting of the late winter sea ice. At this time of the year, the sea ice is near its maximum northern extent, which is limited both by the winds and by the relatively warm underlying ocean. Below the thermocline, deep-water temperatures are everywhere warmer than 2.1°C and in some locations are above 2.3°C. These temperatures are more than 0.3°C higher than those shown in meridional sections for this region (Gordon and Molinelli 1982; Olbers et al. 1992) but appear consistent with some historical data and with recent observations along 67°S (Swift 1993) and 85°W (Read et al. 1995).

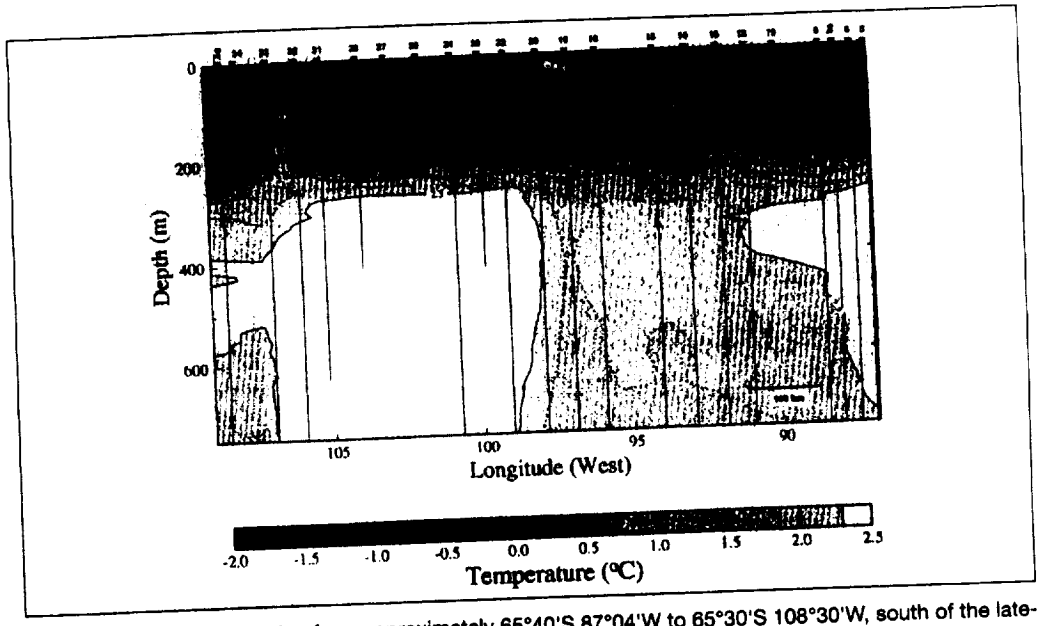

Figure 2. Temperature section from approximately 65°40'S 87°04'W to 65°30'S 108°30'W, south of the late-winter sea ice edge in the Bellingshausen Sea (figure 1) based on CTD stations 2 and 3 (italics) and XBT casts 5–34. Vertical lines show the control after extensive data editing. Automatic contouring at a contour interval of 0.2°C has been supplemented by the +2.3°C isotherm.

The mixed-layer variability displayed in figure 2 extended well to the south and west of CTD station 3. A mixed layer having minimum thickness of 40 m at a temperature of −1.7°C was measured in the southeastern Ross Gyre at CTD station 60 (figure 1) together with thinner sea ice and lower ice concentrations (Jeffries et al. 1995). A coincident anomalous chlorophyll distribution can be related to these features and the freshening of the surface layer due to sea ice melting.

We thank the *Nathaniel B. Palmer* officers and crew, G. Flenner, M. Klas, S. Morgan, S. O'Hara, and Antarctic Support Associates personnel for assistance with the data collection. Carbon dioxide sampling was done by D. Chipman and R. Esmay under grants from the Department of Energy. This research was supported by National Science Foundation grant OPP 92-20009 and the University of Rio Grande, Rio Grande, Brazil.

References

Gordon, A.L., and E.J. Molinelli. 1982. *Southern Ocean atlas: Thermohaline and chemical distributions.* New York: Columbia University Press.

Jacobs, S.S. 1994. Sea-ice evolution in the Amundsen and Bellingshausen seas. *Antarctic Journal of the U.S.*, 29(5), 111–113.

Jacobs, S.S., H.H. Hellmer, P. Schlosser, and W. Smethie. 1994. An oceanographic expedition to the Amundsen and Bellingshausen Seas. *Antarctic Journal of the U.S.*, 29(5), 109–111.

Jeffries, M., R. Jaña, S. Li, and S. McCullars. 1995. Sea-ice and snow-thickness distributions in late winter 1993 and 1994 in the Ross, Amundsen, and Bellingshausen Seas. *Antarctic Journal of the U.S.*, 30(1–4), 18–21.

Langdon, C., and I. Bitte. In preparation. Low-cost, high-precision, automated amperometric oxygen titrator. *Deep-Sea Research.*

Olbers, D., V. Gouretski, G. Seiss, and J. Schröter. 1992. *Hydrographic atlas of the Southern Ocean.* Bremerhaven: Alfred-Wegner-Institute for Polar and Marine Research, Bremerhaven.

Read, J., R. Pollard, A. Morrison, and C. Symon. 1995. On the southerly extent of the Antarctic Circumpolar Current in the southeast Pacific. *Deep-Sea Research II*, 42(4–5), 933–954

Swift, J. 1993. Comparing WOCE data with historical hydrographic data in the southeast Pacific. *EOS, Transactions of the American Geophysical Union.* 74(43), 327. [Abstract]

JOURNAL OF GEOPHYSICAL RESEARCH, VOL. 101, NO. C8, PAGES 18,297–18,313, AUGUST 15, 1996

Cosmonaut polynya in the Southern Ocean: Structure and variability

Josefino C. Comiso

Laboratory for Hydrospheric Processes, NASA Goddard Space Flight Center, Greenbelt, Maryland

Arnold L. Gordon

Lamont-Doherty Earth Observatory, Columbia University, Palisades, New York

Abstract. Along the far eastern margin of the Weddell Gyre is a persistent feature in the middle of the ice pack which we previously reported and called the Cosmonaut polynya. A study of polynya occurrences from 1973 to 1993 reveals that since 1986 the polynya has become more active with an average size of about 7.2×10^4 km^2 and an average location at 52°E and 65°S. Satellite observations indicate that the polynya has recurred several times during winter in recent years with intervals ranging from a few days to a few weeks. The centroid of the polynya varies only slightly with each formation during the year and from one year to another, suggesting a controlling influence of the ocean and bottom topography that may be initially induced by wind. The daily time series indicates two primary modes of formation: one that is initiated in the early winter during a storm at a site usually preceded by an embayment of the ice edge and another that occurs during midwinter often preceded by a coastal polynya event adjacent to Cape Ann. The Cosmonaut polynya region is characterized in this study by compression of the westward flowing coastal current and the eastward flowing southern edge of the Antarctic Circumpolar Current. Following the principle of conservation of potential vorticity, vertical stretching of the water column would ensue, enhancing upwelling. Such a process accelerates the injection of relatively warm salty deep water into the surface layer, inhibiting sea ice growth and causing the polynya formation. This theory appears to explain the general behavior of the polynya in terms of frequency, duration, size, and location.

1. Introduction

Previous studies indicate the existence of long-term or recurring polynyas in the Southern Ocean. Detailed study and characterization of these polynyas is important because of the unique role they play in air-sea interaction and in deep ocean ventilation. A polynya is defined as a region of significantly reduced ice concentration relative to the surrounding region [*Smith et al.*, 1990]. Its spatial and temporal scales are greater than that of the more ephemeral network of leads. Two basic types of polynyas have been observed, each of which has a different role in ice-ocean-atmosphere coupling. One type is the "latent heat polynya" induced by wind removal of newly formed sea ice. The other type is the "sensible heat polynya," which is maintained by the upwelling of heat from the ocean.

The latent heat polynyas generally form along coasts (and may be referred to as coastal polynyas) where offshore wind first encounters the sea. The ensuing sea-air fluxes in the Southern Ocean coastal-latent heat polynyas produce salty and very cold shelf water, a prime ingredient in Antarctic Bottom Water formation. Latent heat polynyas have been referred to as "ice factories," as the constant removal of newly formed ice by the wind may result in tens of meters of winter ice formation. During the slacking of the wind the latent heat polynya may be covered by thin ice, but this would be removed, once more exposing the ocean to the atmosphere with the next wind burst. It has been inferred indirectly that a large fraction of the Antarctic sea ice originates from such polynya regions [*Eicken and Lange*, 1989]. Examples of latent heat polynyas in the Antarctic coastal region have been cited and studied [*Zwally et al.*, 1985; *Cavalieri and Martin*, 1985; *Jacobs and Comiso*, 1989; *Kottmeier and Engelbart*, 1992; *Darby et al.*, 1995].

The sensible heat polynya is associated with deep ocean convection. Atmospheric cooling of warm deep water brought to the sea surface with insufficient melting of local or convergent sea ice to inhibit convection results in a persistent convective condition [*Gordon*, 1991]. The most remarkable example of this type of polynya was the large Weddell polynya observed from 1974 through 1976 [*Zwally and Gloersen*, 1977; *Carsey*, 1980; *Gordon and Comiso*, 1988]. Within the polynya region the ocean to 3000 m depth was on average 0.5° colder in 1977 than in prepolynya years, an indicator of the thickness of the convective layer associated with the Weddell polynya [*Gordon*, 1982].

An alternative form of a sensible heat polynya may not involve convective overturning but rather locally enhanced upwelling of warm deep water induced through circulation and local topography interactions. The deep convection state is not attained because the melting of convergent sea ice is sufficient to inhibit convection. In this type of polynya a surface layer ocean divergence is expected. Examples of such polynyas may be the topographically forced upwelling that occurs over the Maud Rise [*Gordon and Huber*, 1990; *Ou*, 1991] and the Cosmonaut polynya, which was first reported by *Comiso and Gor-*

Paper number 96JC01500.
0148-0227/96/96JC-01500$09.00

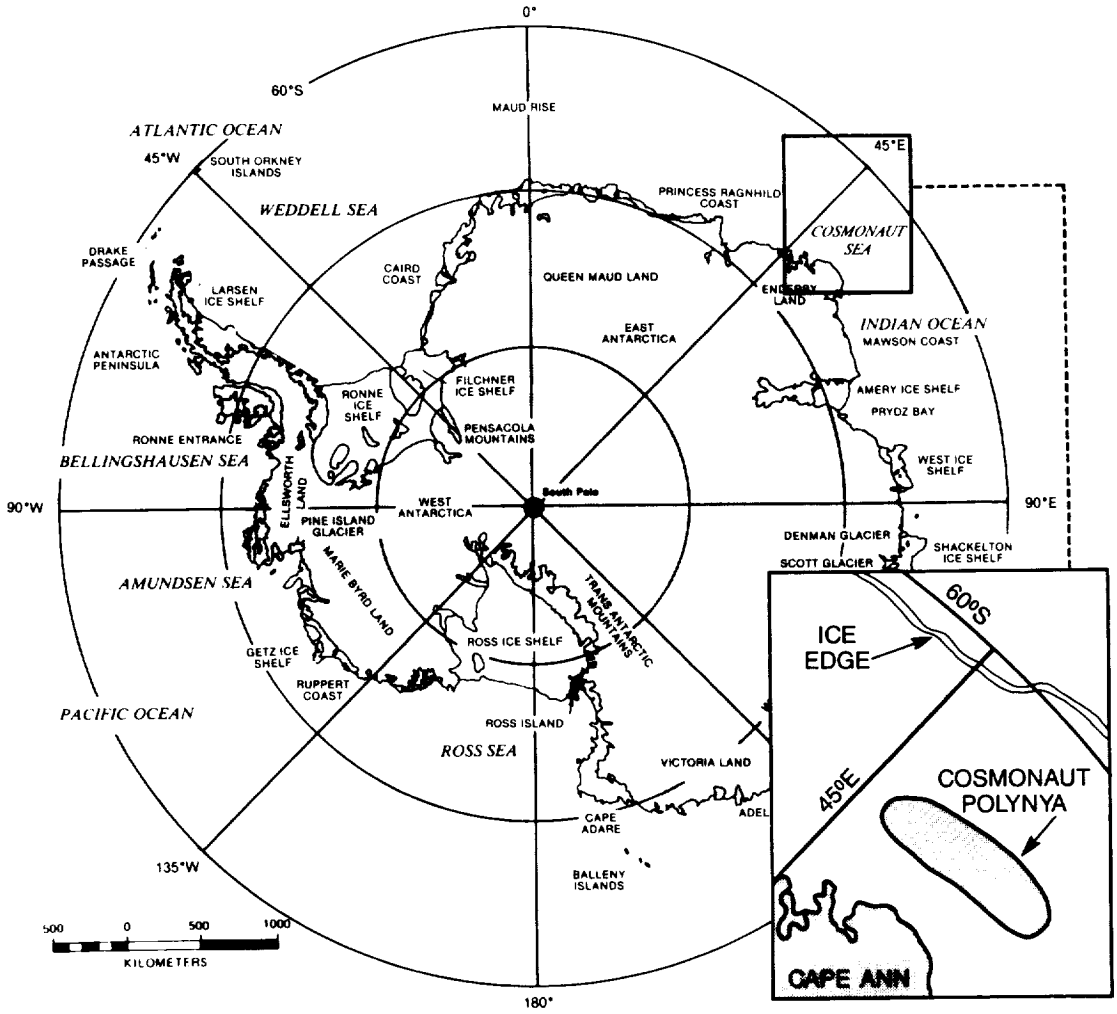

Figure 1. The Antarctic region and (inset) the Cosmonaut Sea study area.

don [1987]. One may expect periods of new or thin ice cover during cold air episodes or during periods of decreased circulation-induced upwelling, but the climatic character of these forms of sensible heat polynya would reappear when the ability of atmosphere to remove oceanic heat is overcome by the latter.

The Cosmonaut polynya, with an average central position at 65°S (range 64°–66°S) and 52°E (range 42°–57°E) in water of 3000–4000 m depth, is situated adjacent to Enderby Land in close proximity to Cape Ann (Figure 1). This polynya is among the most persistent polynyas in the Southern Ocean and has been observed almost every year since satellite passive microwave data became available in December 1972. In this paper we will present a comprehensive characterization of the polynya development, especially the spatial and temporal variation of its area and the location of its centroid. We also evaluate the possible influence of wind using available in situ and other satellite data. Finally, we examine the oceanographic setting in the general polynya region and present the theoretical basis of a vorticity effect, which we think is the likely mechanism that leads to the polynya formation process.

2. Satellite and Other Observations of the Polynya Region

Passive microwave satellite data have been used to study large-scale characteristics of the sea ice cover [*Zwally et al.*, 1983; *Parkinson et al.*, 1987; *Gloersen et al.*, 1992]. Polynya areas are especially difficult to characterize using this technique because such areas are usually covered by new ice, the emissivity of which varies depending on the stage of ice development and is different from those of thick ice [*Grenfell and Comiso*, 1986; *Grenfell et al.*, 1992]. Because of the unstable nature of the emissivity of new ice, algorithms for new ice are effective only when one type of new ice is dominant and thick ice with snow cover is not present. Some new ice algorithms have been used [e.g., *Wensnahan et al.*, 1993; *Cavalieri*, 1994] for some regions, but such techniques are generally not effective in the Antarctic region.

In this study, we do not use a special algorithm for new ice because it is not known which type of new ice is dominant and because thick ice with snow cover is expected in the region. The polynya is characterized instead using ice concentration maps derived from using the Bootstrap algorithm previously developed for the Southern Ocean [*Comiso et al.*, 1984; *Comiso and Sullivan*, 1986]. The technique is generally effective for the dominant Antarctic first-year ice cover and for polynya studies, although it does not take into account the difference in the emissivities of new ice and the thicker ice types. In 100% new ice areas the inferred concentration varies from 50% to 80%, depending on the type of new ice and stage of formation [*Comiso et al.*, 1992]. Thus having ice concentra-

tion values in this range in the middle of the pack may indicate either the presence of open water or the dominance of new ice in the region. In this context, it should be noted that new ice does not form as readily (because of oceanic heat) in sensible heat polynyas as in latent heat polynyas.

We use ice concentration maps from passive microwave data to quantify the following: (1) location and time of occurrence of the polynya, (2) polynya size, and (3) persistence and interannual variability. The study area is shown in Figure 1 (see inset). The location of the centroid of the polynya is inferred through interactive computer analysis and is expected to be good within a few pixels. The time of occurrence is established within the daily resolution of the data set. The size is quantified using estimates of extent and actual open water area. Polynya extent is defined as the sum of the area of all pixels in the study region with less than 80% ice concentration. This is meant to include areas that are covered predominantly by new ice. The actual open water area is the sum of the product of the area of each pixel and the corresponding open water concentration (e.g., 1 minus the ice concentration). The estimate of actual open water area is subject to errors associated with the possible presence of new ice, the emissivity of which during the time of observation is not known.

The primary data set used in this study is that observed by a series of special sensor microwave imagers (SSM/I) onboard Defense Meteorological Satellite Program (DMSP) satellites from July 1987 through 1993. To study the long-term polynya characteristics, we also used data from the Nimbus 7 scanning multichannel microwave radiometer (SMMR), which operated effectively from 1979 through 1987 and from the Nimbus 5 electrically scanning microwave radiometer (ESMR), which provided good data from 1973 through 1976. Daily average images are used instead of weekly or monthly because this polynya may occur only for a few days. The temporal resolution is from about 100 min to daily, but for SMMR, data were available every other day only. For consistency these different data sets have been mapped into the same 25 × 25 km size grids.

Other data sets used are bathymetry maps originally put together by *Vanney and Johnson* [1985], dynamic topography data originally published in the work by *Gordon et al.* [1978] but enhanced with recent data (1979–1989) from the Japanese Antarctic Research Expedition (JARE) data reports supplied by the National Institute of Polar Research in Tokyo, and Antarctic data presented in map format by the Alfred Wegener Institute (AWI) of Germany and the Arctic and Antarctic Research Institute (AARI) of Russia (i.e., AWI/AARI Atlas by *Olbers et al.* [1992]). We also used near-simultaneous European Centre for Medium-Range Weather Forecasts winds which have been enhanced using SSM/I data through a variational analysis method following *Atlas et al.* [1991]. The wind data have been gridded in the same format as the ice data for convenience in the interpretation. Finally, results from the fine resolution Antarctic model (FRAM) developed by *Webb and the FRAM Group* [1991] were utilized for comparative analysis.

3. Spatial and Temporal Variability

The highlight of polynya activities during each year from 1987 through 1993 (except 1989) are presented in the sets of images in Plates 1–6. The time series of daily images over the study area (i.e., see Figure 1) provides a means of qualitatively characterizing the Cosmonaut polynya in terms of persistence, actual size and shape, and duration of each occurrence during the winter season. Although these characteristics are not the same every year, it is apparent that there are unique features that are persistent and tend to be repeated every few years. The polynya is also large and well defined during some years but not every year, while multipolynya systems appear to have become common only in recent years. The polynya will be referred to as active during years in which there was at least one major occurrence that lasted for several days, and inactive, otherwise, as in 1989 (not shown). Also, the appearance of at least 20% open water (i.e., 80% ice concentration) in several pixels within the general study area for a few days will be referred to as a Cosmonaut polynya event.

The sequences of daily ice concentration maps in Plates 1–6 are color-coded and presented in 72-image format for each year. The top left portion of each series of images is provided with four lines showing the 45°E and 55°E longitudes and 60°S and 70°S latitudes for reference of geographical location and scale. Each set does not document all the occurrences of the polynya during the year, but the complete set of available data was used in the quantitative analysis of the phenomenon. Although the error in the absolute value of the ice concentration may be large in the polynya areas because of the likely presence of new ice, the precision of the sensor is within 1K which is equivalent to about 1% ice concentration. Thus temporal changes of the order of 4%, which is the color scale interval, are expected to be caused by real physical changes occurring on the surface. In this study, winter starts in early July and ends in late October. Also, east of about 50°E is considered the eastern part, while to the west of this longitude is considered the western part of the study area. By embayment of ice we mean the formation of ice around an open ocean area (as in a bay).

From the series of images we observed two modes of polynya formation. The first mode, which does not appear every year, generally forms in the western part of the region (near longitude 45°E) during the early part of the winter season only and will be referred to as the western Cosmonaut polynya (WCP). The second mode, which recurs during the winter and early spring, usually preceded by a coastal polynya and located primarily several miles offshore, will be called the eastern Cosmonaut polynya (ECP). In many cases, especially when the two occur simultaneously, the two polynyas merge together. Thus, although the specific forcing mechanisms might be different, the regional conditioning needed to initiate the WCP and ECP may be due to the same oceanographic and atmospheric effects.

3.1. Recent Occurrences (1987–1993)

Period of 1987. On July 10, when SSM/I data became available, a sizable WCP at 42°E was already formed, eventually disappearing after a few days (Plate 1). The occurrence of an ECP during this period is also apparent but only on a relatively small scale and manifested by significant open water fraction in the general area. However, there was a good polynya event on July 15–18 and relatively smaller ones on August 1–3 and August 5–6. The big event of the year occurred from August 15 through the end of the month. The ECP was especially well defined and relatively large from August 20 through August 28, reaching peak value in area on August 21. In this sequence the coastal polynya on August 19 grew in size extending to the north on August 20. In subsequent days the offshore portion became dominant, while the coastal portion was disconnected and became very small. On August 28 the coastal feature

increased in size and got connected to the offshore feature again. The latter feature had a component to the west where reduced concentrations extended all the way into the marginal ice region. The polynya recurred again on September 4–7, October 4–9, October 14–16, and October 24–29, but not as prominently as in August.

Period of 1988. The Cosmonaut polynya was especially active and relatively big in 1988 (Plate 2). The WCP is shown to be preceded by the ECP in the July 6–9 and July 16–23 images. An embayment of ice leading to the formation of the WCP happened during the July 20–27 period. Both polynyas occurred simultaneously and were almost joined together on July 20–23. The biggest polynya event of the year occurred on August 3–11 with the area of occurrence covering both regions of WCP and ECP formations of the previous week. This suggests a strong alliance between the two polynyas. Another ECP event occurred during the period from September 3 through October 15. The persistence and size of the polynya during this period were quite unusual. There was a weakening of the effect from September 15–21, but when it recovered, three of them occurred simultaneously covering the region from 40°E to 60°E. The three polynyas reached their maximum size and were practically all connected on September 28, 1988. The western component of this system outlasted the other two by about a week. However, as soon as the latter disappeared on October 19, another activity to the east started and became significant again on October 30. The system of two or more polynyas in the region may be partly influenced by other air/ocean processes as will be discussed later.

Period of 1989. In 1989 the Cosmonaut Sea was covered by ice early in the season, and the WCP did not occur. The daily images (not shown) indicate that the ECP was not as active as in the two previous years despite strong coastal polynya occurrences during the year and very early in the season. The ECP formed on July 3 and July 4, but the polynya was short-lived and was never fully developed. A possible reason for this is that the upwelling of warm water was not intense enough, and the size did not reach the threshold value that would allow it to survive for a longer period as discussed by *Comiso and Gordon* [1987]. The following summarizes the periods of polynya or near polynya formations: July 2–10, July 13–16, August 3–9, August 11–14, August 17–26, September 29–October 6, and October 18–30.

Period of 1990. The polynya was well defined and very active in 1990 as shown in the time series starting July 1 (Plate 3). On July 1 the eastern polynya formed only briefly but reappeared again on July 8–11 and on July 17–19. The series also shows the embayment of the ice edge leading to the formation of the WCP on July 10. Coastal polynyas near Cape Ann can be observed from July 31 through August 24, but the full ECP did not occur until August 27 through August 31. The polynya then reappeared as a bigger and a more defined feature on September 6–17, September 25–30, and October 17–31. A multipolynya system also occurred during the period (e.g., August 30, August 31, and October 13–17).

Period of 1991. The polynya was again very active in 1991 (Plate 4) though not as active as in 1988. The formation of the ECP is already apparent as reduced concentration in the coastal area on July 1. The WCP did not occur perhaps partly because the ice edge was too far north too early in the winter. Although the region was covered mainly by relatively lower-concentration ice (or new ice), the embayment (July 9–19) did not happen in the location where the polynya usually forms. The ECP was observed to be well-defined on July 15–23, August 3, August 10–11, August 17–23, September 2–8, September 23 to October 10, and October 16–20. The multipolynya system was especially common and occurred several times during the year (e.g., August 18, September 25, and October 7). On October 2–4 an unusual three-polynya system was formed with the shape of a flower with three petals. Oceanic influence originating from the marginal ice zone appears to be partly responsible for such a feature.

Period of 1992. In 1992 the polynya was again active (Plate 5), but its size was not as big as in 1991. The WCP formed but only briefly during early July (see part of it on July 17). The ECP formed on July 24–30, but the size was relatively small and was mainly a coastal phenomenon. From August 8 through August 20 the western part of the region had relatively low-concentration ice, but the latter was not very localized. The ECP formed on August 9, August 17, August 20–21, and August 29–30 but was bigger and better defined on September 2–15, October 2–5, October 16–21, and October 24–27. On September 23–25 a two-polynya system, one north of the other, occurred but were merged together at a later date.

Period of 1993. The Cosmonaut Sea region was covered by sea ice very early in the winter of 1993, and no WCP was observed. The ECP formed on July 1 (Plate 6), lasting for more than a week. During this period the existence of a strong tie between the coastal and the offshore components of the ECP is again apparent. This polynya recurred on July 14–17, August 1–6, August 15–21, September 9–13, September 16–21, September 28 through October 3, October 10–21, and October 23–31. Except for the late October events, the big events of the year occurred on July 2 and August 17.

3.2. Previous Occurrences (1973–1987)

Occurrences of the Cosmonaut polynya before 1987 were partly documented by *Comiso and Gordon* [1987] using SMMR and ESMR data. Because of power limitations on board the Nimbus 7 spacecraft, the SSMR sensor was turned on every other day only and could not provide coverage as detailed as SSM/I. Also, while the ESMR sensor was on continuously, only the 3-day average data, as described by *Zwally et al.* [1983], was available for this study. Despite this lack of temporal detail the data provided a good sense of history of the polynya formations from 1973. During the time period 1973 through 1976, when ESMR data were available, the ECP was observed to be a well-defined feature only in September 1973 and September 1975, but in other months or years it was mainly a coastal phenomenon near Cape Ann. During the SMMR years (1979–1986) one of the big polynya events reported and analyzed by *Comiso and Gordon* [1987] was the WCP of 1980, which occurred concurrently with a polynya over the Maud Rise region. The 1986 polynya cited in the same paper was one of the biggest ECPs observed up to 1993. Other significant ECPs observed are those in September 1979, September 1982, and September 1986. During the other years the coastal polynya near Cape Ann occurred, but the offshore component was seldom seen. Since 1986, however, this polynya appears to have been more active than in previous years, taking into account the more limited data available from SMMR and ESMR and the changes in instrument.

3.3. Variations in Location

Because of constantly varying size and shape, it was difficult to devise an unsupervised technique for finding the exact lo-

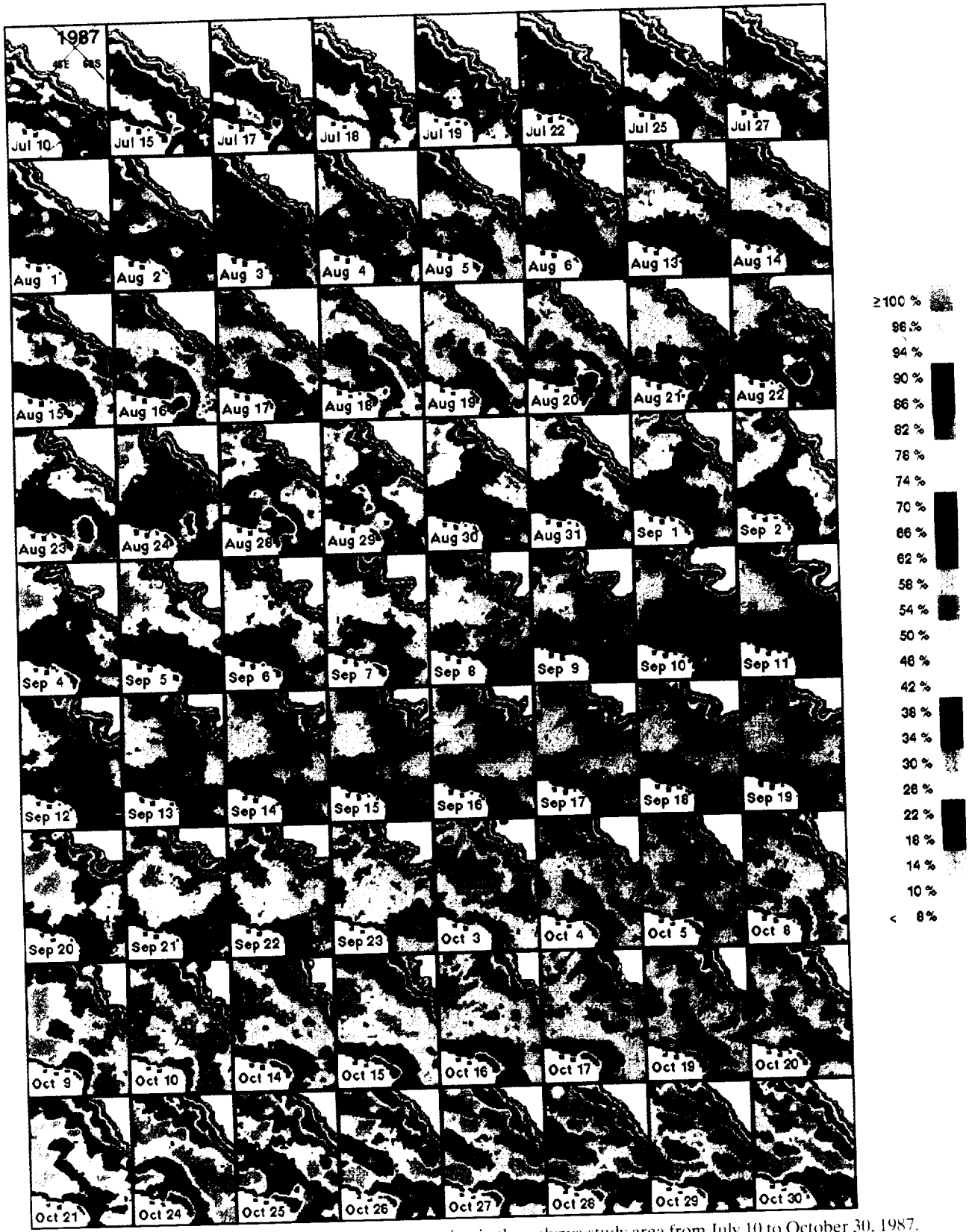

Plate 1. Color-coded images of ice concentration in the polynya study area from July 10 to October 30, 1987. The four lines in the top left image correspond to 45°E and 55°E longitudes and 60°S and 70°S latitudes.

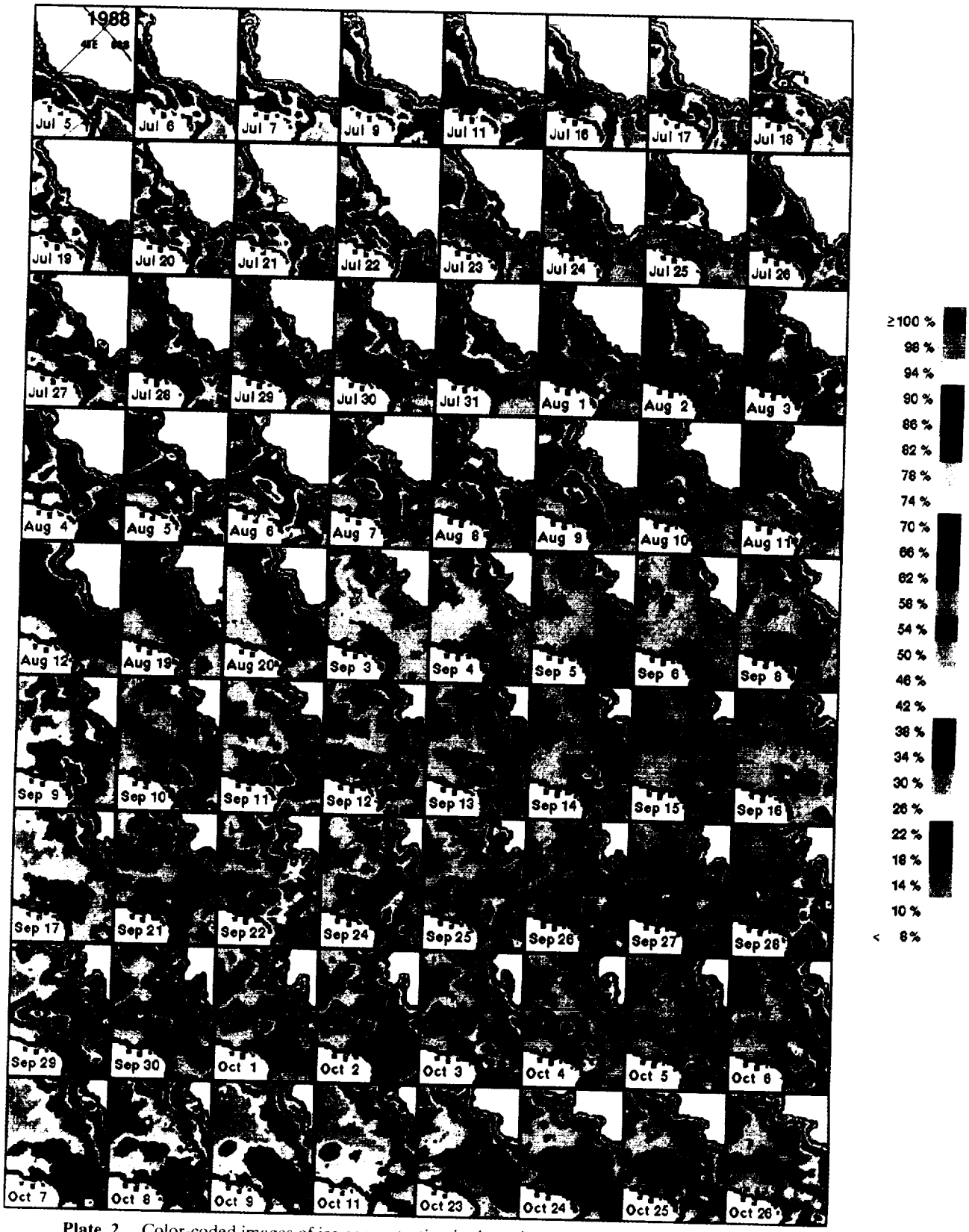

Plate 2. Color-coded images of ice concentration in the polynya study area from July 5 to October 26, 1988.

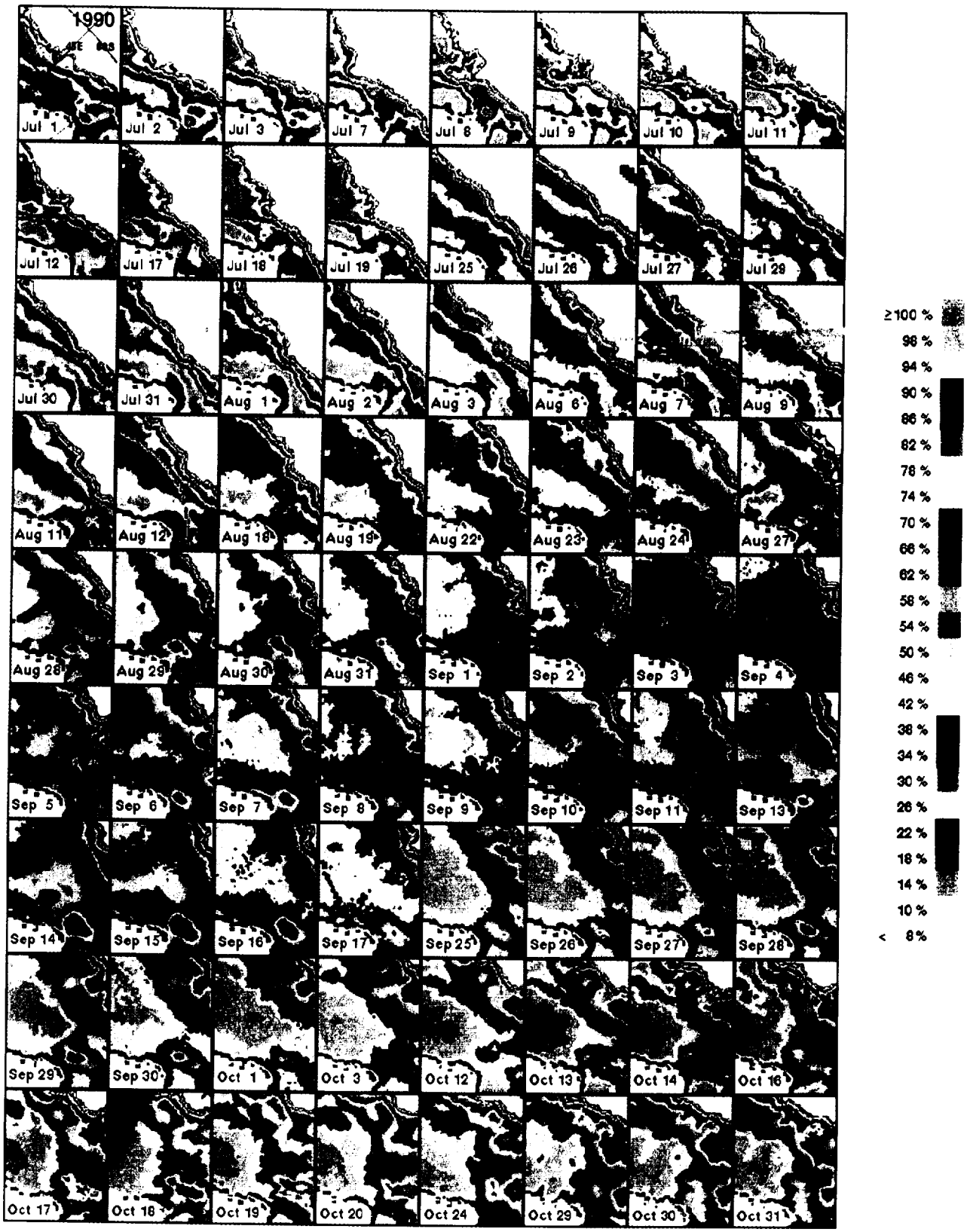

Plate 3. Color-coded images of ice concentration in the polynya study area from July 1 to October 31, 1990.

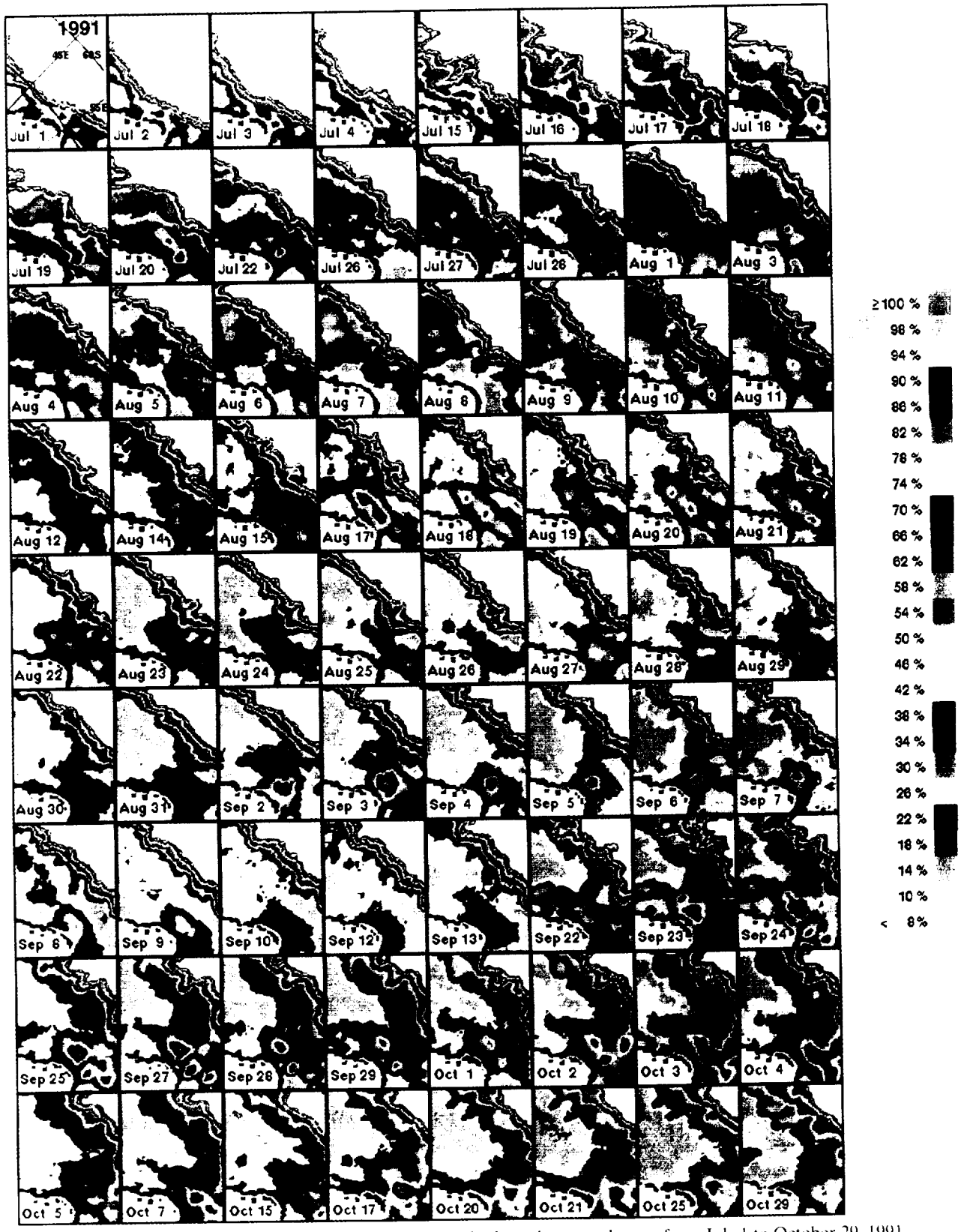

Plate 4. Color-coded images of ice concentration in the polynya study area from July 1 to October 29, 1991.

cation of the centroid of the polynya as it occurred each year. In this study, the location is determined using a Silicon Graphics Indigo^2 workstation and a supervised interactive graphics system. The technique is to display each image on the screen, visually position the cursor at the center location of the polynya, and use the computer to convert this location to geographical coordinates. This procedure may be the only efficient way of identifying the centroid, knowing the complexity of the polynya features as revealed in the series of images (Plates 1–6). Even with this procedure it is sometimes difficult to identify the centroid because of odd shapes and the splitting into two or more polynyas as described earlier. In the latter case, the location of the pixel with the lowest concentration in the largest polynya area is chosen. The error in the positioning of the cursor to the pixel of interest is about a pixel (25 km × 25 km in area).

The centroid of the two polynyas varied significantly in longitude during each winter and from one winter to another (Figure 2). However, the centroid of the ECP tended to be confined between 50°E and 55°E from 1979 through 1993. Also, the WCP tends to be between 40° and 50°E. Sometimes the centroid of the WCP is close to that of the ECP, indicating a strong coupling of the two as mentioned earlier. The plot summarizes the occurrences observed during SMM/I years (Figure 2a) and during SMMR years (Figure 2b). During SMMR years much of the activities in the eastern regions were small features near Cape Ann. Since 1986 the offshore component of the polynya occurred more frequently and with better delineation. Overall, the features occurred in the same general location, suggesting a strong oceanographic influence. The oceanographic setting relevant to the polynya formation will be discussed in the next section.

3.4. Variations in Areal Extent and Actual Open Water Area

The amount of open water during the winter period is a key determinant of the oceanic heat loss. Upward heat flux between ocean and atmosphere may generate over 100 W/m^2 in typical polynya areas, which is at least an order of magnitude greater than that for an ice-covered ocean [*Gordon*, 1982]. The time dependence of the areal extent of open water, as defined earlier, is shown in Figure 3a, while the actual open water area is shown in Figure 3b. Except during overlap (in location of WCP and ECP) the study area excludes the WCP region but includes the coastal region off Cape Ann. Only open water concentrations more than 10% were included in the calculation of actual open water area. Also, when the polynya was close to the marginal ice zone, which was masked out, part of the polynya area may have been excluded. As mentioned earlier, the calculation of ice concentration does not take full consideration of the low emissivity of new ice compared to that of the dominant first-year ice. However, even if the polynya is completely filled by new ice, its feature is still identifiable in the images, and hence its size and extent can still be estimated. This is an important consideration when polynya activities are being studied. The inferred actual ice area, however, does not reflect the true area covered by ice since the area covered by new or thin ice will be underestimated [*Comiso et al.*, 1992]. The errors in these area estimates may thus be higher than those cited (i.e., <5%) by *Zwally et al.* [1983].

The areal plots in Figure 3 quantify the strength and duration of the polynya events presented in the series of images (Plates 1–6). As indicated earlier, the polynya was most active in 1988 when it opened several times during the winter season, and the average daily extent was as high as 2.4 × 10^5 km^2, while the corresponding actual open water area was about 10.0 × 10^4 km^2. The polynya was also very active in 1991 and 1992, but much of the activity occurred after September. During these years the size of the polynyas also approached those of 1988. The polynya was also relatively active and well defined in 1987 and 1990. During these years the daily average open water extent reached 1.2 × 10^5 km^2, while the actual open water area was about 5.1 × 10^4 km^2. In 1989 the polynya was not so active, although the coastal feature near Cape Ann occurred several times during the year. The extent was only about 3.1 × 10^4 km^2, while the actual area was about 1.4 × 10^4 km^2. The varied polynya size suggests large interannual changes in the ocean and atmosphere coupling off Cape Ann.

Table 1. Peak Extent Average, Integrated Daily Average Extent, and Integrated Daily Actual Area of the Polynya for Each Year

Dates	Peak Average, 10^4 km^2	Sum of Daily Extent, 10^6 km^2	Sum of Actual Water Area, 10^6 km^2
July 1 to Oct. 30, 1987	6.5	3.3	2.6
July 1 to Oct. 30, 1988	11.4	6.5	3.6
July 1 to Oct. 30, 1989	3.5	1.5	1.0
July 1 to Oct. 30, 1990	7.4	4.0	2.7
July 1 to Oct. 30, 1991	8.0	6.0	3.5
July 1 to Oct. 30, 1992	6.9	3.5	2.2
July 1 to Oct. 30, 1993	6.8	3.4	2.1

Following the threshold concept suggested by *Comiso and Gordon* [1987], the sizes of these polynyas may be large enough to keep the polynya open for only a few days. However, the maximum size, frequency of occurrence, and persistence appear unpredictable and vary from one year to another (Figure 3). To quantify the interannual changes in total area opening, the average of the peak values for the polynya extent (i.e., extent that is at least 3.0 × 10^4 km^2) from July 1 through October 30 were calculated for each year. Also, the sums of the daily averages of the polynya extents and actual open water areas were calculated for each year. These results are given in Table 1. As expected, the ECP was most active in 1988 with an average peak value for the extent of 11.4 × 10^4 km^2, while it was least active in 1989 with an average peak value of 3.5 × 10^4 km^2. The integrated sum of the daily extents and actual open water areas for 1988 and 1989 are 6.5 × 10^6 km^2 and 1.5 × 10^6 km^2, respectively. Because of the fix time interval (July through October) used in the analysis for all years, some early or late occurrences are not taken into account and may produce slight errors in this analysis, especially in spring.

The frequency of occurrence and persistence of the polynyas can also be inferred from the ice extent data in Figure 3. Polynyas with daily extents greater than 9.0 × 10^4 km^2 occurred 3 times in 1988 and 1991, 2 times in 1987, and 3 times in 1990, 1992, and 1993. Polynyas with daily extents greater than 6.0 × 10^4 km^2 occurred 9 times in 1988, 8 times in 1990, 7 times in 1991, 4 times in 1992 and 1993, and 1 time in 1987. These statistics indicate substantial interannual variability. However, among those with daily extent greater than 6.0 × 10^4 km^2, seven occurred in July, nine in August, eight in September, and nine in October. These results indicate that the

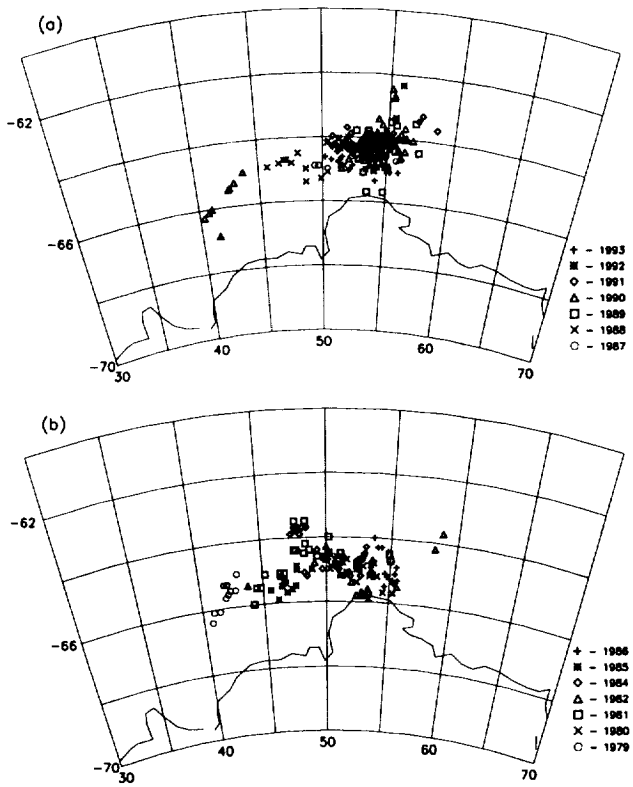

Figure 2. Geographical location of the centroid of the most active region of the Cosmonaut polynya for the time periods (a) 1987–1993 and (b) 1979–1986.

polynya may occur in any month with almost equal probability between July and October.

4. Atmospheric Connections

The role of atmospheric forcing on surface or subsurface conditioning that leads to the advent of a sensible heat polynya has been studied previously using a sea ice model [e.g., *Martinson et al.*, 1981; *Parkinson*, 1983; *Hibler and Ackley*, 1983; *Lemke et al.*, 1990]. To gain an insight into the effect of wind on the formation of the Cosmonaut polynya, near-simultaneous winds as described earlier were utilized. Daily images of ice concentrations on July 21, August 1, and August 6 are shown in Plates 7a, 7c, and 7e, respectively. Differences in daily ice concentration between each day and the previous day are also shown in Plates 7b, 7d, and 7f. The strong role of wind is manifested in the superposition of wind data over both daily ice concentration images and differences of the daily images (Plate 7). Wind data during midnight and noontime for the dates shown are overlaid on the left and right images, respectively.

Three days of data are shown in Plate 7 to demonstrate that the location of a cyclone strongly influences the size and shape of the polynya. In the difference maps, reductions in ice concentration or retreats of the ice edges are represented by brownish colors, while increases in ice concentration or advances of the ice edges are represented by greenish/yellowish colors. The composite images indicate that a cyclone occurred at the Cosmonaut Sea area on July 21. Strong winds caused a general decrease in ice concentration in the region (large brown area north of Cape Ann), eventually causing the embayment that led to the formation of the polynya feature in the western side of the region. The sequence of images that depicts the formation of this polynya in a better temporal detail is shown in Plate 2. The polynya may not have lasted long partly because of constant movement of the center of the cyclone toward the east as shown in Plate 7. The constant movement eventually caused winds to come from the south (see August 6 image) at the polynya study region. This time a strong component of the wind in the northwest direction near Cape Ann led to a coastal feature, advances in the ice edge, and a general reduction in ice concentration in the Cosmonaut Sea area. This event preceded the formation of a fully developed polynya as shown in the sequence from August 1 through August 11 (Plate 2). The process is likely the preconditioning required for the formation of the polynya, which lasted for more than a week.

5. A Proposed Mechanism for the Cosmonaut Polynya

5.1. Oceanographic Setting

We propose that the configuration of the coastline (Figure 4) induces the formation of the persistent Cosmonaut polynya. Cape Ann is the northernmost promontory of elevated glacial surface of Antarctic other than the Antarctic Peninsula. Only low-lying ice shelf regions south of Australia reach further north. In the Cape Ann region, opposing coastal and offshore currents are pressed together, increasing the meridional gra-

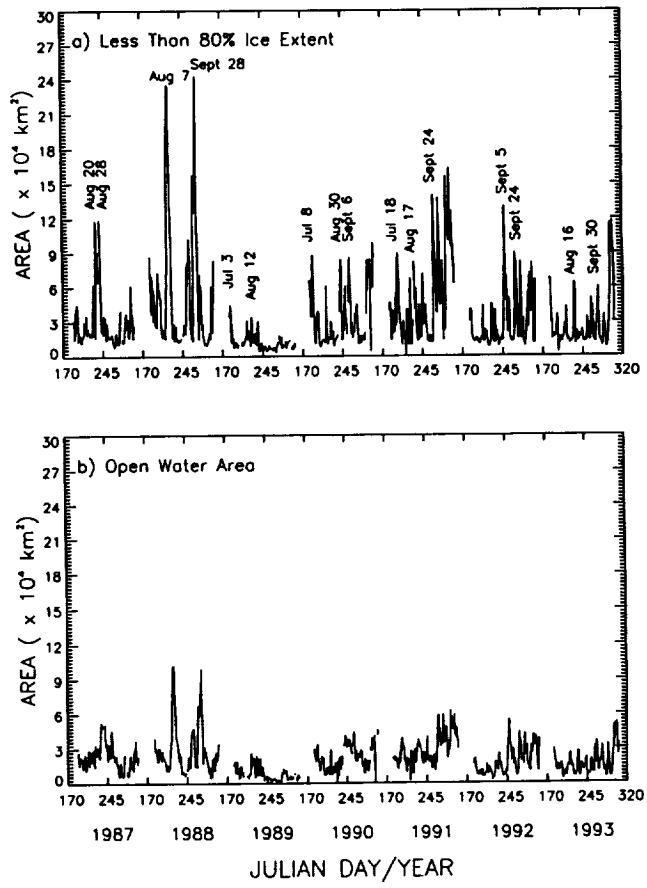

Figure 3. (a) Extent and (b) actual area of open water (<80% ice concentration) in the polynya area for the time period from 1987 through 1993.

dient of zonal flow within the Antarctic Divergence. Following the principle of conservation of potential vorticity, enhanced upwelling ensues. This process accelerates the injection of relatively warm salty deep water into the surface layer, thereby inhibiting sea ice growth.

Gordon and Huber [1990] described a regional balance for the Antarctic zone mixed layer of wind-induced upwelling and buoyancy-induced mixed layer deepening. This balance results in significant upward heat and salt flux that limit winter sea ice thickness. In the region of Maud Rise, enhanced upwelling due to the effect of topography [*Ou*, 1991; *Gordon and Huber*, 1990; *De Veaux et al.*, 1993] forces greater vertical heat flux leading to a Weddell polynya when the heat loss to the atmosphere falls below the topographic enhanced heat flux between the deep water and the mixed layer. In the mid-1970s the Weddell polynya persisted for the full duration of the winters for 3 consecutive years [*Carsey*, 1980]. Since then it has behaved like the Cosmonaut polynya, opening and closing with periods of days to weeks as described earlier and in the work by *Comiso and Gordon* [1987]. The short-period polynyas are not prone to deep-reaching convection, as the supply of meltwater eventually maintains overall stability. A nonconvective sensible heat polynya results. The one-dimensional model of *Martinson* [1981] of a sea ice covered ocean shows that the deep water heat input to the surface layer if it were to melt ice would maintain stable stratification. The polynya closes when the atmosphere becomes colder and/or when a strong sea ice convergence event occurs. Should the deep water salt input to the surface layer overtake the meltwater supply, a convective sensible heat polynya results, as has been hypothesized as the cause for the large Weddell polynya in the 1970s [*Gordon*, 1982].

The oceanic pressure fields in the region as reported in the Atlas of the FRAM [*Webb and the FRAM Group*, 1991] and as inferred from steric height anomalies of the AWI/AARI Atlas [*Olbers et al.*, 1992] show a regional northwest to southeast geostrophic flow field from roughly 50°S, 20°E toward Enderby Land. As the water approaches Antarctica, it bifurcates with the main component turning into an eastward flowing branch,

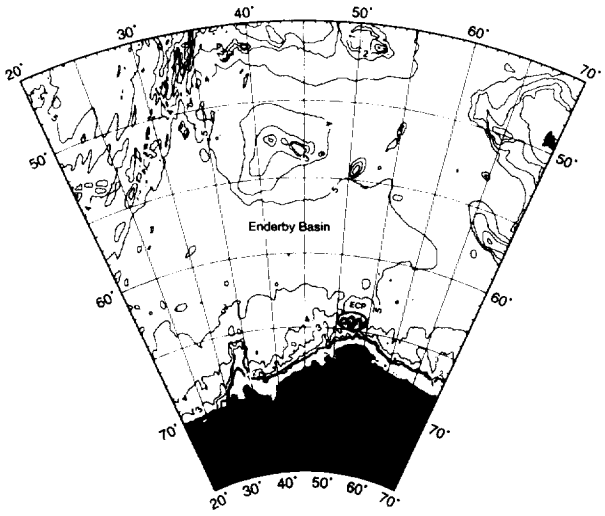

Figure 4. Bottom topography in the study region. The 1-km contour is indicated by a bold solid line. The shaded eliptical region is where the centroids of eastern Cosmonaut polynya events are mainly located.

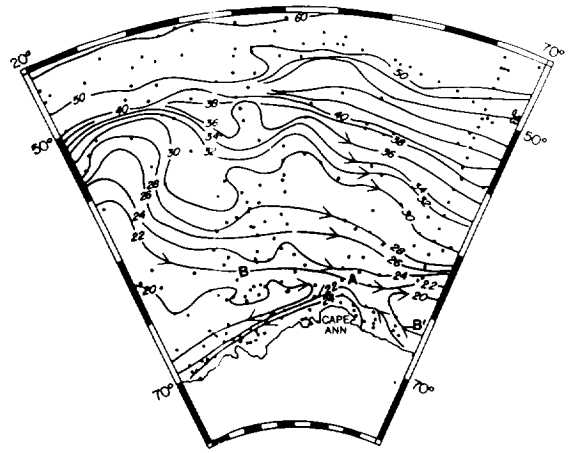

Figure 5. The 0–500 dbar dynamic height based on the Southern Ocean Atlas data set [*Gordon*, 1982] and on the Japanese Antarctic Research Expedition data of 1979–1989 inclusive. Approximate locations of A, B, and B′ discussed in Figure 7 are indicated.

marking the southern edge of the Antarctic Circumpolar Current (ACC) [*Orsi et al.*, 1993] and a branch that turns back to the west to form the southern limb of the Weddell Gyre [*Bagriantsev et al.*, 1989; *Orsi et al.*, 1993]. The 0–500 dbar baroclinic field (Figure 5) produced by updating the Southern Ocean Atlas data set [*Gordon*, 1982], with the JARE data obtained during the period 1979–1989, reveals the more detailed baroclinic circulation pattern in the vicinity of the western and eastern Cosmonaut polynyas. The streamlines of opposing geostrophic flow are strongly compressed adjacent to Cape Ann. The compression prohibits the less than 20 dynamic centimeter sea level trough from passing north of Cape Ann. The trough west of 45°E may be considered as the easternmost extension of the Weddell Gyre.

The AWI/AARI Atlas [*Olbers et al.*, 1992] shows that the topography of the subsurface temperature maximum core layer forms a crest surrounding Antarctica within the 60°–65°S band. Similarly, the oxygen distribution at 200 m (Figure 6) displays a band of low oxygen near 65°S, depicting shallowing of the deep water stratum. These features coincide with a trough of sea level marking a reversal of circulation often referred to as the Antarctic Divergence [*Deacon*, 1937]. To the north of the Antarctic Divergence, the flow is toward the east, as part of the Antarctic Circumpolar Current. To the south, the flow is toward the west, as part of the coastal current. Within the Antarctic Divergence the relatively warm low oxygen deep water rises to its shallowest level. The core layer and sea level steric heights data indicate that the Antarctic Divergence has its closest approach to Antarctica at Cape Ann, which is near the site of the Cosmonaut polynya.

A series of cyclonic eddies have been observed [*Wakatsuchi et al.*, 1994] near 100°–115°E, to the east of the Cosmonaut polynya region. Such eddies within the Antarctic Divergence may be common, forming centers of upwelling along the Antarctic Divergence. Perhaps the centers of the ECP and WCP may be related to cyclonic features. In a more general sense, the Antarctic Divergence with its associated eddy may play a role in demarcating the northern limits of sea ice, where gyre-like ocean circulation does not inject ice into the region north of the Antarctic Divergence, for example, the Weddell Gyre.

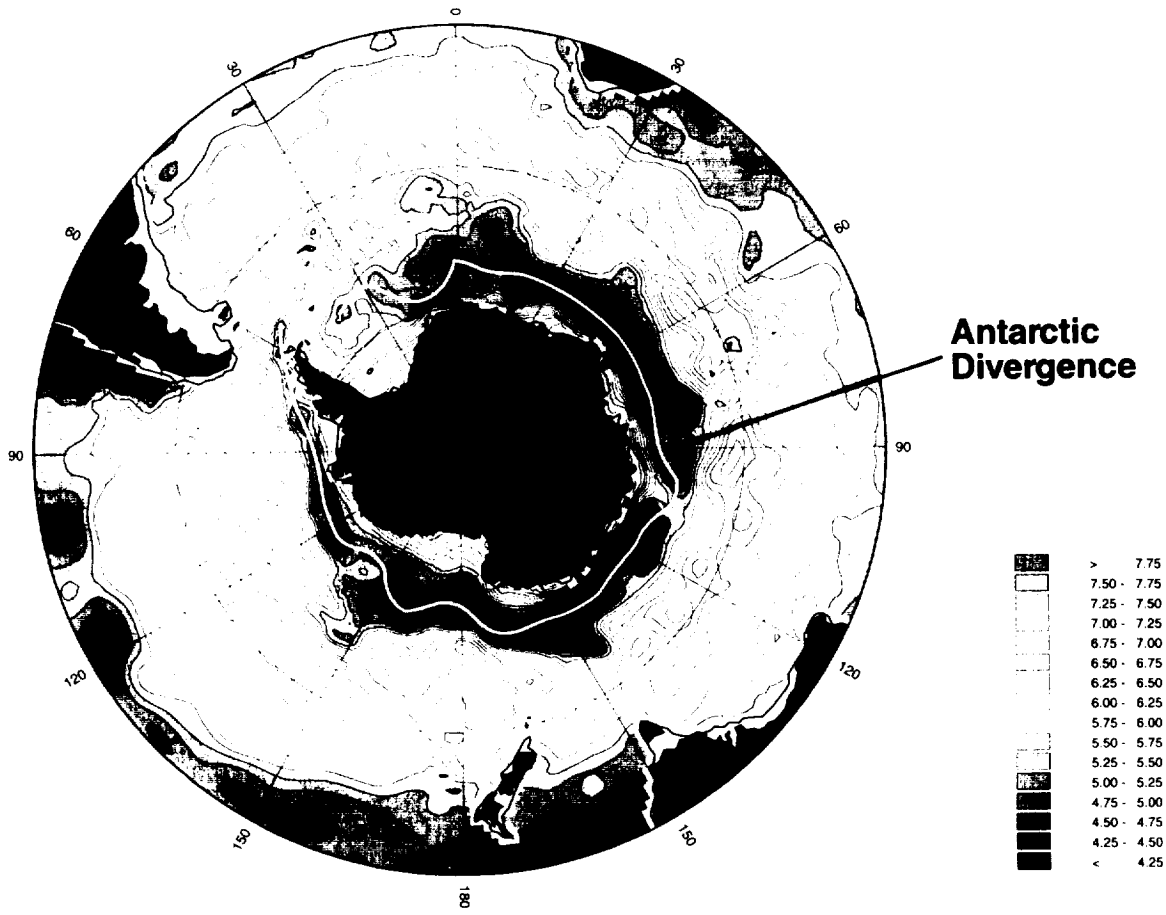

Figure 6. Position of the Antarctic Divergence (AD) (bold white line), as defined by the axis of oxygen minimum at the 200 m horizon taken from the Alfred Wegener Institute and the Arctic and Antarctic Research Institute Atlas [*Olbers et al.*, 1992].

The coastal current speed can be estimated from buoy drifter tracks and iceberg tracking [*Tchernia and Jeannin*, 1983]. Iceberg 1064 was tracked from approximately 63°E to 30°W. From June 1, 1980, to July 1, 1980, it drifted over the 3000-m isobath along Enderby Land from 57°E to 42°E, a distance of about 750 km, indicating a mean speed of about 27 cm/s. We will use this value as the typical current speed in the region in the next section.

5.2. Theoretical Considerations

A schematic illustrating the vorticity and upwelling concept is shown in Figure 7. Water that enters the compressed zone in the vicinity of Cape Ann apparently has a change of relative vorticity as the meridional gradient of zonal flow is greatly increased. As a particle within the ACC or coastal flow approaches the compression near Cape Ann, it would experience a dramatic reduction in relative vorticity (increase in the meridional gradient of zonal flow, more clockwise rotation). As total absolute vorticity is conserved, the water column may move to the south or stretch in place (or some combination). As the coastal margin and current prohibits movement to the south, we suggest that the water column stretches, forcing enhanced upwelling of deep water into the surface layer. This flux would inhibit sea ice formation and allow for the development of the Cosmonaut polynya whenever the atmosphere cannot remove the excess heat flux.

We thus propose that the Cosmonaut polynya is caused by the upwelling of warm deep water and the increase in surface water divergence. This can be justified quantitatively as follows. The conservation of potential vorticity may be expressed as

$$(f + \zeta)/h = \text{const} \qquad (1)$$

where f is the Coriolis parameter; ζ is the relative vorticity, which is equal to $\partial v/\partial x - \partial u/\partial y$; and h is the thickness of the water column. The Coriolis parameter is given by $2\omega\sin\delta$ (where δ is latitude and ω is the angular velocity of the rotation of the Earth), which is <0 in the southern hemisphere. Assuming f = const (the latitudinal spread of the phenomena is small) and $\partial v/\partial x = 0$ (all of the relative vorticity is due to compression of the zonal flow), we can use the conservation of potential vorticity to determine the growth of h as a function of change in $\partial u/\partial y$.

The surface baroclinic flow (Figure 5) indicates approximately a doubling in $\partial u/\partial y$ from points B to point A (i.e., 1.25×10^{-6} to 2.5×10^{-6} cm/s). A particle tracking along the 22 dynamic centimeter isopleth would experience an increase of its relative vorticity in a distance of approximately 500 km (points B to A on Figure 5). Using the characteristic speed of 27 cm/s, as mentioned in the previous section, a particle would traverse this distance in 1.9×10^6 s or about 21 days. During this time the thickness of the water column initially at point B

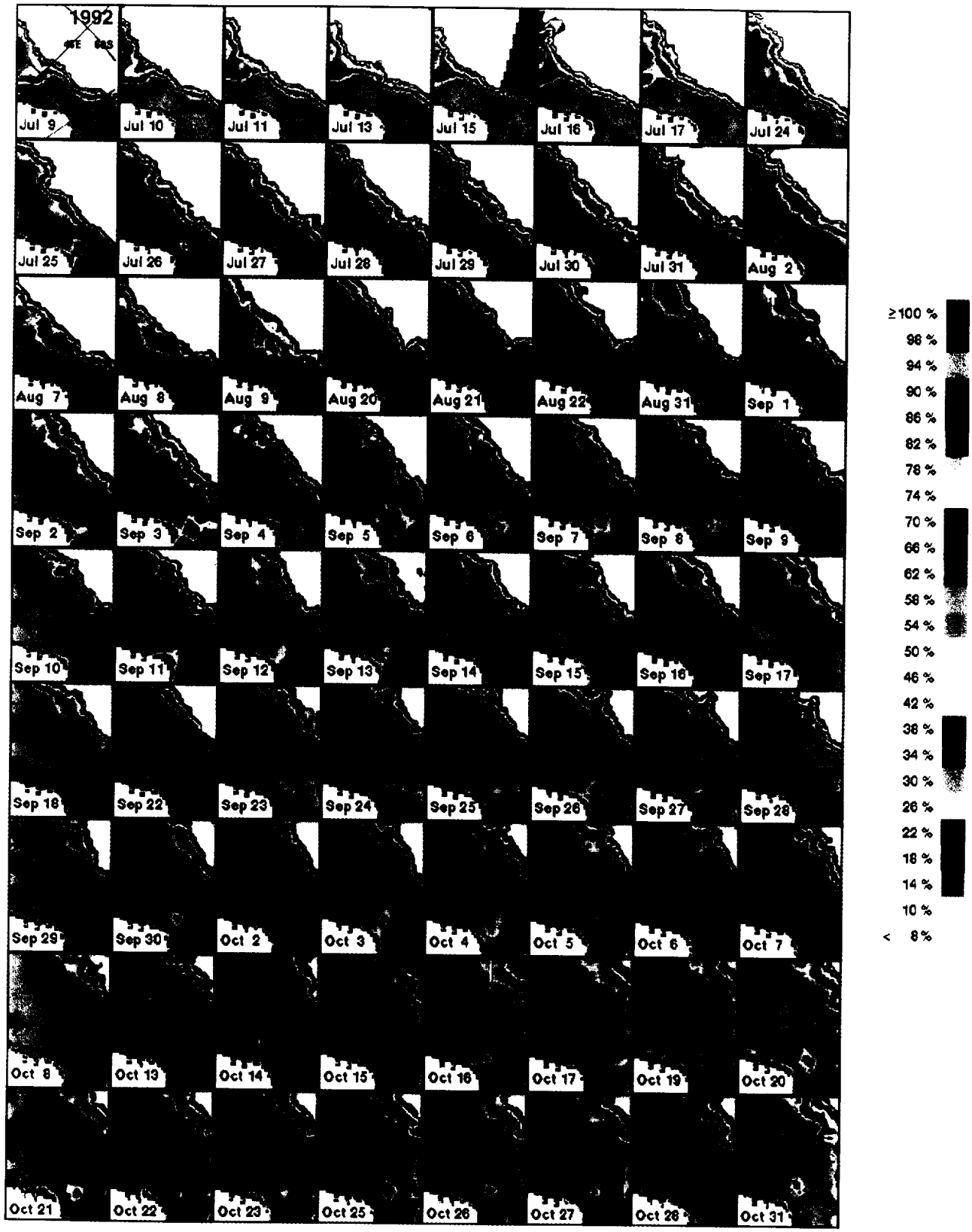

Plate 5. Color-coded images of ice concentration in the polynya study area from July 9 to October 31, 1992.

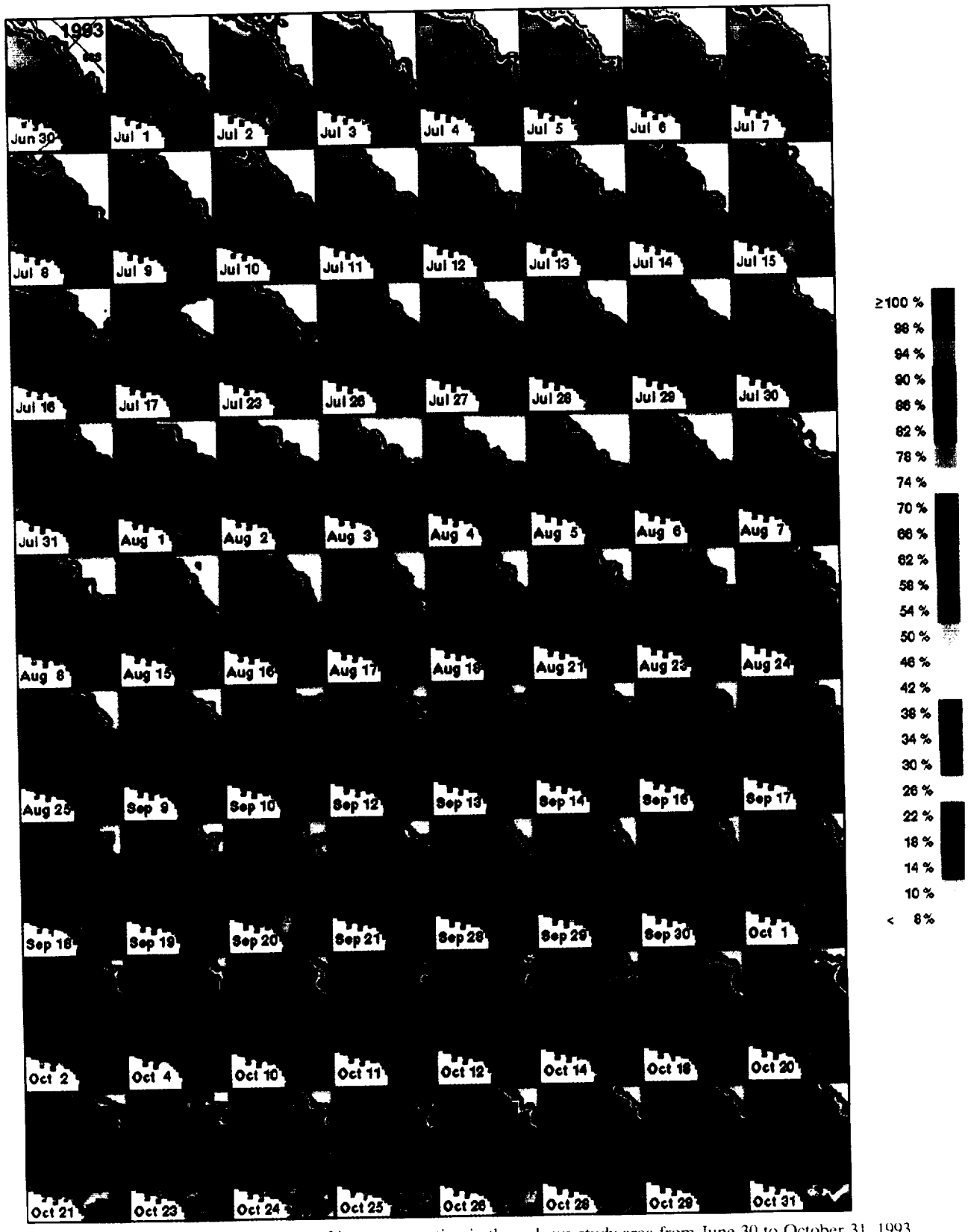

Plate 6. Color-coded images of ice concentration in the polynya study area from June 30 to October 31, 1993.

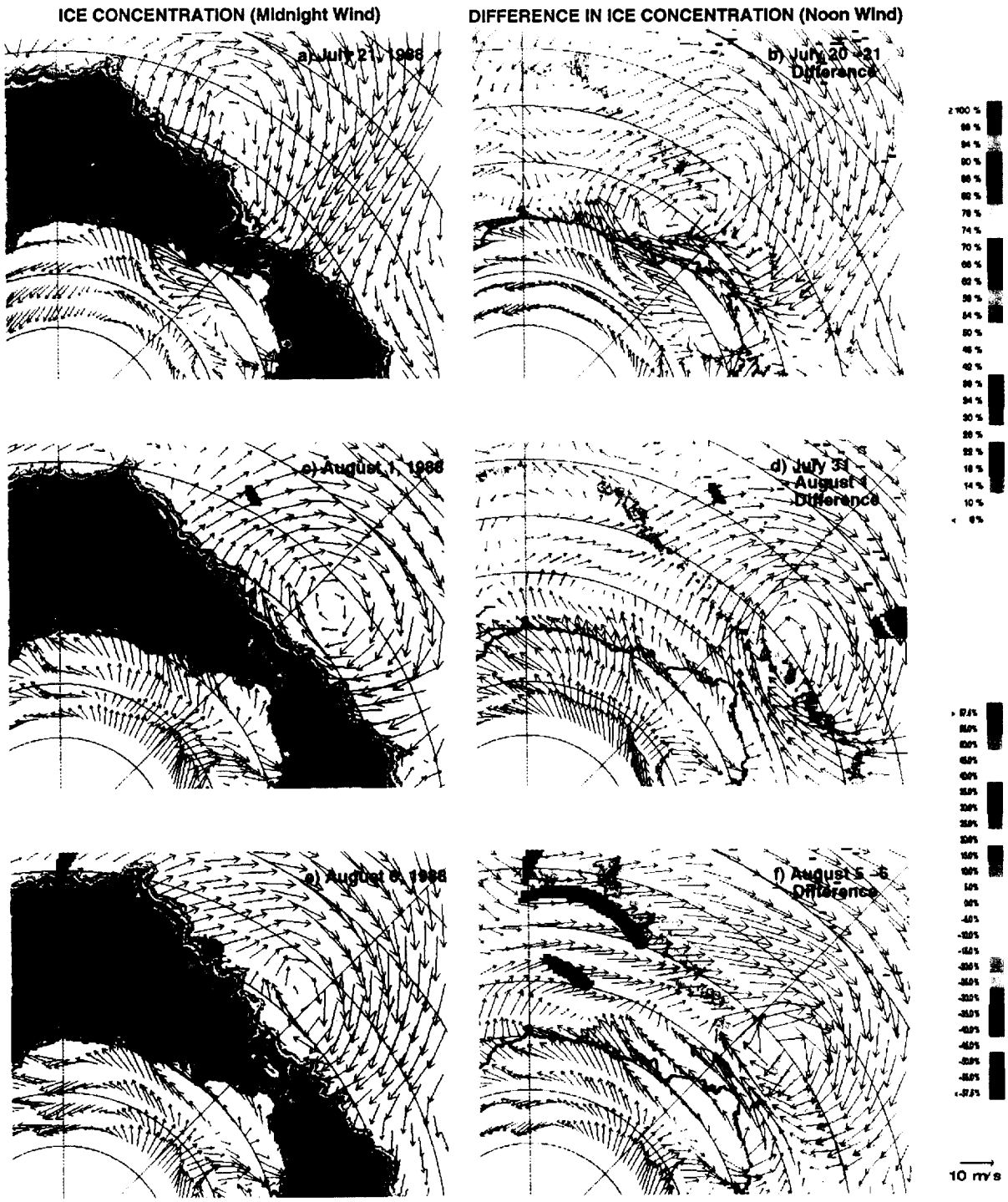

Plate 7. (a) Ice concentration on July 21, 1988, with enhanced European Centre for Medium-Range Weather Forecasts (ECMWF) midnight wind on the same day; (b) difference map of ice concentration from July 20–21, 1988, overlaid by enhanced of ECMWF noontime wind on July 21, (c) and (d) corresponding images for July 31 and August 1, 1988, (e) and (f) corresponding images for August 5 and 6, 1995.

would increase by about 1% when it arrives at point A. It is not clear how much of the water column engages in this stretching, but using 500 m for h, the scale depth of the temperature maximum depth, the water column would stretch by 5 m during the 21-day transient period. This amounts to an upwelling rate of 2.6×10^{-4} cm/s, which is an enhancement over the background regional Ekman-induced upwelling and is about an order of magnitude larger than the latter, estimated to be about 5.7×10^{-5} cm/s [*Levitus*, 1982; *Gordon et al.*, 1978]. The conceptual point that this approach demonstrates, as illustrated in Figure 7, is that compression of the streamlines of flow as occurring north of promontories of Antarctica following the conservation of vorticity is expected to cause enhanced upwelling of warm deep water. Enhanced upwelling shallows

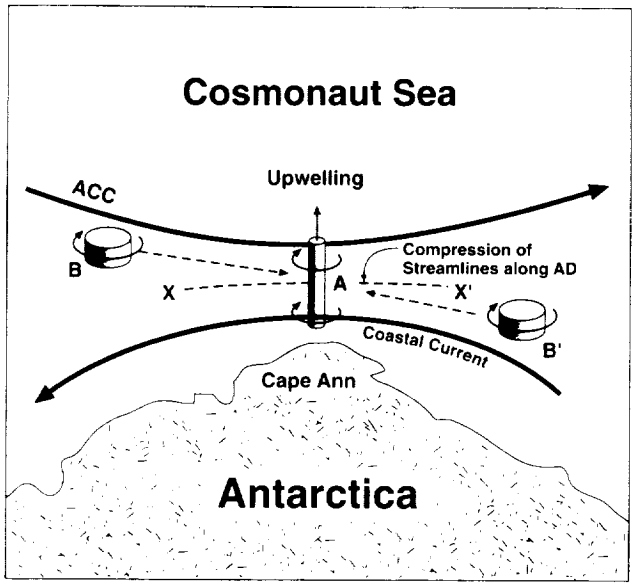

Figure 7. A schematic of the vorticity stretching concept. The relative vorticity of a water column from point B or B′ to point A becomes more negative (clockwise rotation) as it is carried into a region of increased shear as the Antarctic Circumpolar Current and coastal current are pressed together at the Antarctic Divergence (AD) along XX′ by the continental margin configuration. The conservation of absolute vorticity requires the water column to stretch as the alternative poleward flow is blocked by Antarctica. The stretching induces upwelling well in excess of the regional Ekman upwelling, injecting additional warm deep water into the surface mixed layer and causing more ice melt.

the pycnocline and preconditions the surface for polynya generation.

6. Discussion and Conclusions

The Cosmonaut polynya has been one of the most persistent features of the ice-covered portion of the Southern Ocean as observed by more than 2 decades of satellite data. Two modes of the polynya have been identified: the WCP, which occurs in the western region in early winter only, and the ECP, which occurs near Cape Ann one or more times during winter. The historical passive microwave data indicate large interannual variability in size and persistence of the polynya from 1973 through 1993. The five cases in 1975, 1979, 1980, 1982, and 1986 reported by *Comiso and Gordon* [1987] were the most noticeable events up to 1986. Since 1987 the continuous coverage afforded by SSM/I reveals a more active polynya than prior to 1986. The latter data indicate yearly occurrences, multiple events (as many as 4 times) each winter period, and multiple polynyas in the region. Also, large temporal variabilities of the sizes and extents are apparent. During the 1986 through 1993 period the integrated actual open water area was as high as 3.6×10^6 km^2 in 1988 with interannual variability of as much as 65%. Such variation is significant and would have large effects on the regional ocean-atmosphere heat fluxes. The increased activity of the Cosmonaut polynya since 1986 also suggests changing oceanographic or atmospheric conditions in the region. Because of its relatively large size (estimate of average of peak extents was about 7.2×10^4 km^2) and the potential impact on the ventilation of the ocean and bottom water formation, this increase in activity may be an important aspect of climate variability.

The persistence of the ECP in the same general location off Cape Ann suggests a strong oceanographic influence to its formation. The oceanographic setting indicates that the polynya may be caused by a stretching of the water column in the area as a result of a vorticity conserving interaction of Antarctic Circumpolar Current with the coastal current. This hypothesis is supported by the dynamic topography of the region and the configuration of the coastline. Our estimate indicates that a water column stretching can cause an upwelling of warm water at a rate of 2.6×10^{-4} cm/s, which is well above the regional Ekman upwelling rate of 5.7×10^{-5} cm/s [*Gordon and Huber*, 1990]. We suggest that this phenomenon causes the formation of the Cosmonaut polynya.

The large upward heat flux in the large Weddell polynyas of the mid-1970s was maintained by deep-reaching convection [*Gordon*, 1982]. The ECP is a sensible heat polynya which is also maintained by oceanic heat. However, recent oceanographic data (e.g., JARE) reveal that the deep water in the Cosmonaut Sea is not anomalously cold, suggesting that deep ocean convection has not been occurring. This is consistent with the transient nature of the polynya in that the size has not been large enough to overcome melt effects of ice "blown" from the sides. Only when conditions for enhanced upwelling are strong and persistent enough and abundant sea ice is no longer available for melting that deep ocean convection might occur. This appears not to be the case with the Cosmonaut polynya, which we hereafter type as a "nonconvective sensible heat polynya." This type of polynya is unique in that the upwelled water feeds a divergence of surface water rather than local convective cells.

Further research is needed to verify the vorticity hypothesis and better understand the threshold phenomenon. The recent increase in frequency and activity of the feature should make it likely that a ship-based observational program can be done at the same time the polynya actually occurs. This would enable measurements of crucial oceanographic parameters when the process is actually going on. Such research would at the same time help establish if these events have profoundly changed the oceanography of the region. High-resolution satellite data (e.g., synthetic aperture radar and Landsat) should also help resolve some of the ambiguities of surface conditions within the Cosmonaut polynya and may allow for improved classification of the polynya type.

Acknowledgments. The authors are grateful to Rico Allegrino of Hughes STX for help in the processing of satellite and ancillary data. The authors also wish to thank Stan Jacobs of Lamont-Doherty Earth Observatory of Columbia University, Robert Thomas of NASA headquarters, and three anonymous reviewers for very useful comments and suggestions. Data used in this study are enhanced ECMWF winds (VAM winds) provided by R. Atlas of GSFC, JARE oceanographic data in the Cosmonaut Sea region provided by the National Institute of Polar Research of Japan, and gridded SSM/I brightness temperature data supplied by NSIDC of the University of Colorado. The research of J.C.C. was supported by NASA RTOP 461-62-09 under NASA's Cryosphere Processes Program, while that of A.L.G. was supported by NASA grant NAGW 3362, and NSF grant OPP 93-13700 to Lamont Doherty Earth Observatory of Columbia University, Lamont-Doherty Earth Observatory contribution number 5462.

References

Atlas, R., S. C. Bloom, R. N. Hoffman, J. V. Ardizzone, and G. Brin, Space-based surface wind vectors to aid understanding of air-sea interactions, *Eos Trans. AGU*, *72*(18), 201, 204, 205, and 208, 1991.

Bagriantsev, N., A. Gordon, and B. Huber, Weddell Gyre: Temperature maximum stratum, *J. Geophys. Res.*, *94*(C06), 8331–8334, 1989.

Carsey, F. D., Microwave observations of the Weddell polynya, *Mon. Weather Rev.*, *108*, 2032–2044, 1980.

Cavalieri, D. J., A passive microwave technique for mapping new and young sea ice in seasonal sea ice zones, *J. Geophys. Res.*, *99*(C6), 12,561–12,572, 1994.

Cavalieri, D. J., and S. Martin, Microwave study of Wilkes Land polynyas, in *Oceanology of the Antarctic Continental Shelf*, *Antarc. Res. Ser.*, vol. 43, edited by S. Jacobs, pp. 227–252, AGU, Washington, D. C., 1985.

Comiso, J. C., and A. L. Gordon, Recurring polynyas over the Cosmonaut Sea and the Maud Rise, *J. Geophys. Res.*, *92*(C3), 2819–2834, 1987.

Comiso, J. C., and C. W. Sullivan, Satellite microwave and in situ observations of the Weddell Sea ice cover and its marginal ice zone, *J. Geophys. Res.*, *91*(C8), 9663–9681, 1986.

Comiso, J. C., S. F. Ackley, and A. L. Gordon, Antarctic sea ice microwave signature and their correlation with in situ ice observations, *J. Geophys. Res.*, *89*(C1), 662–672, 1984.

Comiso, J. C., T. C. Grenfell, M. Lange, A. Lohanick, R. Moore, and P. Wadhams, Microwave remote sensing of the Southern Ocean ice cover, in *Microwave Remote Sensing of Sea Ice*, Geophys. Monogr. Ser., vol. 68, edited by F. Carsey et al., pp. 243–260, AGU, Washington, D. C., 1992.

Darby, M. S., A. J. Willmott, and T. A. Somerville, On the influence of coastline orientation on the steady state width of a latent heat polynya, *J. Geophys. Res.*, *100*(C7), 13,625–13,633, 1995.

Deacon, G. E. R., The hydrology of the Southern Ocean, *Discovery Rep.*, *XV*, 1–24, 1937.

De Veaux, R., A. L. Gordon, J. C. Comiso, and N. E. Chase, Modeling of topographical effects on Antarctic sea ice using multivariate adaptive regression splines, *J. Geophys. Res.*, *98*(C11), 20,207–20,319, 1993.

Eicken, H., and M. A. Lange, Development and properties of sea ice in the coastal regime of the southeastern Weddell Sea, *J. Geophys. Res.*, *94*(C6), 8193–8206, 1989.

Gloersen, P., W. Campbell, D. Cavalieri, J. Comiso, C. Parkinson, and H. J. Zwally, Arctic and Antarctic Sea Ice, 1978–1987: Satellite passive microwave observations and analysis, *NASA Spec. Publ.*, *511*, 1992.

Gordon, A. L., Weddell deep water variability, *J. Mar. Res.*, *40*, suppl., 199–217, 1982.

Gordon, A. L., Two stable modes of Southern Ocean winter stratification, in *Deep Convection and Water Mass Formation in the Ocean*, edited by J. Gascard and P. Chu, pp. 17–35, Elsevier, New York, 1991.

Gordon, A. L., and J. C. Comiso, Polynyas and the Southern Ocean, *Sci. Am.*, *258*, 90–97, 1988.

Gordon, A. L., and B. A. Huber, Southern Ocean winter mixed layer, *J. Geophys. Res.*, *95*(C7), 11,655–11,672, 1990.

Gordon, A. L., E. Molinelli, and T. Baker, Large-scale relative dynamic topography of the Southern Ocean, *J. Geophys. Res.*, *83*(C6), 3023–3032, 1978.

Grenfell, T., and J. C. Comiso, Multifrequency passive microwave observations of first year sea ice grown in a tank, *IEEE Trans. Geosci. Remote Sens.*, *GE-24*, 826–831, 1986.

Grenfell, T. C., D. J. Cavalieri, J. C. Comiso, M. R. Drinkwater, R. G. Onstott, I. Rubinstein, K. Steffen, and D. P. Winebrenner, Microwave signatures of new and young ice, in *Microwave Remote Sensing of Sea Ice*, edited by F. Carsey, chap. 14, pp. 291–301, AGU, Washington, D. C., 1992.

Hibler, W. D., III, and S. F. Ackley, Numerical simulation of the Weddell Sea pack ice, *J. Geophys. Res.*, *88*(C5), 2873–2887, 1983.

Jacobs, S., and J. C. Comiso, Sea ice and oceanic processes on the Ross Sea, Continental shelf, *J. Geophys. Res.*, *94*(C12), 18,195–18,211, 1989.

Kottmeier, C., and D. Engelbart, Generation and atmospheric heat exchange of coastal polynyas in the Weddell Sea, *Boundary Layer Meteorol.*, *60*, 207–234, 1992.

Lemke, P., W. B. Owens, and W. D. Hibler III, A coupled sea ice-mixed layer-pycnocline model for the Weddell Sea, *J. Geophys. Res.*, *95*(C6), 9513–9525, 1990.

Levitus, S., Climatological atlas of the world ocean, *NOAA Prof. Pap.*, *13*, 173 pp. Natl. Oceanic and Atmos. Admin., Washington, D. C., 1982.

Martinson, D. G., P. D. Killworth, and A. L. Gordon, A convective model for the Weddell polynya, *J. Phys. Oceanogr.*, *11*(4), 466–488, 1981.

Olbers, D., V. Gouretski, G. Seib, and J. Schroter, *Hydrographic Atlas of the Southern Ocean*, 82 plates, Alfred Wegener Inst., Bremerhaven, Germany, 1992.

Orsi, A., W. Nowlin, and T. Whitworth, On the circulation of the Weddell Gyre, *Deep Sea Res.*, *40*, 169–177, 1993.

Ou, H. W., Some effects of a seamount on oceanic flows, *J. Phys. Oceanogr.*, *21*(12), 1835–1845, 1991.

Parkinson, C. L., On the development and cause of the Weddell polynya in a sea ice simulation, *J. Phys. Oceanogr.*, *13*(3), 501–511, 1983.

Parkinson, C. L., J. C. Comiso, H. J. Zwally, D. J. Cavalieri, P. Gloersen, and W. J. Campbell, Arctic sea ice 1973–1976 from satellite passive microwave observations, *NASA Spec. Publ.*, *489*, 1987.

Smith, S., R. Muench, and C. Pease, Polynyas and leads: An overview of physical processes and environment, *J. Geophys. Res.*, *95*(C6), 9461–9479, 1990.

Tchernia, P., and P. F. Jeannin, *Quelques aspects de la circulation Antarctique reveles par l'observation de la derive d'icebergs (1972–83)*, Musee Natl. D'Hist. Nat., Paris, 1983.

Wakatsuchi, M., K. I. Ohshima, M. Hishida, and M. Naganobu, Observations of a street of cyclonic eddies in the Indian Ocean sector of the Antarctic Divergence, *J. Geophys. Res.*, *99*(C10), 20,417–20,426, 1994.

Webb, D. J., and the FRAM Group, An eddy-resolving model of the Southern Ocean, *Eos Trans. AGU*, *72*(15), 169, 1991.

Wensnahan, M., G. A. Maykut, T. C. Grenfell, and D. P. Winebrenner, Passive microwave remote sensing of thin sea ice using principal component analysis, *J. Geophys. Res.*, *98*(C12), 12,453–12,468, 1993.

Vanney, J. R., and G. L. Johnson, GEBCO bathymetric sheet, in *Oceanology of the Antarctic Continental Shelf*, edited by S. Jacobs, *Antarc. Res. Ser.*, vol. 43, pp. 1–4, AGU, Washington, D. C., 1985.

Zwally, H. J., and P. Gloersen, Passive microwave images of the polar regions and research applications, *Polar Rec.*, *18*, 431–450, 1977.

Zwally, H. J., J. C. Comiso, C. L. Parkinson, W. J. Campbell, F. D. Carsey, and P. Gloersen, Antarctic sea ice 1973–1976 from satellite passive microwave observations, *NASA Spec. Publ.*, *459*, 1983.

Zwally, H. J., J. C. Comiso, and A. L. Gordon, Antarctic offshore leads and polynyas and oceanographic effects, in *Oceanology of the Antarctic Continental Shelf*, *Antarc. Res. Ser.*, vol. 43, edited by S. Jacobs, pp. 203–226, AGU, Washington, D. C., 1985.

J. C. Comiso, NASA Goddard Space Flight Center, Mail Code 971, Greenbelt, MD 20771.

A. L. Gordon, Lamont-Doherty Earth Observatory, Columbia University, Route 9W North, Palisades, NY 10964.

(Received July 21, 1995; revised April 12, 1996; accepted April 22, 1996.)

Profiling the South Pacific Antarctic Continental Shelf

C. GIULIVI and S. JACOBS
Lamont Earth Observatory of Columbia University
Palisades, NY 10964

Field support of a biogeochemical study in the Ross Sea Polynya continued on N.B. Palmer cruise 9508, with 150 CTD (conductivity-temperature-depth) stations taken during December 1995 and January 1996 in the southwest Ross Sea (figure 1). Three long sections were reoccupied along 76.5°S, three short transects along 165°E and 172°E, and several casts directly north of Ross Island (~77.5S, 168E). Eighty six of the stations reached within a few meters of the sea floor, thereby accessing a bottom boundary layer that often displays higher turbidity and salinity (Jacobs 1989). Equipment and water sampling procedures were as described in Jacobs et al. (1995), and the data from N.B. Palmer cruise 9406 appear in Giulivi et al. (1995). The sea surface was sampled for oxygen isotopes enroute to the Ross Sea from Lyttleton, New Zealand.

Work also continued on other Southern Ocean data obtained on the N.B. Palmer and USCGC Polar Sea. Representative coastal stations from those cruises (figure 1) reveal a temperature field that varies substantially from the Antarctic Peninsula to the Ross Sea (figure 2). Relatively warm Circumpolar Deep Water (CDW) floods the deeper parts of the continental shelf in the Bellingshausen and Amundsen Seas. Colder shelf water west of the central Amundsen Sea is caused by more rapid sea ice removal and greater surface freezing in the Ross Sea Polynya, and in smaller but similar coastal features. Typically perennial and snow-covered sea ice over the continental shelf in the Amundsen & Bellingshausen Seas is a result of more onshore winds in that sector. Record low sea ice extents in this region during the late 1980's and early 1990's (Jacobs and Comiso 1996) had returned to its two-decade mean by the first half of 1996.

The warmer water at depth in the eastern region of figure 2 leads to much higher melt rates of its small floating ice shelves and many icebergs. The CDW/meltwater mixture is colder but lighter than the CDW, and upwells into the near-surface layers, as shown by the shoaling -1.5°C isotherm in the Amundsen Sea. Oceanic melting at

the base of Pine Island Glacier, near station 92, averages more than 10 m yr^{-1}, roughly equivalent to its iceberg calving rate (Jacobs et al. 1996; Jenkins et al. 1996). A numerical model of the sub-ice circulation suggests local melt rates in excess of 20 m yr^{-1}, and chemical analyses of the outflow indicate that precipitation on the glacier catchment basin will have an oxygen-18 ratio of ~ -29 $^{o}/_{oo}$ (Hellmer et al. 1996).

A second volume of the Antarctic Research Series dedicated to the oceanology of the Antarctic continental shelf (Jacobs and Weiss 1997) includes reports based upon some of this recent field work, and related studies in the Weddell Sea and along the east Antarctic continental margin. Shipboard support on NBP 9508 was provided by J. Ardai and S. O'Hara. CTD data reduction and analysis is supported by National Science Foundation grant OPP 94-18151; sub-ice shelf modelling by Department of Energy grant DE FG02 93ER61716; sea ice research by NASA grant NAGW 3362.

References

Giulivi, C., S. Jacobs, S. O'Hara and J. Ardai. 1995. Ross Sea Polynya Project, 1994, Oceanographic Data, N.B. Palmer cruise 9406. Tech. Rept. LDEO-95-1, 316 pp.

Hellmer, H., S. Jacobs, A. Jenkins and S. Khatiwala. 1996. Ocean erosion of a fast-moving Antarctic glacier in the Amundsen Sea. subm. to *Deep-Sea Res.*

Jacobs, S. 1989. Marine controls on modern sedimentation on the Antarctic continental shelf. *Mar. Geol.*, 85, 121-153.

Jacobs, S., C. Giulivi, S. O'Hara and J. Ardai. 1995. Plumbing the Ross Sea Polynya. *Ant. J. of the U.S.*, 30, in press.

Jacobs, S. and J. Comiso. 1996. Climate variability in the Amundsen and Bellingshausen Seas. *J. of Climate*, in press.

Jacobs, S. and R. Weiss (eds). 1997. Oceanology of the Antarctic Continental Margin, *Ant. Res. Ser.*, in prep.

Jacobs. S., H. Hellmer and A. Jenkins. 1996. Antarctic ice sheet melting in the Southeast Pacific. *Geophys. Res. Lett.*, 23(9), 957-960.

Jenkins, A., D. Vaughan, S. Jacobs, H. Hellmer and J. Keys. 1996. Glaciological and oceanographic evidence of high melt rates beneath Pine Island Glacier, West Antarctica. *J. of Glaciology*, in press.

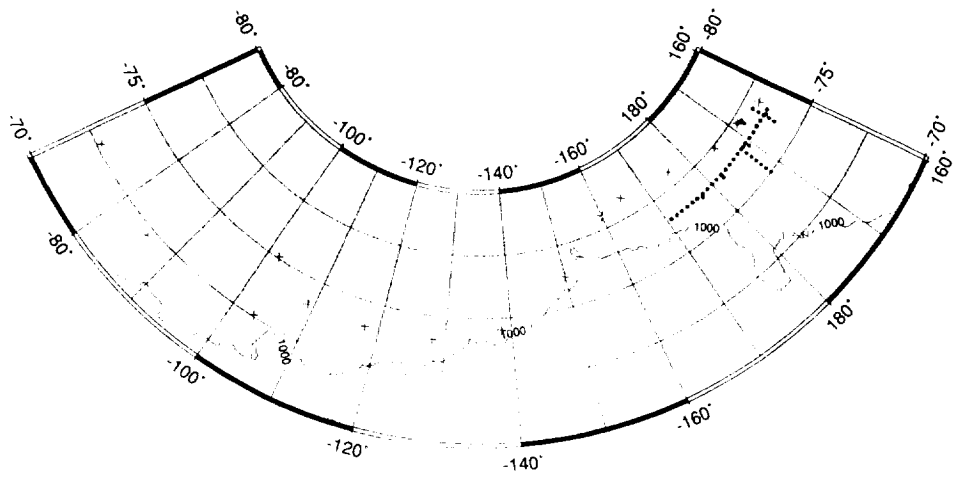

Figure 1. The locations of CTD stations occupied on N.B. Palmer cruise 9508 (dots), and selected stations from N.B. Palmer 9402 and Polar Sea 94 (crosses), near the southern limit of the Pacific Ocean. The edge of the Antarctic ice sheet (shaded) and the 1000 m bathymetric contour roughly define the limits of the open continental shelf from 70-80°S and 70°W-160°E.

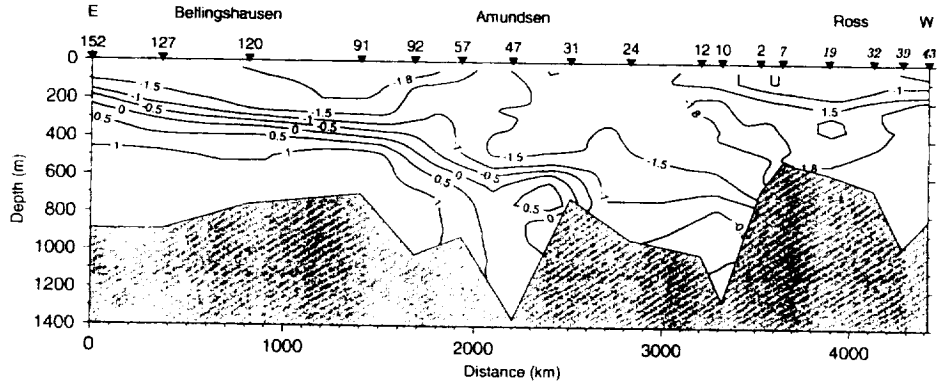

Figure 2. Temperature field near the Antarctic coastline in Feb/Mar 1994, as defined by CTD stations at the crosses in figure 1. [The easternmost station (152) was in Marguerite Bay (~68.5S, 68.5W), off the upper right of figure 1.] Temperatures are in degrees celsius; distances are along great circles between CTD casts.

Made in United States of America
Reprinted from JOURNAL OF CLIMATE
Vol. 10, No. 4, April 1997

Climate Variability in the Amundsen and Bellingshausen Seas*

STANLEY S. JACOBS

Lamont-Doherty Earth Observatory, Palisades, New York

JOSEFINO C. COMISO

NASA/Goddard Space Flight Center, Greenbelt, Maryland

(Manuscript received 17 January 1996, in final form 18 July 1996)

ABSTRACT

Satellite data reveal a 20% decline in sea ice extent in the Amundsen and Bellingshausen Seas in the two decades following 1973. This change is negatively correlated with surface air temperatures on the west side of the Antarctic Peninsula, which have increased ~0.5°C decade $^{-1}$ since the mid-1940s. The recession was strongest during summer, when monthly average minima in 1991–92 removed much of the incipient multiyear ice over the continental shelf. This would have lowered the regional-mean ice thickness, impacting snow ice formation, brine production, and vertical heat flux. The northern ice edge contracted by ~1° of latitude in all seasons from 1973–79 to 1987–93, returning toward mean conditions in 1993–95. The decline included multiyear cycles of several years in length, superimposed on high interannual variability. A review of atmospheric forcing shows winds consistent with mean and extreme ice extents, and suggests links to larger-scale circulation changes in the South Pacific. Historical ocean measurements are sparse in this sector, but mixed-layer depths and upper pycnoclines beneath the sea ice resemble those in the Weddell Sea. Weaker surface currents or changes in the upwelling of Circumpolar Deep Water on the continental shelf could have contributed to the anomaly persistence.

1. Introduction

On 30 January 1774, in what we now call the Amundsen Sea (Fig. 1), heavy sea ice near 71°S, 107°W forced Captain James Cook to abandon his attempt to reach the fabled southern continent. In 1820, Admiral Thaddeus von Bellingshausen was able to reach far enough south to discover Peter I Island and sight what is now Alexander Island. The first expedition to the south and west of those islands, in 1898–99 on the *Belgica*, was beset for more than a year in sea ice (Cook 1900). Sealers had earlier wintered over on the Antarctic Peninsula (Campbell 1992), but the *Belgica* crew, sustained in its ordeal by the fledgling polar explorers Roald Amundsen and Fred Cook, were probably the first to winter south of the Antarctic Circle. Since that time, the sea ice of the southeastern Pacific has enjoyed a reputation of being of "much greater age and thickness than usual, [making] the continental coasts between Alexander Island and the Ross Sea the most inaccessible" (Heap 1964).

Routine satellite monitoring of sea ice in the polar regions began in 1973. In 1993 we reported that a major decrease in sea ice extent had occurred in the Bellingshausen Sea from mid-1988 through early 1991. That retreat was strongly correlated with surface air temperatures on the west coast of the Antarctic Peninsula (AP), which reached a historic high in 1989 (Morrison 1990). The sea ice decline coincided with more northerly surface winds and greater cyclonic activity, and was particularly evident during the austral summer, extending during 1992 into the adjacent Amundsen Sea. The timing of the record Bellingshausen Sea ice recession corresponded with the low-ice phase of a double wave that propagates eastward around Antarctica every 7–10 yr, with regional ice edge expansion and contraction every 3–5 yr (Murphy et al. 1995; White and Peterson 1996).

In this paper we describe a longer-term sea ice recession over the larger Amundsen and Bellingshausen Seas (Fig. 1). We note that errors in quantification of the ice cover due to gridding, moisture effects and precipitation are small compared with the interannual variability. A discussion of the spatial and temporal extent of the regional temperature anomaly is followed by an evaluation of probable atmospheric and

* Lamont-Doherty Earth Observatory Contribution Number 5597.

Corresponding author address: Stanley Jacobs, Lamont-Doherty Earth Observatory, P.O. Box 1000, Palisades, NY 10964.
E-mail: sjacobs@lamont.columbia.edu

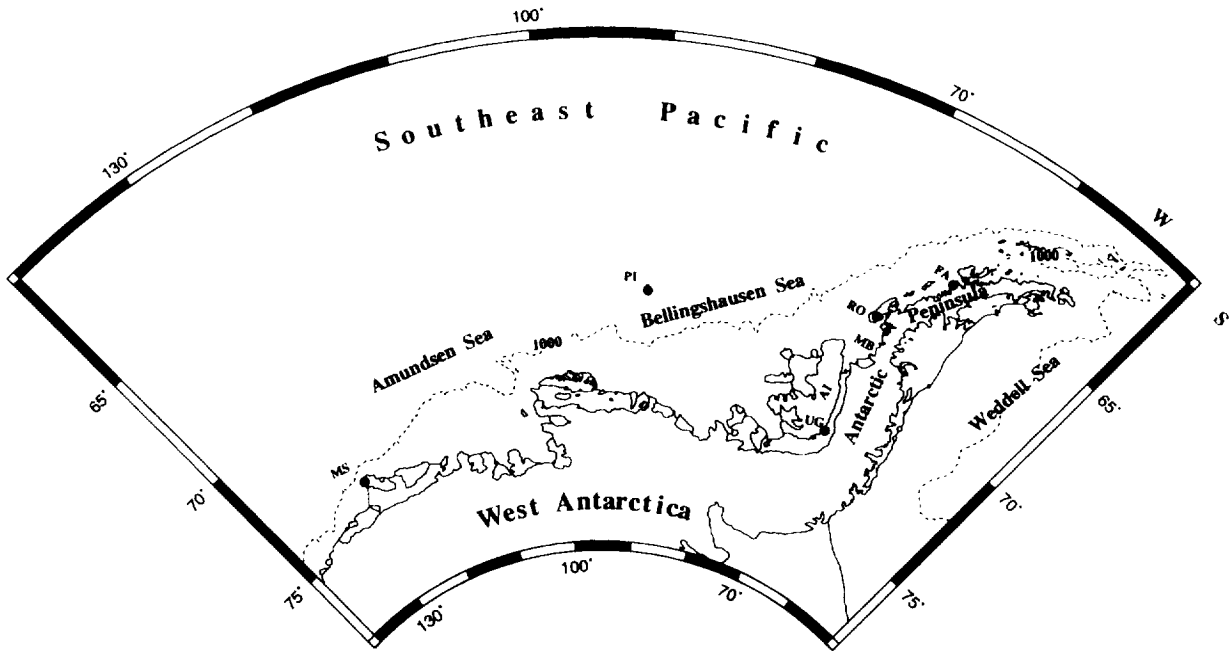

FIG. 1. The Amundsen and Bellingshausen Seas (100°–130°W and 60°–100°W) in the southeastern Pacific Ocean. South of 65°S, the Bellingshausen sector is restricted to the region between 100°W and the Antarctic Peninsula, as the more conventional 60°W boundary now includes a small portion of the Weddell Sea. Here, MS is Mount Siple, UG is Uranus Glacier, AI is Alexander Island, PI is Peter I Island, MB is Marguerite Bay, RO is Rothera Station, and FA is Faraday Station. The dashed line shows the 1000-m bathymetric contour.

oceanic forcing of and response to sea ice anomalies in this region. In reviewing the regional literature, we consider implications of the observations for model projections of future sea ice cover on the Southern Ocean.

2. The Amundsen and Bellingshausen (A and B) sea ice record

a. Data

Sea ice extent and concentration in the A and B near the annual extremes are shown in Fig. 2. The February 1985 and September 1982 panels represent typical summer and winter values during the 1973–94 period. The satellite passive microwave data we used were obtained from the *Nimbus-5* Electrically Scanning Microwave Radiometer (ESMR; 1973–76), the *Nimbus-7* Scanning Multichannel Microwave Radiometer (SMMR; 1978–87), and the Special Sensor Microwave Imagers (SSMI; 1987–94) of the Defense Meteorological Satellite Program. To fill gaps in these records during the 1970s, we used information derived from National Ice Center (NIC) charts, compiled from visible, thermal infrared, and passive microwave observations (NOCDA 1985). Weatherly et al. (1991) found no systematic difference between NIC and ESMR ice extents, but noted a slight negative bias relative to the SMMR records of Gloersen et al. (1992). During 6 full yr of overlap (1974, 1976, and 1979–82), our calculated ESMR and SMMR ice extents averaged 7% higher than the NOCDA data.

b. The sea ice extent anomaly

The A and B sea ice displays a low seasonal range relative to other Southern Ocean sectors, with a late summer ice field exceeded only by that in the Weddell Sea (Zwally et al. 1983b; Enomoto and Ohmura 1990). Gloersen et al. (1992) noted that these ice features might be caused by below-freezing temperatures for most of the year and by diversion of the Circumpolar Current (ACC) by the AP. However, the former condition applies to all of the circumpolar coastal region, and the ACC widens southward upstream of the A and B (Gordon and Molinelli 1982; Orsi et al. 1995). The west side of the AP is about 6°C warmer than the east side (Reynolds 1981), as northward barrier winds prevail in the Weddell Sea and the westerlies have a southward component in the Bellingshausen Sea (Schwerdtfeger 1984; Jacobs and Comiso 1993). These factors limit northward ice advance west of the AP, while southward retreat in the summer has, until recently, not penetrated widely onto the continental shelf.

At the summer minimum, monthly average ice extents from passive microwave observations in the A and B have ranged from a high of 1.03 Mkm^2 in 1983 to a low of 0.40 Mkm^2 in 1992, with no minima since 1987 above the 22-yr means of 0.76 and 0.82 Mkm^2. In the separate Bellingshausen and Amundsen Seas, minima of 0.06 and 0.08 Mkm^2 in February of 1991 and 1992 were 80% below average, near the threshhold achievable with sensor resolution and continental mask accuracy. Using the National Aeronautics and Space Administra-

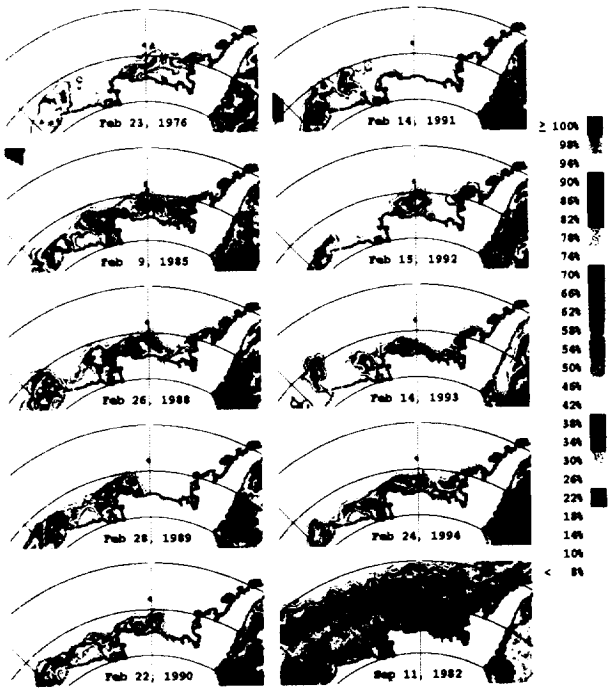

FIG. 2. Sea ice cover in the Amundsen and Bellingshausen Seas, 130°W to the Antarctic Peninsula, with the colors depicting ice concentration. Each image represents a 1–3-day average from satellite passive microwave brightness temperatures, using the algorithm of Comiso (1995). The February panels depict conditions near the summer minimum ice extent; the September panel shows ice cover near a winter maximum. Data were obtained from the *Nimbus*-5 ESMR, 1973–76; the *Nimbus*-7 SMMR, 1978–87, and the SSMI, 1987–94 of the Defense Meteorological Satellite Program.

tion (NASA) team algorithm, Parkinson (1995) indicated that "summertime ice extents were comparable" in 1989–91 and in 1974–76, but we find the February–March average in 1989–91 to be only half that in 1974–76 in the Bellingshausen Sea (east of 100°W) and only three-quarters that of the earlier period in the A and B. Prior to 1987, the summer minimum was most often in March; since that time it has consistently occurred in February. During the recent minima, much of the presumably thicker, multiyear ice over the continental shelf was removed, so that late summer residual ice extent was lower in the A and B than in the Ross Sea.

First observed during the summer months, the recent A and B ice retreat has extended through all seasons. Dividing the 1973–93 interval into septennial periods (Fig. 3), it is apparent that the open water season north of the ice edge increased by more than a month at all latitudes. Most of the winter change occurred between 1973–79 and 1980–86, and most of the summer latitude increase occurred between 1980–86 and 1987–93. The passive microwave data show that all but one of the record-low ice extent months occurred between July 1988 and August 1992. The lowest winter maximum, in 1988, was less than twice the highest summer minimum 10 yr earlier. A record-low annual mean of 1.33 Mkm^2 occurred in 1992, versus a two-decade average of 1.65 Mkm^2 and a 1986 maximum of 1.91 Mkm^2.

c. *Spatial and temporal variability*

Heap (1964) indicated that mean sea ice conditions from 7° to 92°W were "less significant than the frequently enormous departures from the average," and Gloersen et al. (1992) noted a large interannual variability in A and B monthly mean ice extents. On the other hand, Fig. 3 in Parkinson (1992) and Fig. 1 in Simmonds and Jacka (1995) suggest that variability in this region is below the Southern Ocean average, and generally lower than in the adjacent Weddell and Ross Seas. More recently, Parkinson (1995) observed that "the time series for the Bellingshausen Sea shows marked multiyear fluctuations, with increased wintertime ice coverage in the 1988–91 period [when] the summertime coverage was unusually low." The longer record over the larger A and B region (Fig. 4) shows multiyear cycles of large and small annual range (1.14 to 2.15 Mkm^2). The winter peaks suggest an interannual periodicity of 3–5 yr, which is also reflected in the summer minima, as noted earlier for shorter portions of the

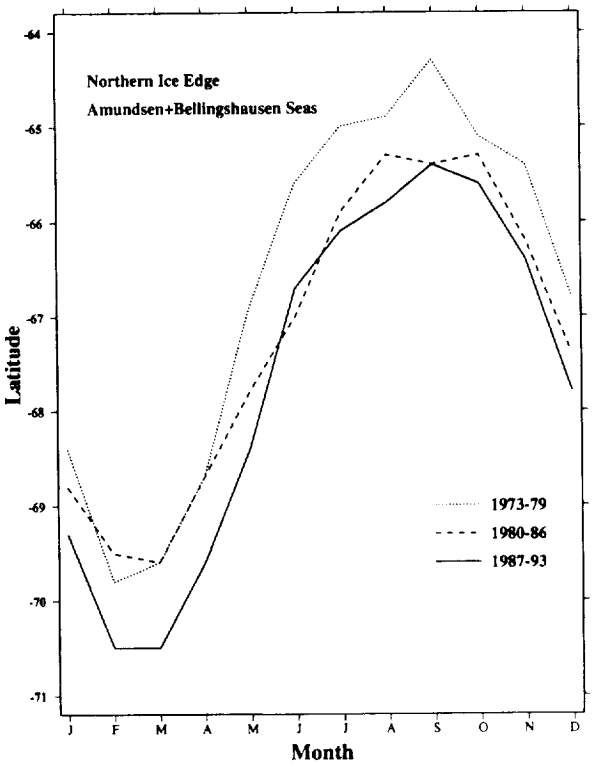

FIG. 3. Latitude of the northern ice edge in the Amundsen and Bellingshausen Seas (70°–130°W), averaged over septennial periods. From a midmonth compilation of National Ice Center charts at 10° longitudes provided by H. Jacka, extended for 1993 from weekly northern ice limit charts (NPOC 1993).

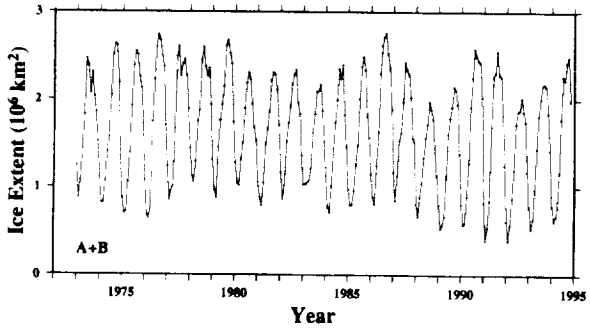

FIG. 4. Monthly average sea ice extent in the Amundsen and Bellingshausen Seas from January 1973 to November 1994. For ice concentrations >15% where passive microwave data were available and >10% when NOCDA (1985) data were used (41% of months prior to November 1978).

sea ice record (Zwally et al. 1983b). To evaluate longer-term variability, 5-yr moving means of seasonally averaged ice extent are shown in Fig. 5. The smoothed data reveal generally negative trends during all seasons, superimposed on shorter cycles that roughly coincide with the circumpolar wave (White and Peterson 1996). Linear regressions over the full record have slopes ranging from -0.14 Mkm^2 decade^{-1} in winter (July–September) to -0.20 Mkm^2 decade^{-1} in summer [January–March (JFM)], significant at the 90% to 99% levels, respectively. Over the shorter SMMR/SSMI period (1979–94), the trends were significantly negative only during autumn (April–June, >90%) and summer (JFM, >99%).

d. Potential errors due to gridding, instrumentation, algorithm, and surface wetness

Constructing a long time series of sea ice cover requires a combination of data from different sensors and satellites that can provide dissimilar information. To improve consistency, we have regridded the SMMR data to the format now used for SSMI. Land masking has been updated (Martino et al. 1995), and some additional land–ocean boundaries have been masked, based upon Advanced Very High Resolution Radiometer (AVHRR) and 85-GHz passive microwave observations. Residual errors in ice edge and concentration may remain due to the different sensor frequencies, antenna patterns, side lobes, and resolution. For example, ice concentration derived from ESMR data relied upon a 19.35-GHz channel at zero incidence angle, whereas SMMR (SSMI) used 18- (19.35) GHz and 37-GHz channels at vertical polarization and 50° (53°) incidence angles. A comparison of SMMR and SSMI ice extents during the July–August 1987 overlap period shows a discrepancy of less than 1%. The algorithm we used (Comiso 1995) gave ice concentrations that were typically 5% to 15% higher than the NASA team algorithm for most of 1992 in the A and B (Figs. 7 and 8 in Comiso et al. 1996).

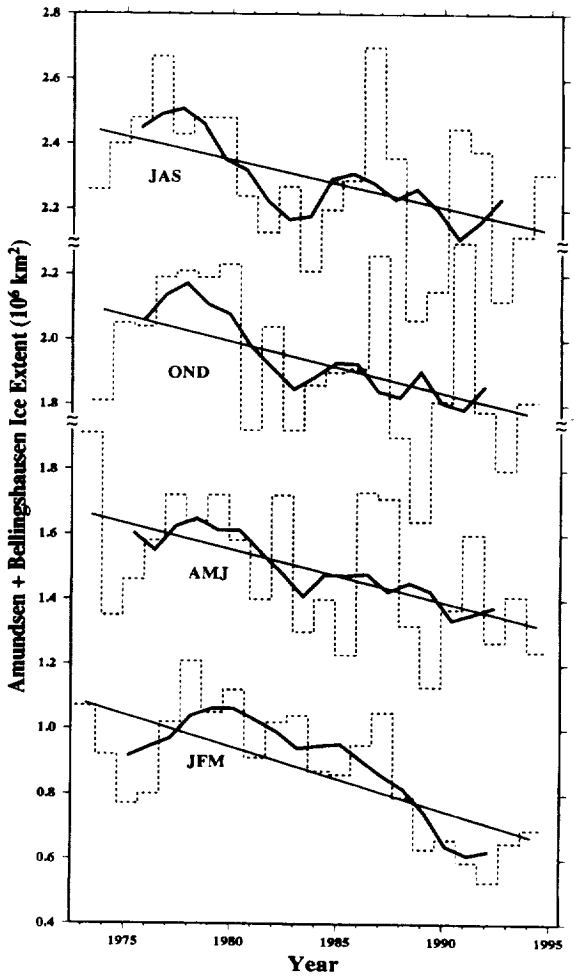

FIG. 5. Five-year moving means (heavy solid lines) and least square regressions (light solid lines) of seasonal average (dashed lines) sea ice extent in the Amundsen and Bellingshausen Seas. Ice seasons (JFM is summer) lag the atmospheric seasons by 1 month, as in Zwally et al. (1983b).

ESMR winter brightness temperatures of apparent multiyear ice are ~20°C colder in the A and B than in much of the rest of the Southern Ocean (Zwally et al. 1983b). While an apparent shift of ~20% in ice concentration could result from this colder signature on the one-channel ESMR sensor, the use of data from at least two channels of SMMR or SSMI substantially reduces any error due to the multiyear ice signature (Comiso et al. 1992). During early spring, when the surface is slightly wet and highly emissive, the multiyear ice signature would be masked, making even an ESMR retrieval fairly accurate. During midspring and summer, other factors such as flooding, melted snow, or a slushy surface may cause underestimates in ice concentration. However, snow wet by flooding and wicking of the brine (Jeffries et al. 1994a; Aldworth 1995) would tend to be masked by the formation of crusts and ice lenses reported by these authors (and by Cook 1900). Warm,

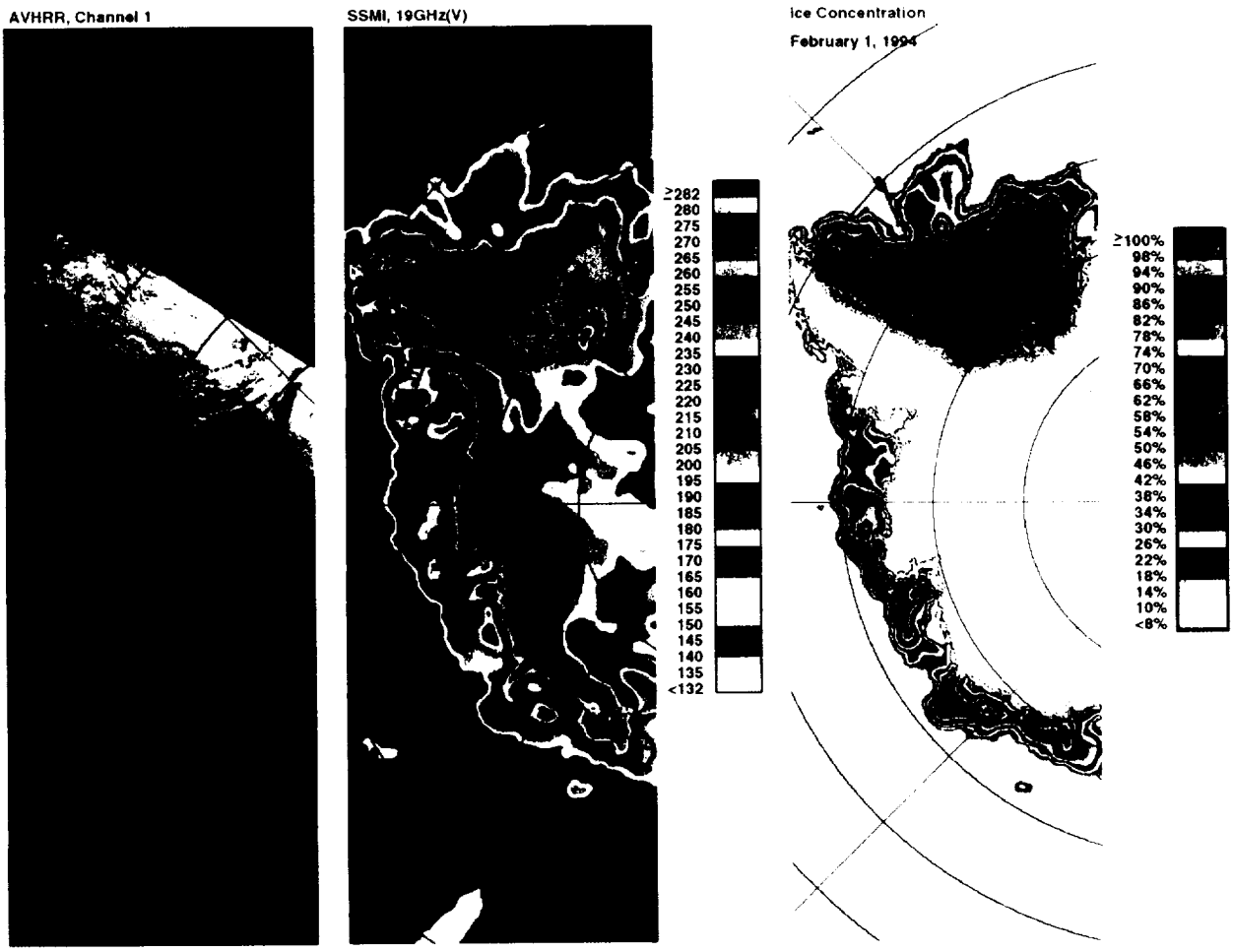

FIG. 6. Composite images of the western Antarctic region encompassing the Amundsen and Bellingshausen Seas on/or about 1 February 1994. From left to right, the panels show: AVHRR channel 1 (0.72 μm) data, SSMI passive microwave brightness temperatures (K) at 19.35 GHz with vertical polarization, and percent ice concentration derived from both 19.35- and 37-GHz data. The meridional lines are spaced at 45° of longitude around 90°W, and the zonal lines are at 5° of latitude, with most A and B ice between 70 and 75°S.

moist, northerly winds were frequently recorded on the beset *Belgica*: "A few days ago temperature rose to +0.5°C and has remained near −1°C for several days . . . everything is wet" (10 May log entry in Cook 1900). Air and snow surface temperatures above freezing were also encountered in the central A and B during August and September 1993 (Jeffries et al. 1994a). Time series and in situ ice observations are unavailable, but little surface wetness and no melt ponds were evident during a late summer cruise through the A and B (Jacobs et al. 1994). This suggests that wetness effects may be intermittent and not a significant source of error in monthly averaged data.

Inaccuracies in ice extent determination (the sum of areas with ice concentration >15%) should be minimal, due to the strong concentration gradient near the ice edge. Although high water vapor content in the atmosphere is typical near the ice edge and can affect estimates of ice extent, the use of a combination of 19-, 22-, and 37-GHz data minimizes this effect (Comiso 1995). From a comparison of microwave and AVHRR imagery at a time of particularly low ice cover (Fig. 6), the ice edge is better and more consistently defined with the SSMI than with the AVHRR data. The latter do not appear to give a larger ice extent, but more quantitative analyses of the AVHRR data can be compromised by the persistent cloud cover (Stammerjohn and Smith 1996). The fact that the observed A and B ice retreat was similar during all seasons (Fig. 2) is further evidence that surface effects do not cause large, fictitious reductions in ice extent.

e. Precipitation and basal melting

Sea ice fields on both sides of the AP are known to experience freeboard submergence and flooding at the ice–snow interface (Heap 1964; Lange et al. 1990; Eicken et al. 1994; Jeffries et al. 1994b). Moisture trans-

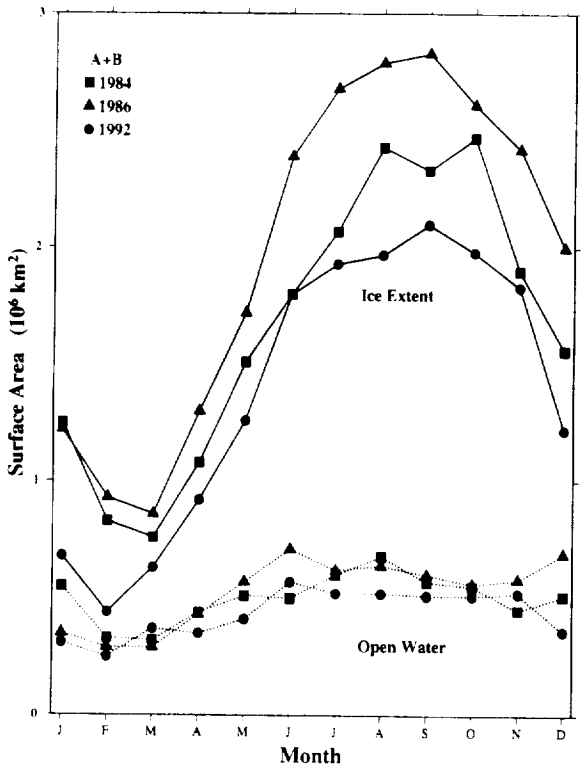

FIG. 7. Annual cycles of "open water" area (dotted lines) and ice extent >10% (solid lines) in the A and B during years with average (1984), high (1986), and low (1992) ice extents. Open water will include thin ice, which can have a similar microwave emissivity.

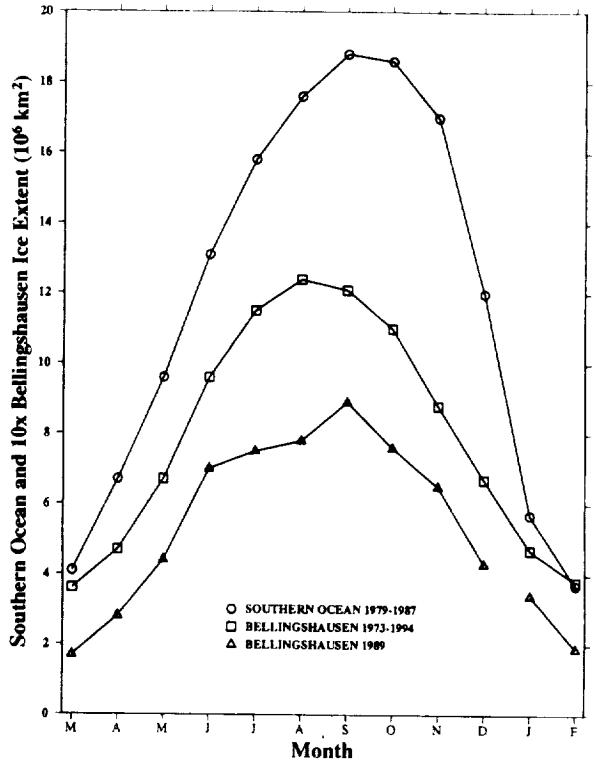

FIG. 8. The asymmetric annual cycle of sea ice extent in the Southern Ocean (upper curve, from Gloersen et al. 1992) versus the symmetric mean cycle and the year with minimum ice extent in the Bellingshausen Sea (middle and lower curves). For this comparison the Bellingshausen vertical scales are 10 times the actual values, and the abscissa has been shifted by 2 months to better display the growth and retreat periods.

port and accumulation on the continent is high in this region (Giovinetto and Bentley 1985; Bromwich et al. 1995) and may lead to thicker snow on the sea ice. There is very limited information on temporal variability of the snow cover, but precipitation events rose by 10% on the west side of the AP as surface pressure declined from 1956 to 1993 (Turner and Colwell 1995). High and variable precipitation, in combination with high heat flux from the ocean, could induce or reinforce multiyear periodic variations in ice extent (Ledley 1985). Late refreezing followed by a thinner, less insulating snow cover would facilitate the growth of thicker and colder ice, whereas ice beneath thicker snow will be warmer and more susceptible to decay. Eicken et al. (1995) modeled a decrease in ice thickness and no change in ice extent with increasing precipitation, but hypothesized that a thick snow cover could also shield the ice from summer melting. In winter, higher oceanic heat flux to the base of Southern Ocean sea ice would melt ice, lower the freeboard, and enhance flooding.

f. Open water and annual cycles

The SE Pacific sea ice field has a higher percentage of open water than the adjacent sectors, with annual means ranging from 26% to 33% of ice extent since 1978, versus 19% to 22% in the Weddell Sea. Greater ice divergence in the A and B could result from higher synoptic variability of sea level pressure (Bromwich et al. 1995; White and Peterson 1996), or from stronger upwelling. Divergence is limited in the Weddell Sea by the AP, which blocks westward ice drift, and by the colder temperatures, which will cause more rapid freezing in newly opened leads. The area of open water (including thin ice) within the A and B pack increases gradually from a minimum in late summer to a maximum in late autumn–early winter, ranging from 19% to 28% during the winter months (Fig. 7). Open water seasonality was low and did not change markedly during the recent ice extent anomaly. Open water averaged 0.49 Mkm^2 from 1979 to 1993, much larger than the 0.29 Mkm^2 exposed by the recent ice edge retreat (Fig. 2). Persistent open water and thin ice in this region will tend to mask changes associated with the retreat of the northen ice edge.

An unusual characteristic of the Bellingshausen Sea is its symmetric annual cycle of ice growth and retreat. Roughly equal February–March minima are followed by 5 months of advance to an August–September maxima, then 5 months of retreat (Fig. 8). The more typical

Southern Ocean cycle is one of slow growth and rapid retreat (Rayner and Howarth 1979). Stammerjohn and Smith (1996) identified an even shorter ice advance than retreat period in a smaller Bellingshausen sector, plausibly inferring a regional surplus of ice import and melting. However, the northern Amundsen Sea imports ice from the Ross Gyre and displays an asymmetric cycle. For most of the Southern Ocean, rapid spring retreat exceeds the available air–sea heat flux, a deficit that must be made up from the underlying deep water (Gordon 1981). A more gradual retreat in the Bellingshausen Sea could therefore imply less deep water influence, consistent with a relatively low-salinity surface layer (section 5).

3. Air temperatures and ice extents

a. The observed temperature anomaly

Since the report of a warm period on the northwestern side of the AP in the early 1970s (Schwerdtfeger 1976), several authors have cited the lengthening period of positive temperature anomalies in this region (e.g., Weatherly et al. 1991; Chapman and Walsh 1993). Sansom (1989) found no statistically significant trend in the 1958–88 air temperatures at Faraday Station, due to the large interannual variability, particularly during winter. However, King (1994) indicated that the more recent record-high temperatures have increased the statistical significance of the trends and that warmer winters have caused a decrease in the annual temperature range [see also Stark (1994)]. A composite record from the southwestern AP region confirms a secular climate change since the 1960s (Harangozo et al. 1995, unpublished manuscript). A longer melt season on the surface of eastern AP ice shelves (Ridley 1993) shows that warming was not limited to the Bellingshausen side of the peninsula. Raper et al. (1984) and Jones (1990) cited the strength and persistence of the AP warming relative to other Antarctic regions. Figure C5 of Folland et al. (1992) suggests that it also extended northwest from the AP to the region south of New Zealand, one of the largest regional annual surface temperature anomalies (>+0.5°C) in the global ocean from 1981–90 (vs 1951–80).

The Faraday–Rothera (western AP) air temperature record begins in the mid-1940s and shows an increase of ~0.05°C yr^{-1} from 1944 to 1991, averaging 1.1°C colder than at Orcadas Station northwest of the Weddell Sea (Fig. 9). The coherence of these time series is not high (r^2 = 0.56), but is consistent with the observation by Heap (1964) that similar climatic conditions prevail in the Bellingshausen and northwestern Weddell Seas. Linear regressions of the records show a slower rate of increase at Orcadas, +0.026°C yr^{-1} during the overlap period (1945–91) and +0.018°C yr^{-1} over the full term (1904–91), but both are significant at the 99% level. Although regional warming was apparent prior to the

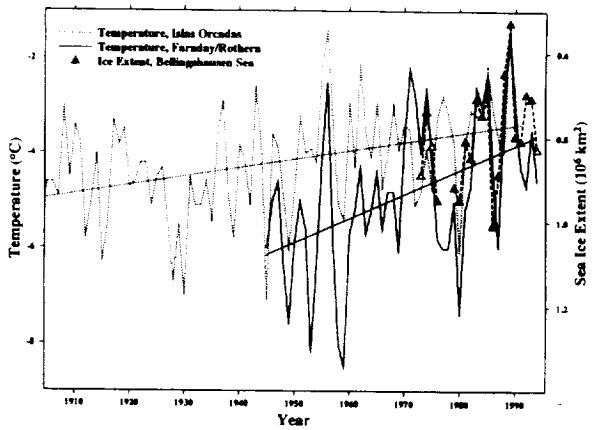

FIG. 9. Annual average air temperatures (1904–91) at Orcadas Station, 60°44′S, 44°44′W on the South Orkney Islands in the northwest Weddell Sea and from 1945 to 1994 at Faraday-Rothera Stations (Fig. 1), with least square regressions. The Faraday–Rothera record is a composite average, or a Faraday mean minus 0.6°C for years with incomplete Rothera records. Data are from Jones and Limbert (1987), H. Jacka, and the British Antarctic Survey. The triangles show annual-mean ice extent in the Bellingshausen Sea (note inverted scale), open in years where data gaps were filled by estimates from adjacent months and the mean annual cycle.

1940s (Jones et al. 1993) and western AP temperatures have occasionally exceeded those at Orcadas, the lower Orcadas maxima from 1904 to 1944 suggest that the AP did not experience an episode earlier this century warmer than that in 1988–92. An ice core from the crest of the AP indicates that the last two decades have been the warmest in the last five centuries (Thompson et al. 1994).

b. Air temperature versus sea ice extent

A 1956 peak in the Faraday–Rothera temperature record (Fig. 7) coincides with a time of early ice breakout in Marguerite Bay (Heap 1964). Schwerdtfeger (1976) correlated the AP warmth in the early 1970s with more open water there, consistent with low summer ice extents in the southeastern Pacific during the ESMR period (Parkinson 1992). The Bellingshausen ice extent has been negatively correlated with western AP surface air temperatures (Weatherly et al. 1991; Chapman and Walsh 1993; Jacobs and Comiso 1993; King 1994), as is apparent from Fig. 7. From 1973 to 1993, western AP annual-mean air temperatures ranged over 6°C, while the upstream sea ice extent varied by 0.48 Mkm^2 (Fig. 10). Low annual-mean temperatures of −6.0°C in 1977 and 1978 fit the relatively high ice extents for those years in the NOCDA (1985) data. From the Fig. 10 regression (r^2 = 0.77), a 1°C rise in surface air temperature corresponds to ~0.11 Mkm^2 less sea ice. The Amundsen Sea coastline lacks long instrumental temperature records, but Fig. 3 shows that the mean A and B ice edge shifted southward by ~1° latitude in the time between the first and last periods, comparable to a

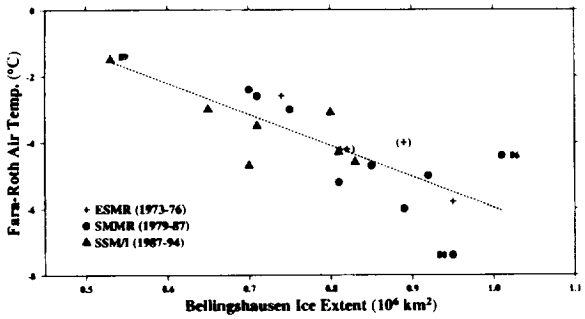

FIG. 10. Annual-mean ice extent in the Bellingshausen Sea (60°–100°W) versus the Faraday–Rothera air temperature mean. Sea ice data gaps in 1973 and 1975 (+) were filled as noted in the Fig. 9 caption. Years that diverge most from the linear regression, 1980 and 1986, also appear as extremes in Fig. 12.

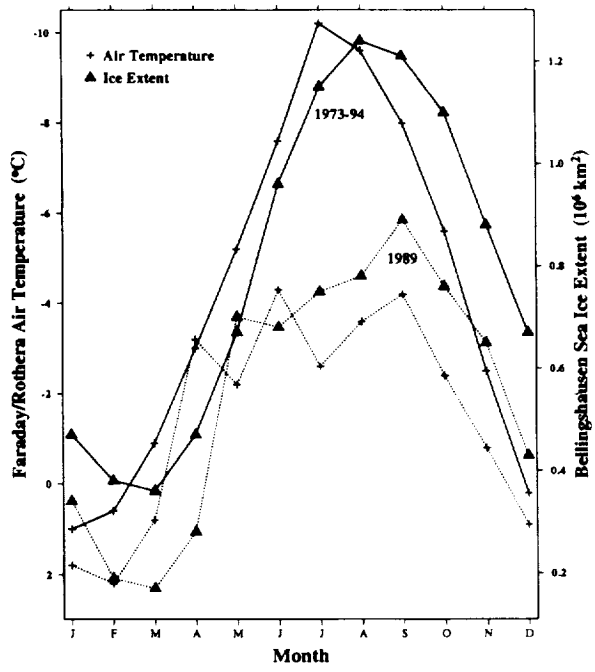

FIG. 11. Annual cycles of monthly average ice extent in the Bellingshausen Sea and surface air temperature (note inverted scale) at Faraday–Rothera (Fig. 9 caption). The solid curves show means for the 1973–94 period, and the dotted curves show the historically warm 1989.

1.5°latitude/°C projection for the circumpolar region (Jacka and Budd 1991).

The mean annual cycle of ice extent in the Bellingshausen Sea lags air temperature by 1–2 months in all seasons (Fig. 11). Ice extent during the record-warm 1989 also lagged temperatures by about a month in summer and fall, but not during late winter and spring. While ice extent typically lags air temperature by several weeks in the Southern Ocean (Cavalieri and Parkinson 1981; Jacobs and Comiso 1989; Chapman and Walsh 1993), Weatherly et al. (1991) also found that ice leads the winter temperatures. Fletcher (1972) noted a correlation between winter iciness of the Southern Ocean and Southern Hemispheric zonal circulation intensity. Ackley and Keliher (1976) reported that ice extent influences synoptic-scale weather patterns, air temperatures, and the regional atmospheric circulation.

4. Atmospheric forcing

From changes in sea level pressure gradients between Antarctic coastal stations, Schwerdtfeger (1976) inferred that warmer air temperatures in the early 1970s were caused by increased northwesterly winds toward the AP. Westerlies in the Bellingshausen Sea typically have a southward component in the 1977–89 Australian Bureau of Meteorology records (Jacobs and Comiso 1993). Here, we estimate wind stress directions over the larger A and B region and divide the record at 68°S, roughly separating the prevailing westerlies and easterlies. Incorporating winds from the European Center for Medium-Range Weather Forecasting extends the wind record, but reveals an offset during the overlap period (Fig. 12). Wind speeds appear to increase through 1989 and then to decrease, but the scarcity of supporting instrumental data means that little significance can be attributed to these fluctuations. Seasonal variability in speed (direction) is strongest in the northern (southern) zone. For most of the year the sea ice edge lies north of 68°S (Fig. 3), where the typical wind stress will aid ice advance due to Ekman drift. The summer edge is south of 68°S, where the more southward wind stress will tend to retain ice along the coastline.

Sea ice advance in the A and B is typically monotonic through August or September, with a midwinter pause or retreat in some years, particularly near the AP (Ackley 1981; Harangozo 1994; Figs. 4 and 9). Summer and winter maxima in cyclone densities east of the Ross Sea, an area of frequent system stagnation and decay, also lie in the confluence of lows that have spiraled southeast from the Tasman Sea region (Jones and Simmonds 1993). These extremes differ in season from those reported by van Loon (1971), but both support the existence of a semiannual wave that could induce a midyear retreat. While storms will alter the sea ice cover by breaking up and rafting floes and by increasing leads and surface water divergence, evidence for decadal changes in storminess is lacking. The marked "southward" ("northward") peak in wind stress direction during 1980 (1986) in the 60°–68°S zone of Fig. 12 is consistent with convergence (divergence) and lower (higher) ice extent than might be expected from the air temperature that year in Fig. 10. However, the longest period of sustained southerly winds in the zone from 68° to 75°S (Fig. 12) extended into the period of record-low early summer ice extent in 1992. Since southerly winds will usually transport colder air and promote freezing, this suggests an oceanic role as the sea ice was advected into warmer waters.

Changes in the Southern Hemispheric atmospheric

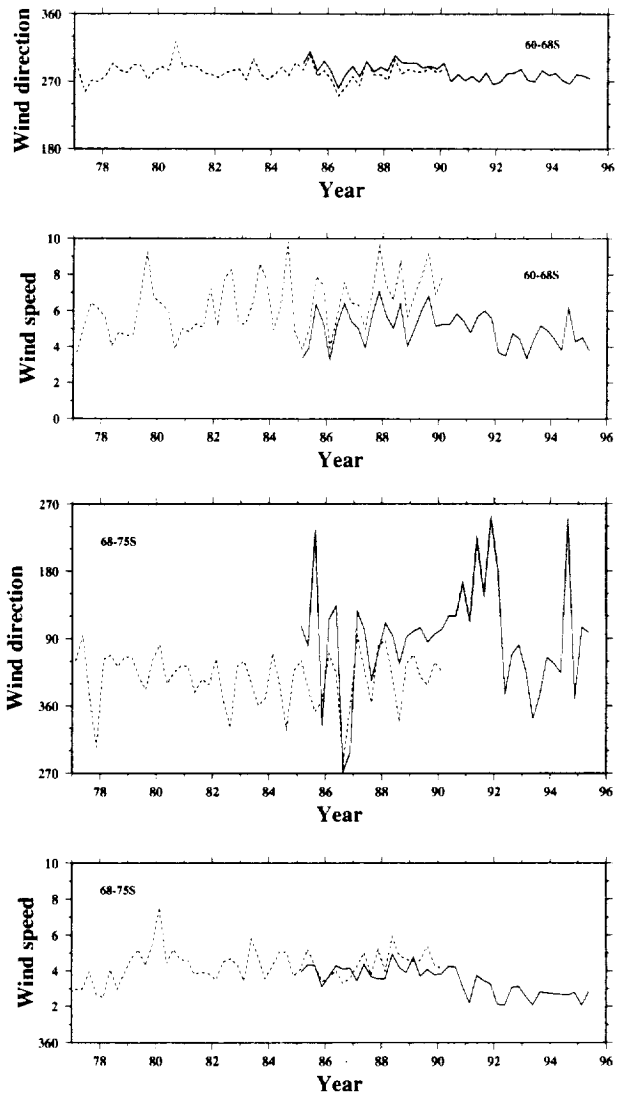

FIG. 12. Seasonal average wind speed and direction in the southeastern Pacific from 60° to 68°S (upper panels) and from 68° to 75°S (lower panels). Dashed lines denote Australian Bureau of Meteorology (ABM) and solid lines European Center for Medium-Range Weather Forecasting (ECMWF) records. Wind direction is the surface stress direction, with the coordinate system rotated 30° clockwise to account for ice drift to the left of the wind in the Southern Hemisphere. The shading indicates where ice will be advected northward. ABM and ECMWF wind speed and direction changes are generally coherent during the 5-yr overlap period, with typically stronger ABM winds. The lower-resolution ABM grid contains only five points in the 68°–75°S region.

circulation over the past two decades were largest in the South Pacific (van Loon et al. 1993). These have involved the semiannual oscillation, circumpolar trough, and polar vortex, and may be related to the concurrent rise of sea surface temperature at low latitudes (Hurrell and van Loon 1994). El Niño–Southern Oscillation (ENSO) cycles occur every several years, and have been characterized by more positive tropical Pacific air temperature anomalies since about 1976 (Folland et al. 1990). ENSO influence extends to high latitudes (Chiu 1983; Smith and Stearns 1993; Gloersen 1995) and could account for some of the low-frequency variability in Figs. 4 and 5. White and Peterson (1996) indicated that the 4–5-yr circumpolar wave in the Southern Ocean surface pressure, wind, temperature, and sea ice extent (see also Zwally et al. 1983a; Murphy et al. 1995) is probably associated with El Niño activity in the equatorial Pacific. It is not yet clear how large-scale changes in the atmospheric circulation over the South Pacific might focus a climate anomaly in the A and B – Antarctic Peninsula region.

5. Oceanic response

Air–sea interactions in the Bellingshausen Sea may have led to the warmer temperatures in the western AP region (King 1994). Lying downwind from the prevailing westerlies, the peninsula would have experienced a more maritime climate as the ice edge moved southward (Fig. 3). The A and B sea ice retreat was comparable in area and latitude, but more persistent than the Weddell Polynya, which was well developed for only 3 yr in the mid-1970s (Carsey 1980). Air–sea interactions will be less intense in the warmer A and B, but winter sea–air heat flux is much larger over open water than over sea ice (Gordon 1981). In summer, the lower albedo accompanying a smaller sea ice cover will allow greater radiational heating of the surface layer. It is thus quite likely that the recent increase in the open water area in the A and B was a factor in the AP warming.

An initial sea ice anomaly would tend to be maintained by the greater thermal inertia of the ocean versus that of the atmosphere. Heat storage in the mixed layer has been correlated with longer summer seasons (Jacobs and Comiso 1989). Abnormal summer air temperatures can predispose near-surface waters to more or less ice the next fall or winter (Weatherly et al. 1991) and are a possible source of multiyear anomalies (Gloersen et al. 1992). However, persistence within a limited area implies relatively weak surface currents or continual reinforcement. A mixed-layer temperature anomaly in the central A and B would drift east-northeast toward the Drake Passage (Sievers and Nowlin 1984; Webb et al. 1991). If it moved at more than 10 cm s^{-1}, a perturbation would be advected out of the A and B in less than 6 months; at half that speed, an anomaly could propagate beyond a single annual cycle within the region. Velocities near fronts in the deep Bellingshausen Sea exceed 10 cm s^{-1} against a background of weaker currents (Pollard et al. 1995). From the wind data in Fig. 10, stronger currents could be expected northward in the ACC and a weaker flow with a more southward component toward the Antarctic continent.

Northeast drift of surface water and ice over the deep ocean west of the AP is one limb of a clockwise circulation, with southward flow on the continental shelf

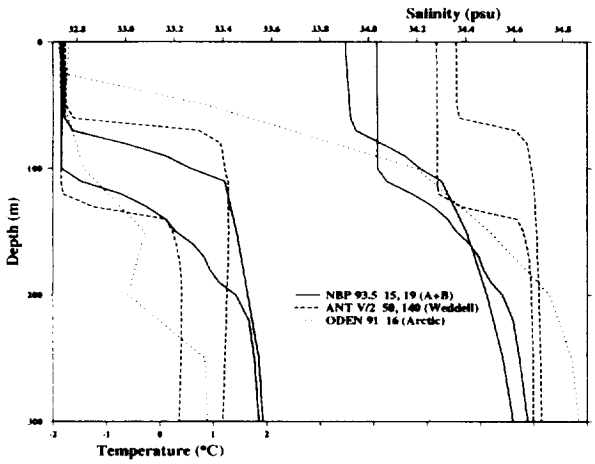

FIG. 13. Profiles of temperature and salinity versus depth beneath the sea ice in the Amundsen and Bellingshausen Seas, the Weddell Sea, and the Arctic Ocean. The A and B examples are from a September–October 1993 cruise between 88° and 110°W, north of the continental shelf (Jeffries et al. 1994a), where mixed-layer depths ranged from ~50 to 130 m. The 1986 Weddell examples are characterized by Gordon and Huber (1990) as representative of the warm and cold regimes in that sector. The 1991 Arctic station was near 88°N, 60°E (Bauch 1995).

(Hofmann et al. 1996). Scattered islands, bays, and grounded icebergs along the irregular A and B coastline would retard and recirculate shelf currents, contributing to persistence of the anomaly. The *Belgica* track revealed slow and erratic ice motion in the southern Bellingshausen Sea, with a stronger westward drift near the shelf break. Extensive open water areas on the Amundsen shelf in the summers of 1976 and 1992 lagged similar features on the Bellingshausen shelf by about 1 yr. If related to the transport of a heat storage anomaly, this would be equivalent to a westward drift of ~4 cm s^{-1}. That direction conforms with the prevailing winds and with observed and modeled ice and ship drifts (Ackley 1981; Pollard and Thompson 1994; Read et al. 1995). Modeled eastward surface currents along this coastline (Webb et al. 1991) may have resulted from the use of a wind stress field that did not resolve the coastal easterlies.

It is not apparent that the Circumpolar Deep Water (CDW) played a strong role in the recent A and B sea ice retreat. Hofmann et al. (1996) note that heat flux from CDW west of the AP may moderate the amount of ice cover and regional climate. For sea ice extent to be reduced on a decadal timescale by that flux, more heat must reach the surface water, presumably through a more active vertical circulation. The relatively fresh surface water, lack of bottom water formation, and historically low seasonal range in ice extent have made the A and B region seem more like the Arctic than the rest of the dynamic Southern Ocean. However, its mixed-layer depths and salinities are similar to those in the Weddell Sea (Fig. 13), and its upper-pycnocline dT/dS ratios are intermediate between those of the Weddell "warm and cold" regimes. The A and B sea ice growth will thus be constrained by the high ratio of heat to salt across this gradient (Martinson 1990). Its entire pycnocline is stronger than in the Weddell Sea (greater salinity range from 50 to 300 m), limiting deep convection forced by sea ice formation. CDW entrainment during brine-driven mixed-layer deepening also implies ice growth prior to the observed decline. Greater upwelling of CDW could result from increased wind-driven divergence of the ice and surface water, as inferred from deeper lows during 1989 in the Bellingshausen Sea (Jacobs and Comiso 1993) and suggested by slight changes in modeled wind strength (Fig. 10).

Did deep water temperatures in the A and B change during the last two decades? At reoccupied stations along 67°S in the Bellingshausen Sea, the CDW temperature maximum was often 0.05°–0.15°C warmer in 1992 than a few decades earlier (Swift 1993). However, greater warm anomalies in the deep waters can be found in the archives, suggesting a variability related to mesoscale features or to movements of the southern ACC boundary and deep frontal zone near 67°S (Orsi et al. 1995). Read et al. (1995) reported that transport and frontal structure from 85° to 88°W in the Bellingshausen Sea did not change substantially between 1964 and 1992. On the other hand, a recent southward shift of the ACC position in the southeastern Pacific is supported by temperature differences between the World Ocean Circulation Experiment meridional sections and archived data (Swift 1995), and consistent with a retreat of the northern ice edge. The evidence is thus mixed, and the limited historical data make it difficult to separate any possible trend from natural variability in the A and B deep water.

There are indications that a recent change may have occurred in the rate of upwelling of CDW onto the continental shelf. Deep water floods the deeper regions of the southeastern Pacific continental shelves and is only slightly cooled and freshened in the process (Jacobs et al. 1996). At depths below 200 m near Alexander Island (Fig. 1), CDW was up to several tenths of a degree warmer in 1994 than in the early 1980s data of Potter et al. (1988). Warmer CDW would enhance melt-driven upwelling near the coastline, but better time series data and models are needed to evaluate the potential impacts of such changes on mixed-layer temperatures and sea ice extent.

6. Discussion

a. Modeling implications

Coupled air–sea general circulation models (GCMs) incorporate feedback mechanisms, such as variable surface albedo, and project decreasing sea ice extents as atmospheric temperature rises. These results agree with the generally negative correlations found between ice extent and surface air temperature (Jacka and Budd

1991; Weatherly et al. 1991). Early model simulations with enhanced greenhouse gases did not include ice dynamics, leads, or salinity effects, compromising quantitative projections of sea ice extent and thickness (Mitchell et al. 1990). Some GCMs now incorporate sea ice dynamics (e.g., Pollard and Thompson 1994), and future models may benefit from the inclusion of variable snow cover and surface mixed layers. Zonally variable warming over the Antarctic sea ice in a model that includes the response to aerosols (Taylor and Penner 1994) is consistent with recent warming near the AP.

A few models emphasize the tendency for warming and freshening to stabilize the ice–ocean system with a deeper pycnocline and weaker ice divergence (Martinson 1990; Manabe et al. 1991). The latter project thicker sea ice on the Southern Ocean in a warmer climate as a cap of lower-salinity surface water caused by higher P – E and continental runoff strengthens the pycnocline and damps the vertical ocean circulation and heat flux. However, with a surface water residence time of ~2 yr (Gordon and Huber 1990), an improbable 5 m yr^{-1} of freshwater would be needed to produce mixed-layer salinities as low as those in the Arctic (Fig. 13)—that is, sufficient to greatly decrease heat flux from the CDW. Manabe et al. (1991) modeled an air temperature increase of ~0.05°C yr^{-1}, similar to that observed in the A and B, and obtained a high runoff by transferring to the ocean any P – E > 20 cm yr^{-1} on Antarctica. They noted that precipitation may be overestimated at high southern latitudes, a typical problem in current GCMs (Chen et al. 1995). A lower ice extent and a reduction of multiyear ice seems incompatible with greater ice thickness, and would imply that the observed warming and any related freshening in the A and B did not markedly increase the regional stability of the upper ocean.

b. Circumpolar ice extent

Satellite observations of sea ice extent now extend over more than two decades, revealing interannual changes and a declining sea ice cover in the A and B. While decadal and longer trends are common in regional records (e.g., Fletcher 1972), this retreat probably exceeded that at any other time this century and diminished the regional-mean sea ice thickness. In the full Southern Ocean, decreases in sea ice extent in one area are typically balanced by increases elsewhere (Ackley 1981; Zwally et al. 1983b; Parkinson 1994). Over the 1979–87 period, Gloersen and Campbell (1991) did not find a significant change in Antarctic sea ice extent, but Johannessen et al. (1995) reported a net decline of 0.13 Mkm^2 from 1978 to 1994. That would correspond to a warming of ~0.14°C over the full sea ice region if the air temperature–ice extent relationship in Fig. 8 were extrapolated to the circumpolar ice edge. In addition, the A and B ice edge recession of ~1° of latitude (Fig. 2), or 0.29 Mkm^2, implies sufficient net growth in other sectors to compensate about half of this regional decline. The retreat depicted in Fig. 4 may be reversed over the next several years, but continued warming in high southern latitudes (Jones 1990; Jacka and Budd 1991) will eventually register as a significant loss of circumpolar sea ice cover.

c. Future work

The significance of the recent southeastern Pacific sea ice retreat has been its duration and association with a lengthy regional warming trend. The forcing is not yet clear, but probably lies external to the region, associated with large-scale changes in the state and circulation of the atmosphere and ocean. The high variability of sea level pressure and increased open water in the southeastern Pacific sector probably enhanced air–sea interactions, heat and moisture fluxes, and divergence of the mixed layer. In situ ocean data are as yet inadequate to define reliable time series, but evidence of A and B surface water alterations might be found downstream in the ACC or in the Antarctic Intermediate Water. Sea ice time series should be lengthened by continued satellite monitoring, and by the use of ice core and tree ring proxies (e.g., Cook et al. 1992; Thompson et al. 1994). Understanding the cause and course of this kind of climate variability would benefit from the identification and monitoring of key indices of the subsurface ocean circulation, application of regional coupled circulation models, and more regular field measurements.

Acknowledgments. We thank R. Allegrino, S. Peng, E. Simpson, Y. Tourre, and the British Antarctic Survey for assistance with source material, calculations, and figures. The ECMWF data were provided by the National Center for Atmospheric Research, Boulder, CO. Several individuals made helpful comments on earlier versions of the manuscript. This work is supported by the NASA Polar Research Program (NAGW 3362).

REFERENCES

Ackley, S. F., 1981: A review of sea-ice weather relationships in the Southern Hemisphere. *Sea Level, Ice and Climatic Change*, Vol. 131, I. Allison, Ed., International Association Scientific Hydrology, 127–159.

——, and T. E. Keliher, 1976: Antarctic sea ice dynamics and its possible climatic effects. *AIDJEX Bull.*, **33,** 53–76.

Aldworth, E., 1995: Snow and ice characteristics of the Bellingshausen Sea, during the spring melt. *Deep-Sea Res.*, **42,** 1021–1046.

Bauch, D., 1995: The distribution of $\delta^{18}O$ in the Arctic Ocean: Implications for the freshwater balance of the halocline and the sources of deep and bottom waters. *Berichte zur Polarforschung*, Vol. 159, 144 pp.

Bromwich, D. H., R. I. Cullather, F. M. Robasky, X. Pan, and M. van Woert, 1995: The moisture budget in high southern latitudes as evaluated from atmospheric numerical analyses. Preprints, *Sixth Symp. on Global Change Studies*, Dallas, TX, Amer. Meteor. Soc., 192–197.

Campbell, D., 1992: *The Crystal Desert.* Houghton-Mifflin, 308 pp.

Carsey, F., 1980: Microwave observation of the Weddell Polynya. *Mon. Wea. Rev.*, **108,** 2032–2044.

Cavalieri, D. J., and C. L. Parkinson, 1981: Large-scale variations in observed Antarctic sea ice extent and associated atmospheric circulation. *Mon. Wea. Rev.*, **109,** 2323–2336.

Chapman, W. L., and J. E. Walsh, 1993: Recent variations of sea ice and air temperature in high latitudes. *Bull. Amer. Meteor. Soc.*, **74,** 33–47.

Chen, B., D. H. Bromwich, K. M. Hines, and X. Pan, 1995: Simulations of the 1979–88 polar climates by global climate models. *Ann. Glaciol.*, **21,** 83–90.

Chiu, L. S., 1983: Variation of Antarctic sea ice: An update. *Mon. Wea. Rev.*, **111,** 578–580.

Comiso, J. C., 1995: SSM/I sea ice concentrations using the bootstrap algorithm. NASA Ref. Publ. 1380, 57 pp. [Available from NASA Center for Aerospace Information, 800 Elkridge Landing Rd., Linthicum Heights, MD 21090-2934.]

——, T. C. Grenfell, M. Lange, A. W. Lohanick, R. K. Moore, and P. Wadhams, 1992: Microwave remote sensing of the Southern Ocean ice cover. *Microwave Remote Sensing of Sea Ice*, F. Carsey, Ed., *Geophys. Monogr.*, No. 68, Amer. Geophys. Union, 243–259.

——, D. J. Cavalieri, C. L. Parkinson, and P. Gloersen, 1996: Passive microwave algorithms for sea ice concentration—Two techniques. *J. Remote Sens. Environ.*, in press.

Cook, E., T. Bird, M. Peterson, M. Barbetti, B. Buckley, R. D'Arrigo, and R. Francey, 1992: Climatic change over the last millennium in Tasmania reconstructed from tree-rings. *The Holocene*, **2,** 205–217.

Cook, F. A., 1900: *Through the First Antarctic Night*. Heinemann, 413 pp.

Eicken, H., M. A. Lange, H.-W. Hubberten, and P. Wadhams, 1994: Characteristics and distribution patterns of snow and meteoric ice in the Weddell Sea and their contribution to the mass balance of sea ice. *Ann. Geophys.*, **12,** 80–93.

——, H. Fischer, and P. Lemke, 1995: Effects of the snow cover on Antarctic sea ice and potential modulation of its response to climate change. *Ann. Glaciol.*, **21,** 369–376.

Enomoto, H., and A. Ohmura, 1990: Influences of atmospheric half-yearly cycle on the sea ice extent in the Antarctic. *J. Geophys. Res.*, **95,** 9497–9511.

Fletcher, J. O., 1972: Ice on the ocean and world climate. *Proc. Symp. Beneficial Modifications of the Marine Environment*, Washington, DC, Nat. Acad. Sci., 4–49.

Folland, C. K., T. R. Karl, and K. Ya. Vinnikov, 1990: Observed climate variations and change. *Climate Change, The IPCC Scientific Assessment*, J. T. Houghton, G. J. Jenkins, and J. J. Ephraums, Eds., Cambridge University Press, 195–238.

——, ——, N. Nichols, B. S. Nyenzi, D. E. Parker, and K. Ya. Vinnikov, 1992: Observed climate variability and change. *Climate Change 1992, The Supplementary Report to the IPCC Scientific Assessment*, J. T. Houghton, B. A. Callander, and S. K. Varney, Eds., Cambridge University Press, 135–170.

Giovinetto, M. B., and C. R. Bentley, 1985: Surface balance in ice drainage systems of Antarctica. *Antarct. J. U.S.*, **20,** 6–13.

Gloersen, P., 1995: Modulation of hemispheric sea-ice cover by ENSO events. *Nature*, **373,** 503–506.

——, and W. J. Campbell, 1991: Recent variations in Arctic and Antarctic sea-ice covers. *Nature*, **352,** 33–36.

——, ——, D. J. Cavalieri, J. C. Comiso, C. L. Parkinson, and H. J. Zwally, 1992: Arctic and Antarctic sea ice, 1978–1987: Satellite passive-microwave observations and analysis. NASA SP-511, 290 pp. [Available from P. Gloersen, Code 971, NASA/GSFC, Greenbelt, MD 20771.]

Gordon, A. L., 1981: Seasonality of Southern Ocean sea ice. *J. Geophys. Res.*, **86,** 4193–4197.

——, and E. J. Molinelli, 1982: Thermohaline and chemical distributions and the atlas data set. *Southern Ocean Atlas*, Columbia University Press, 10 pp. and 233 plates.

——, and B. A. Huber, 1990: Southern Ocean winter mixed layer. *J. Geophys. Res.*, **95,** 11 655–11 672.

Harangozo, S. A., 1994: Interannual atmospheric circulation–sea ice extent relationships in the Southern Ocean: An analysis for the west Antarctic Peninsula region. Preprints, *Sixth Conf. on Climate Variations*, Nashville, TN, Amer. Meteor. Soc., 364–372.

Heap, J. A., 1964: Pack ice. *Antarctic Research*, R. Priestley, R. Adie, and G. Robin, Eds., Butterworths, 308–317.

Hofmann, E. E., J. M. Klinck, C. M. Lascara, and D. A. Smith, 1996: Water mass distribution and circulation west of the Antarctic Peninsula and in Bransfield Strait. *Foundations for Ecological Research West of the Antarctic Peninsula*, R. Ross, E. Hoffman, and L. Quetin, Eds., *Antarctic Research Series*, No. 70, Amer. Geophys. Union, 61–81.

Hurrell, J. W., and H. van Loon, 1994: A modulation of the atmospheric annual cycle in the Southern Hemisphere. *Tellus*, **46,** 325–338.

Jacka, T. H., and W. F. Budd, 1991: Detection of temperature and sea ice extent changes in the Antarctic and Southern Ocean. *Proc. Int. Conf. on the Role of the Polar Regions in Global Change*, Fairbanks, AK, University of Alaska, 63–70.

Jacobs, S. S., and J. C. Comiso, 1989: Sea ice and oceanic processes on the Ross Sea continental shelf. *J. Geophys. Res.*, **94,** 18 195–18 211.

——, and ——, 1993: A recent sea-ice retreat west of the Antarctic Peninsula. *Geophys. Res. Lett.*, **20,** 1171–1174.

——, H. H. Hellmer, P. Schlosser, and W. M. Smethie Jr., 1994: An oceanographic expedition to the Amundsen and Bellingshausen Seas. *Antarct. J. U.S.*, **29,** 109–111.

——, ——, and A. Jenkins, 1996: Antarctic ice sheet melting in the Southeast Pacific. *Geophys. Res. Lett.*, **23,** 957–960.

Jeffries, M. O., K. Morris, A. P. Worby, and W. F. Weeks, 1994a: Late winter characteristics of the seasonal snow cover on sea-ice floes in the Bellingshausen and Amundsen Seas. *Antarct. J. U.S.*, **19,** 9–10.

——, R. A. Shaw, K. Morris, A. L. Veazey, and H. R. Krouse, 1994b: Crystal structure, stable isotopes ($\delta^{18}O$), and development of sea ice in the Ross, Amundsen and Bellingshausen Seas, Antarctica. *J. Geophys. Res.*, **99,** 985–995.

Johannessen, O. M., M. Miles, and E. Bjorgo, 1995: The Arctic's shrinking sea ice. *Nature*, **376,** 126–127.

Jones, D. A., and I. Simmonds, 1993: A climatology of Southern Hemisphere extratropical cyclones. *Climate Dyn.*, **9,** 131–145.

Jones, P. D., 1990: Antarctic temperatures over the present century—A study of the early expedition record. *J. Climate*, **3,** 1193–1203.

——, and D. W. S. Limbert, 1987: A data bank of Antarctic surface temperature and pressure data. U.S. Dept. of Energy Tech. Rep. 038, 52 pp. [Available from National Technical Information Services, U.S. Dept. of Commerce, Springfield, VA 22161.]

——, R. Marsh, T. M. L. Wigley, and D. A. Peel, 1993: Decadal timescale links between Antarctic Peninsula ice-core oxygen-18, deuterium and temperature. *The Holocene*, **3,** 14–26.

King, J. C., 1994: Recent climate variability in the vicinity of the Antarctic Peninsula. *Int. J. Climatol.*, **14,** 357–369.

Lange, M. A., P. Schlosser, S. F. Ackley, P. Wadhams, and G. S. Dieckmann, 1990: $\delta^{18}O$ concentrations in sea ice of the Weddell Sea, Antarctica. *J. Glaciol.*, **36,** 315–323.

Ledley, T. S., 1985: Sea ice: Multiyear cycles and white ice. *J. Geophys. Res.*, **90,** 5676–5686.

Manabe, S., R. J. Stouffer, M. J. Spelman, and K. Bryan, 1991: Transient response of a coupled ocean–atmosphere model to gradual changes of atmospheric CO_2. Part I: Annual mean response. *J. Climate*, **4,** 785–818.

Martino, M. G., D. J. Cavalieri, P. Gloersen, and H. J. Zwally, 1995: An improved land mask for the SSM/I grid. NASA Tech. Memo. 104625, 9 pp. [Available from NASA Center for Aerospace Information, 800 Elkridge Landing Rd., Linthicum Heights, MD 21090-2934.]

Martinson, D. G., 1990: Evolution of the Southern Ocean winter mixed layer and sea ice: Open ocean deep water formation and ventilation. *J. Geophys. Res.*, **95,** 11 641–11 654.

Mitchell, J. F. B., S. Manabe, V. Meleshko, and T. Tokioka, 1990: Equilibrium climate change and its implications for the future.

Climate Change: The IPCC Scientific Assessment, J. T. Houghton, G. L. Jenkins, and J. J. Ephraums, Eds., Cambridge University Press, 131–172.

Morrison, S. J., 1990: Warmest year on record on the Antarctic Peninsula. *Weather*, **45**, 231–232.

Murphy, E. J., A. Clarke, C. Symon, and J. Priddle, 1995: Temporal variation in Antarctic sea-ice: Analysis of a long term fast-ice record from the South Orkney Islands. *Deep-Sea Res.*, **42**, 1045–1062.

NOCDA, 1985: *Sea Ice Climatic Atlas*. Vol. I, *Antarctic*, Naval Oceanography Command, 132 pp.

NPOC, 1993: *Antarctic Ice Charts, 1991–92*. National Ice Center, 104 pp.

Orsi, A. H., T. Whitworth III, and W. D. Nowlin Jr., 1995: On the meridional extent and fronts of the Antarctic Circumpolar Current. *Deep-Sea Res.*, **42**, 641–673.

Parkinson, C. L., 1992: Interannual variability of monthly Southern Ocean sea ice distributions. *J. Geophys. Res.*, **97**, 5349–5363.

——, 1994: Spatial patterns in the length of the sea ice season in the Southern Ocean, 1979–1986. *J. Geophys. Res.*, **99**, 16 327–16 339.

——, 1995: Recent sea ice advances in Baffin Bay/Davis Strait and retreats in the Bellingshausen Sea. *Ann. Glaciol.*, **21**, 348–352.

Pollard, D., and S. L. Thompson, 1994: Sea-ice dynamics and CO_2 sensitivity in a global climate model. *Atmos.–Ocean*, **32**, 449–467.

Pollard, R. T., J. F. Read, J. T. Allen, G. Griffiths, and A. I. Morrison, 1995: On the physical structure of a front in the Bellingshausen Sea. *Deep-Sea Res.*, **42**, 955–982.

Potter, J. R., M. H. Talbot, and J. G. Paren, 1988: Oceanic regimes at the ice fronts of George VI Sound, Antarctic Peninsula. *Cont. Shelf Res.*, **8**, 347–362.

Raper, S. C. B., T. M. L. Wigley, P. R. Mayes, P. D. Jones, and M. J. Salinger, 1984: Variations in surface air temperatures. Part 3: The Antarctic, 1957–82. *Mon. Wea. Rev.*, **112**, 1341–1353.

Rayner, J. N., and D. A. Howarth, 1979: Antarctic sea ice: 1972–1975. *Geogr. Rev.*, **69**, 202–223.

Read, J. F., R. T. Pollard, A. I. Morrison, and C. Symon, 1995: On the southerly extent of the Antarctic Circumpolar Current in the southeast Pacific. *Deep-Sea Res.*, **42**, 933–954.

Reynolds, J. M., 1981: Distribution of mean annual temperatures in the Antarctic Peninsula. *Br. Antarct. Survey Bull.*, **54**, 123–133.

Ridley, J., 1993: Surface melting on Antarctic Peninsula ice shelves detected by passive microwave sensors. *Geophys. Res. Lett.* **20**, 2639–2642.

Sansom, J., 1989: Antarctic surface temperature time series. *J. Climate*, **2**, 1164–1172.

Schwerdtfeger, W., 1976: Annual temperature and ice condition changes in the Antarctic Peninsula area. *Antarct. J. U.S.*, **11**, 152.

——, 1984: *Weather and Climate of the Antarctic*. Vol. 15, *Developments in Atmospheric Science*, Elsevier, 261 pp.

Sievers, H. A., and W. D. Nowlin Jr., 1984: The stratification and water masses at Drake Passage. *J. Geophys. Res.*, **89**, 10 489–10 514.

Simmonds, I., and T. H. Jacka, 1995: Relationships between the interannual variability of Antarctic sea ice and the Southern Oscillation. *J. Climate*, **8**, 637–647.

Smith, S. R., and C. R. Stearns, 1993: Antarctic pressure and temperature anomalies surrounding the minimum in the Southern Oscillation index. *J. Geophys. Res.*, **98**, 13 071–13 083.

Stammerjohn, S. E., and R. C. Smith, 1996: Spatial and temporal variability in western Antarctic Peninsula sea ice coverage. *Foundations for Ecological Research West of the Antarctic Peninsula*, R. Ross, E. Hoffman, and L. Quetin, Eds., Antarctic Research Series, Amer. Geophys. Union, in press.

Swift, J. H., 1993: Comparing WOCE data with historical hydrographic data in the southeast Pacific. *Eos, Trans. Amer. Geophys. Union*, **74**, 327.

——, 1995: Comparing WOCE and historical temperatures in the deep southeast Pacific. *Int. WOCE Newsletter*, **18**, 15–17.

Stark, P., 1994: Climatic warming in the central Antarctic Peninsula area. *Weather*, **49**, 215–220.

Taylor, K. E., and J. E. Penner, 1994: Response of the climate system to atmospheric aerosols and greenhouse gases. *Nature*, **369**, 734–737.

Thompson, L. G., D. A. Peel, E. Mosley-Thompson, R. Mulvaney, J. Dai, P. N. Lin, M. E. Davis, and C. F. Raymond, 1994: Climate since AD 1510 on Dyer Plateau, Antarctic Peninsula: Evidence for recent climate change. *Ann. Glaciol.*, **20**, 420–426.

Turner, J., and S. R. Colwell, 1995: Temporal variability of precipitation over the western Antarctic Peninsula. Preprints, *Fourth Conf. on Polar Meteorology and Ocean*, Dallas, TX, Amer. Meteor. Soc., 113–116.

van Loon, H., 1971: A half-yearly variation of the circumpolar surface drift in the Southern Hemisphere. *Tellus*, **6**, 511–515.

——, J. W. Kidson, and A. B. Mullan, 1993: Decadal variation of the annual cycle in the Australian dataset. *J. Climate*, **6**, 1227–1231.

Weatherly, J. W., J. E. Walsh, and H. J. Zwally, 1991: Antarctic sea ice variations and seasonal air temperature relationships. *J. Geophys. Res.*, **96**, 15 119–15 130.

Webb, D. J., P. D. Killworth, A. C. Coward, and S. R. Thompson, 1991: *The FRAM Atlas of the Southern Ocean*. Natural Environmental Research Council, 67 pp.

White, W. B., and R. G. Peterson, 1996: An Antarctic circumpolar wave in surface pressure, wind, temperature and sea ice extent. *Nature*, **380**, 699–702.

Zwally, H. J., C. L. Parkinson, and J. C. Comiso, 1983a: Variability of Antarctic sea ice and changes in carbon dioxide. *Science*, **220**, 1005–1012.

——, J. C. Comiso, C. L. Parkinson, W. J. Campbell, F. D. Carsey, and P. Gloersen, 1983b: Antarctic sea ice, 1973–1976: Satellite passive-microwave observations. NASA SP-459, 206 pp. [Available from J. Zwally, Code 971, NASA/GSFC, Greenbelt, MD 20771.]

Deep Coastal Oceanography from McMurdo Sound to Marguerite Bay

Stanley S. Jacobs

Lamont-Doherty Earth Observatory

of Columbia University

Palisades NY 10964

Thirty years ago Lamont investigators made the first continuous vertical 'STD' (salinity-temperature-depth) profiles in the Ross Sea, casting from the *Eltanin* with an early model of the now widely-used 'CTD'. The original acronym has long since been abandoned to the public health sector, and the 'C' now stands for seawater conductivity, from which salinity is calculated (as is 'D' from pressure). From the many 'bottle' and CTD casts made in the Ross Sea before and since that time, a rough time series of summer temperature and salinity measurements can be compiled (Jacobs and Giulivi 1998a). Unlike local meteorological observations and satellite-derived information on sea ice extent, the oceanographic data are highly discontinuous in space and time. In spite of geographical biases (e.g., Giulivi and Jacobs 1997a) and a curious year-round salinity record (from McMurdo Sound), it is apparent that interannual salinity variability is substantial on the Ross Sea continental shelf. The salinity changes are correlated with sea ice range (Figure 1), which has a periodicity of several years. Superimposed on the large short-term variability is a slight decline in shelf water salinity over the past four decades in the southwest Ross Sea (Jacobs and Giulivi 1998b).

Over the past 150 years even the area of the open Ross Sea continental shelf has changed. Continued monitoring of the position of the Ross Ice Shelf front (Keys, Jacobs and Brigham 1997) reveals that the western portion of the ice front is now more than 75 kilometers (km) north of its location in 1911, around the time that Amundsen and Scott

trekked to the South Pole. The 'B-9' iceberg released by the eastern ice front in 1987 removed an area larger than the island between Manhattan and Montauk, but steady advance along the entire ice front since then has more than regained the ice shelf real estate lost in that calving event. The growth of the Ross and other ice shelves stands in contrast to well-publicized retreats along the Antarctic Peninsula, and suggests that the circumpolar inventory of shelf ice may be little changed in recent times.

Three years ago, on cruise 9402 of the *Nathaniel B. Palmer,* we made the first oceanographic measurements in some Antarctic coastal regions between the eastern Ross Sea and Marguerite Bay (Giulivi and Jacobs 1997b). Using new Amundsen Sea data for validation, Hellmer, Jacobs and Jenkins (1998) modeled the flow of circumpolar deep water beneath Pine Island Glacier, where the basal melt rate appears to exceed 10 meters per year (Jacobs, Hellmer and Jenkins 1996). In combination with a calving rate obtained from radar satellite observations, that melting roughly balances the estimated flow of ice across the deep grounding line (Jacobs, Jenkins and Hellmer 1996). Meltwater increases the dissolved oxygen content of the deep water that upwells beneath the glacier, but lowers its oxygen isotope ($\delta^{18}O$) content, from which the $\delta^{18}O$ of precipitation on the glacier catchment basin can be inferred (Figure 2). Relatively shallow and warmer than the ambient environment, outflows from beneath the glacier are likely to influence local sea ice formation.

Following up on an earlier finding of higher seabird populations near the Antarctic Slope Front, Ainley et al. (1998) evaluated bird distributions observed during *Palmer* cruise 9402, late enough in the season that summer colonies had been abandoned. They found that ocean thermohaline fronts in the Amundsen and Bellingshausen regions are more diffuse and less related to the continental shelf break than in the Ross Sea. Interpretations

were complicated by overly wide ocean station spacing, by the lack of prey data and unavoidable time gaps in the observations, and by large flocks of birds roosting by day and feeding at night. It remains to be determined how deep subsurface features compete with or enhance the ice edge environment as a magnet for top-gun predators.

From the limited historical ocean data available, it is difficult to determine whether significant temporal changes have occurred in waters on the Southeast Pacific Antarctic continental shelf. Nearly 100 years ago oceanographic measurements were made from the *Belgica*, beset for more than a year in the close pack of the southern Bellingshausen Sea. Their southernmost temperatures are substantially colder than the *Palmer* CTD profile at the same location (Figure 3), with a deep temperature maximum in March ~0.3°Celsius below that of our March 1994 data. Ongoing analyses of such comparisons may allow any long-term temperature change to be separated from the short-term variability.

Acknowledgments: C. Giulivi and H. Hellmer assisted with data reduction and figures. This research was supported by the National Science Foundation (OPP-94-18151), with assistance from the National Aeronautics and Space Administration (NAGW-1344), the Department of Energy (DE-FG02-93ER61716) and Lamont-Doherty Earth Observatory.

References

Ainley, D. G., S. S. Jacobs, C. A. Ribic and I. Gaffney. 1998. Seabirds and oceanic features of the Amundsen and southern Bellingshausen Seas, late summer - early autumn 1994. Antarctic Science, in press.

Giulivi, C. F. and S. S. Jacobs. 1997a. A zonal oceanographic section in the southern Ross Sea: Oceanographic data taken from the USCGC *Polar Sea*, February 1994. Technical Report 97-2, Lamont-Doherty Earth Observatory, Palisades, 95 pp.

Giulivi, C. F. and S. S. Jacobs. 1997b. Oceanographic data in the Amundsen and Bellingshausen Seas: *N.B.Palmer* cruise 9402, February-March 1994. Technical Report 97-3, Lamont-Doherty Earth Observatory, Palisades, 330 pp.

Hellmer, H. H., S. S. Jacobs and A. Jenkins. 1998. Oceanic erosion of a floating Antarctic glacier in the Amundsen Sea. In: Antarctic Research Series, vol 75, S. Jacobs and R. Weiss (eds), American Geophysical Union, in press.

Jacobs, S., H. Hellmer and A. Jenkins. 1996. WAIS underbelly melting at Pine Island Glacier? IN: Filchner-Ronne Ice Shelf Programme, Report # 10, H. Oerter (ed), Alfred-Wegener-Institute, Bremerhaven, 38-40.

Jacobs, S. S., A. Jenkins and H. H. Hellmer. 1996. On the mass balance of West Antarctica's Pine Island Glacier. In: Glaciers, Ice Sheets and Volcanoes: A tribute to Mark F. Meier, S. Colbeck (ed), Special Report 96-27, Cold Regions Research and Engineering Laboratory, Hanover, 52-56.

Jacobs, S. S. and C. F. Giulivi. 1998a. Thermohaline data and ocean circulation on the Ross Sea continental shelf. In: Oceanography of the Ross Sea, Antarctica, G. Spezie and G. Manzella (eds), Springer-Verlag, Heidelberg, in press.

Jacobs, S. S. and C. F. Giulivi. 1998b. Interannual ocean and sea ice variability in the Ross Sea. In: Antarctic Research Series vol 75, S. Jacobs and R. Weiss (eds), American Geophysical Union, in press.

Keys, H. J. R., S. S. Jacobs and L. W. Brigham. 1998. Continued northward expansion of the Ross Ice Shelf. Annals of Glaciology, 27, in press.

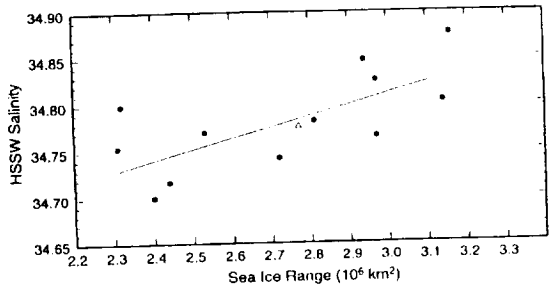

Figure 1. Average salinity at 450-550 m-depths in the
continental shelf in the western Ross Sea (160E-180) vs
represents salinity data for one summer, usually December t
from the Ross sector preceding winter maximum minus the

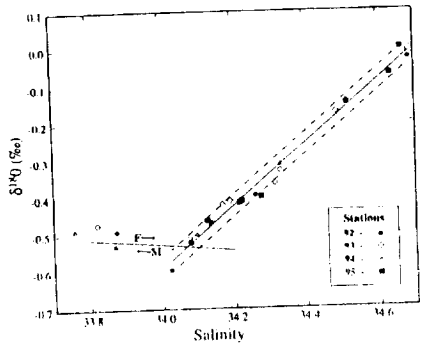

Figure 2. Oxygen isotope/salinity diagram for stations in Pine Island Bay (74°50'S, 102°40'W) in the southeast Amundsen Sea. The solid line fit to the deeper samples extrapolates to a zero-salinity $\delta^{18}O$ content near -29 o/oo, the probable mean value for precipitation on the Pine Island Glacier (75°10'S, 100°00'W) catchment basin. Dashed lines indicate the precision of $\delta^{18}O$ measurements by S. Khatiwala at Lamont-Doherty.

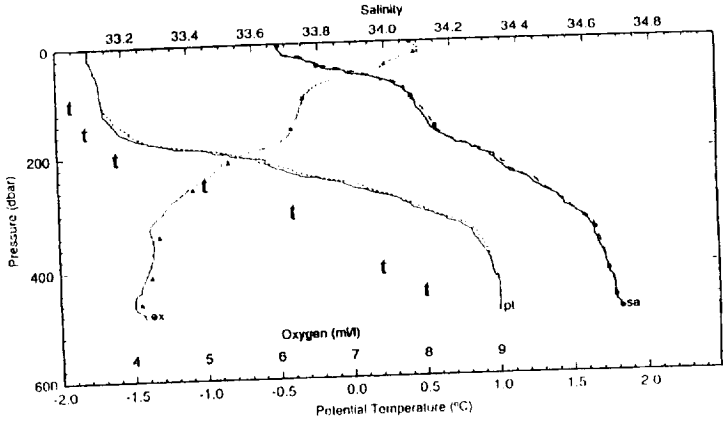

Figure 3. CTD temperature (pt), salinity (sa) and dissolved oxygen (ox) vs. pressure (in decibars) from *Palmer* station 9402-119 on 21 March 1994 at 71°31'S, 85°19'W. Solid symbols on the downcast oxygen profile and upcast (dashed) salinity profile indicate 'bottle' values. The 't' symbols show temperatures at and below 100 m from *Belgica* station 19 on 02 March 1898, occupied at the same location on the Bellingshausen Sea continental shelf.

Thermohaline Data and Ocean Circulation on the Ross Sea Continental Shelf

S.S. Jacobs and C.F. Giulivi

Lamont-Doherty Earth Observatory

of Columbia University

Palisades, NY 10964, USA

Abstract

The ocean station data base on the Ross Sea continental shelf includes measurements from more than fifty cruises, and a few observations through ice holes. Using representative salinity and temperature transects from the summers of 1962-63, 1976-77 and 1983-84, we briefly review the ocean stratification and circulation, identifying five primary water masses. Year-round salinity profiles at a single location in 1960-61 and early winter temperature profiles along the dateline in 1995 are discussed in relation to anticipated seasonal changes. A strong zonal salinity gradient and substantial differences between two representations of the shelf data base reveal the need for caution in modelling and bottom water investigations. Long term observations of shelf water salinity and studies of the inflow of modified deep water would help in the evaluation of recent evidence for marked interannual and decadal variability on the continental shelf.

1. Introduction

Analyses of historical ocean temperature and salinity measurements on the Antarctic continental shelf require a careful consideration of original sources, data processing, and variability in space and time. The effects of stronger winter forcing must be inferred from predominantly late summer observations. Considerable variability over small distances can influence the choice of areas over which data can meaningfully be averaged. Lengthening time series display substantial variability on interannual and longer temporal scales. Here we revisit these caveats in the context of the

increasing utilization of gridded, archived data for modelling and climate change work. Available ocean station data on the Ross Sea continental shelf are summarized, and some differences that can arise from alternate treatments of a similar data base are illustrated. We also evaluate a venerable set of year-long salinity profiles, and a transect of recent May temperature measurements.

The region north of the Ross Ice Shelf is better sampled than most of the remaining circumpolar continental shelf, thanks to a minimal sea ice cover during the austral summer and a location adjacent to McMurdo Station and other Antarctic bases. Aspects of its ocean circulation have been described in numerous papers [e.g., 1-14] and the references therein. Here we present a comparable set of representative zonal and meridional transects, along with a brief description of the primary water masses and their probable sources and sinks. Temporal variability in the ocean thermohaline data over recent decades in this sector is discussed in more detail by Jacobs & Giulivi [15].

2. The data base and seasonal variability

Temperature and salinity data south of the 600m isobath near the continental shelf break were winnowed from NODC archives and supplemented by additional observations (Figure 1). Since the Ross Ice Shelf ice front advances for decades, followed by rapid retreat [16], some stations appear south of the apparent coastline. The seasons (years) and months that ocean station data were obtained are listed in Table 1, along with ship name or other source. The vast majority of the ~1200 profiles utilized were occupied from December through February, and have an areal distribution that is biased toward the southern and western sectors. We did not use data from far beneath the ice shelf [17], at instrument moorings [18, e.g.] or from very recent cruises (http:/usjgofs.whoi.edu/).

Data quality and seasonal cycles are paramount issues in studies of coastal regions. We have long been aware of apparently large (>0.15) salinity changes from one summer to the next in the deep

shelf water of the southwest Ross Sea [19]. While those changes exceeded the measurement accuracy by an order of magnitude, they seemed confounded by a year-round series of stations taken through the sea ice in McMurdo Sound (Figure 2). Extending to depths exceeding 500m, the temperatures showed relatively little variability, but the salinities displayed a greater range than the interannual summer changes noted above. As in the summer profiles [19], temporal shifts were simultaneous over most of the water column, with salinities increasing from May through October, and decreasing in December and February. An unexpected January reversal resulted in the highest annual values from 350-550m, and between 21 February and 07 March most of the water column plunged by more than 0.2 in salinity.

A closer look at the Tressler and Ommundsen report [20] indicates that the authors made their last measurements on 21 February and then left McMurdo, presumably with the salinity samples taken up to that time. A follow-on program by another group was unceremoniously terminated after one cast (March in Figure 2) by a storm that swept away the ice floe, hole and hut. The anomalously low salinity on the March profile may thus have resulted from the program change, perhaps related to different sampling and analysis protocols. This points up the value of thorough data reports (metadata) detailing the methods and problems that are unlikely to appear in large ocean data archives. Nevertheless, this year-round series of ocean stations in McMurdo Sound remains a valuable and unique data set, suggesting a strong seasonal variability in response to surface forcing and circulation within the shelf water.

3. Data products and areal variability

Large portions of the Antarctic continental shelf serve as production sites and temporary storage reservoirs for dense shelf waters. Formed mainly by winter cooling and freezing at the sea surface, shelf waters supply much of the salt that drives thermohaline circulation beneath the large ice shelves, and the properties by which new bottom water is identified [21,6]. At the cold temperatures that characterize the Ross Sea continental shelf, salinity variations exert a greater

control over the density field. Ocean general circulation models often 'restore' salinity near Antarctica to observed conditions, e.g. as represented by the NODC World Ocean Atlas [22]. Model results can vary markedly and have global impacts [23,24] depending upon whether salinities are restored to values as low as 34.0, characteristic of zonal average summer surface waters, or as high as 35.0, which exceed anything reported on the shelf for the past three decades.

Substantial differences are also evident between our summer observations and NODC Atlas objectively-averaged one-degree grid data over the same months in each meridional band (Figure 3). The Atlas data are consistently saltier, perhaps because more recent, lower-salinity measurements [15] were not in the NODC archive. Atlas temperatures also tend to be higher and more variable and, like salinities, do not extend below 500 m. These anomalies might result from mislocated stations, from the incorporation of bathythermograph data into the Atlas, and from irregular shelf depths over which isolated deep values are removed [25]. Atlas data on the shelf may also be biased by different water types from north of the shelf break, near which the strong Antarctic Slope Front [26] could also influence data averaged on pressure surfaces, as in the North Atlantic [27]. Gridded and averaged data are valuable for many purposes, but caution must be exercised in their use for modelling or other work on the Antarctic continental shelf.

Annual averages are compromised by the scarcity of non-summer measurements, and spatial averages can show a high variance due to the strong east-west gradient resulting from the variable salt fluxes and wind fields [2,28]. The zonal gradients in Figure 3 are largest below the upper hundred meters, with the highest salinities and coldest temperatures in the western sector. The salinity gradient may have implications for classical bottom water formation arguments, which frequently hinge on much lower changes in density (salinity). Indeed, the entire region below 350m is saltier than the Pacific continental shelf average of 34.46 [29]. If bottom water formation simply required a shelf component with a salinity above ~34.51 [30], then most water on the Ross Sea continental shelf would qualify. However, the Ross Sea is widely believed to produce much

less bottom water than the Weddell Sea [e.g., 29], in spite of similar environments. This may in part be an artifact of water mass definitions, or be a consequence of the greater warmth of the Ross Gyre, elements of which intrude onto the continental shelf. An apparent drift toward lower shelf water salinities in the Ross Sea over recent decades might also have altered the regional bottom water production rate or properties [15].

4. Water masses

Circumpolar Deep Water evolves into several new water masses on and near the Antarctic continental shelves. As these waters mix and interact with the atmosphere, sea ice and shelf ice, some of them ventilating the deep ocean, their properties and variability are of more than taxonomic interest in this region. Names and definitions have evolved over time, but common usage has tended to follow Carmack [29]. The north-south and east-west temperature and salinity sections across the shelf in Figures 4 and 5 are plotted at the same vertical scale, with the following water mass abbreviations and characteristics:

HSSW (High Salinity Shelf Water), identified by salinities >34.6 and temperatures at the sea surface freezing point, dominates the subsurface western sector in summer. Previously referred to as Ross Sea Shelf Water (and Western Shelf Water in the Weddell Sea), HSSW appears on all sections but the one in Figure 5d.

LSSW (Low Salinity Shelf Water), at a slightly warmer sea surface freezing temperature corresponding to its lower (~34.4-34.6) salinities, is best developed on Figures 5c and 5d. Similar to Eastern Shelf Water in the Weddell Sea, LSSW is hard to differentiate in T/S space from the 'winter water' temperature minimum at the base of the surface water.

ISW (Ice Shelf Water), with subsurface temperatures below the sea surface freezing point, is rarely supercooled in situ. ISW is concentrated in the west-central sector (Figure 5b), where it emerges from beneath the Ross Ice Shelf.

MCDW (Modified Circumpolar Deep Water), derived from Circumpolar Deep Water near the continental shelf break and typed by temperatures between +1.0 and -1.5, intrudes at least to the

ice shelf front in Figure 5c. MCDW has been referred to as a Warm Core in the Ross Sea (and as Modified Warm or Weddell Deep Water in the Weddell Sea).

AASW (Antarctic Surface Water), typically warmer (to ~+2°C) and fresher (<34.5) in summer than the deeper shelf waters from which it evolves, is comprised of a mixed layer of variable thickness, with or without an underlying 'winter water' layer. As AASW cools, thickens, and becomes saltier in winter, much of it is transformed back into shelf waters.

5. General circulation

The large scale ocean circulation on the Ross Sea continental shelf consists of AASW, LSSW and MCDW inflows from the north and east (Figures 4 & 5) that are seasonally cooled and warmed, salinized by sea ice formation and freshened by meltwater. Surface circulation on the open shelf generally moves ice and water to the west and north, and is bounded by a strong, narrow coastal current along the Ross Ice Shelf and another westward flow near the continental shelf break [26]. Intense winter sea ice formation and its removal from the coastlines produces the nearly isothermal LSSW and HSSW. Coastal upwelling in these same regions is consistent with the large-scale density field [2] and with predominant offshore winds.

Shelf waters contribute directly to bottom water formation near the continental shelf break [1,6]. In addition, some portion of the HSSW and LSSW drains into the deeper cavity beneath the Ross Ice Shelf, where glacial ice is melted, probably most strongly near the deep grounding lines. This occurs because seawater freezing temperature decreases with increasing pressure, and results in a deep ISW plume that emerges in the central Ross Sea (Figure 4). Both that outflow and shallower filaments near the ice front may contain ice crystals, produced as the rising water reacts to supercooling [31,7]. Circulation, melting and subsequent freezing beneath the shelf ice have been inferred from measurements near, on and beneath the ice, and from models of the sub-ice circulation [e.g.,3,6,32-38]. The strength of the sub-ice circulation and its exchanges with the

open Ross Sea are likely to vary considerably over interannual and longer periods in response to changes in HSSW salinity and volume[15].

The Ross Sea continental shelf is covered by sea ice for most of the year, with decay and growth both starting near the ice shelf front, typically in late October and late February. Northward transport of sea ice is strongest in the western sector, where barrier and katabatic winds maintain the large Ross Sea Polynya adjacent to the ice shelf front [39] and a small, persistent polynya near 75°S on the Victoria Land coast [40]. The volume and salinity of HSSW will depend in part on the volume of sea ice produced on the continental shelf and exported from it each year. Detailed records of ice transport are not yet available, however, and sea ice thickness data are scarce [41]. The length of the sea ice season on the shelf varied by about a month from 1979-87, with little apparent interannual change in winter ice concentration [9]. A longer Comiso sea ice record from the entire Ross Sea displays strong interannual changes in the sea ice extent [15] at a period comparable to that of the 'Antarctic Circumpolar Wave' [42].

MCDW intrudes year-round at intermediate depths onto the continental shelf [18,10], and overrides the HSSW at some locations in the western sector. Since the HSSW shoals rapidly westward, the 'warm' MCDW that penetrates that sector will lie directly beneath the AASW, from which it cannot easily be discriminated with summer temperature and salinity measurements. MCDW may extend for some distance beneath the ice shelf, as current measurements accompanying the stations in Figure 4a revealed inflow and outflow, respectively, in the eastern and western 'cores' defined by the -1.2°C contours. This recirculation appears to be persistent, and may account for a slight thinning of the ice shelf in that region[10,16].

Temperatures from a May 1995 section across the shelf (Figure 6) were obtained about two months after sea ice had covered this region. By this time any traces of summer AASW and shallow ISW had been eliminated, and the mixed layer was deepest near the Ross Ice Shelf where

surface forcing is strongest. The main ISW outflow remained around 450m, and the MCDW inflow with temperatures warmer than -1°C appeared on several stations. In some locations this MCDW reached above 100m, probably accounting for mixed layer temperatures warmer than the surface freezing point. The corresponding salinities (not shown) were relatively low, either due to the general decline [15] or because 3-4 months of winter brine production remained ahead.

6. Future work

An improved understanding of the ocean circulation on this shelf could be gained by additional long-term high-quality measurements, particularly of salinity in the HSSW. A detailed study of the seasonal and interannual variability of the Antarctic Slope Front, including the cross-slope transport of water masses and sea ice, could also be extremely valuable. At present the imported MCDW may contribute more to the maintenance of the Ross Sea Polynya than to basal melting of the Ross Ice Shelf, but neither impact is well documented. Exported shelf waters contribute to bottom water formation, but neither the volume nor the spatial and temporal variability of deep ventilation is known in this sector. AASW properties and biological productivity will respond to interannual changes in the sea ice formation and concentration. Satellite data continue to provide valuable information about the annual sea ice cycle, but we know much less about the sources, sinks and residence time of AASW on the continental shelf. One thing that is not lacking, apparently, is a host of unsolved problems for the coming millenium.

7. Acknowledgments

We thank the individuals and institutions that provided the data utilized in this study, and the polar programs of the National Science Foundation and National Space and Aeronautics Administration that supported our work. We are grateful to the C.L.I.M.A. Project for its organization of the Lerici Conference on the Oceanography of the Ross Sea, where elements of the material herein and in Jacobs and Giulivi [15] were first presented. This is contribution #0000 of the Lamont-Doherty Earth Observatory of Columbia University.

8. References

1. Jacobs SS, Amos AF, Bruchhausen PM (1970) Ross Sea oceanography and Antarctic Bottom Water formation. Deep Sea Res17:935-962

2. Killworth PD (1974) A baroclinic model of motions on Antarctic continental shelves. Deep Sea Res 21(10):815-838

3. Jacobs SS, Gordon AL, Ardai JL (1979) Circulation and melting beneath the Ross Ice Shelf. Science 203:439-442

4. Ainley DG, Jacobs SS (1981) Sea-bird affinities for ocean and ice boundaries in the Antarctic. Deep Sea Res 28A(10):1173-1185

5. Dunbar RB, Anderson JB, Domack EW, Jacobs SS (1985) Oceanographic influences on sedimentation along the Antarctic continental shelf. In: Jacobs SS (ed) Oceanology of the Antarctic Continental Shelf, Ant Res Ser 43. AGU, Washington, pp 291-312

6. Jacobs SS, Fairbanks RG, Horibe Y (1985) Origin and evolution of water masses near the Antarctic continental margin: Evidence from $H_2{}^{18}O/H_2{}^{16}O$ ratios in seawater. In: Jacobs SS (ed) Oceanology of the Antarctic Continental Shelf, Ant Res Ser 43. AGU, Washington, pp 59-85

7. Lewis EL, Perkin RG (1985) The winter oceanography of McMurdo Sound, Antarctica. In: Jacobs SS (ed) Oceanology of the Antarctic Continental Shelf, Ant Res Ser 43. AGU, Washington, pp 145-166

8. Jacobs SS (1989) Marine controls on modern sedimentation on the Antarctic continental shelf. Mar Geol 85:121-153

9. Jacobs SS, Comiso JC (1989) Sea ice and oceanic processes on the Ross Sea continental shelf. J Geophys Res 94:18195-18211

10. Keys HJR, Jacobs SS, Barnett D (1990) The calving and drift of iceberg B-9 in the Ross Sea, Antarctica. Antarct Sci 2(3):243-257

11. Trumbore S, Jacobs SS, Smethie W (1991) Chlorofluorocarbon evidence for rapid ventilation of the Ross Sea. Deep Sea Res 38(7):845-870

12. Locarnini RA (1994) Water masses and circulation in the Ross Gyre and environs. PhD thesis. Dept Ocean Texas A&M Univ, College Station, 86 pp

13. Jaeger JM, Nittrouer CA, DeMaster DJ, Kelchner C, Dunbar RB (1996) Lateral transport of settling particles in the Ross Sea and implications for the fate of biogenic material. J Geophys Res 101(C8):18479-18488

14. Hofmann EE, Klinck JM (1997) Hydrography and circulation of Antarctic continental shelves: 150°E eastward to the Greenwich Meridian. In: Robinson AR, Brink KH (eds) The Sea 11. The Global Coastal Ocean, Regional Studies and Synthesis. Wiley, New York, in press

15. Jacobs SS, Giulivi CF (1998) Interannual ocean and sea ice variability in the Ross Sea. In: Jacobs SS, Weiss RF (eds) Ant Res Ser 75. AGU, Washington, in press

16. Keys HJR, Jacobs SS, Brigham LW (1997) Continued northward expansion of the Ross Ice Shelf. Subm to Ann Glaciol

17. Jacobs SS, Haines WH (1982) Ross Ice Shelf Project, Oceanographic Data, 1976-1979. TR LDGO-82-1 Columbia Univ, Palisades, 505 pp

18. Pillsbury RD, Jacobs SS (1985) Preliminary observations from long-term current meter moorings near the Ross Ice Shelf, Antarctica. In: Jacobs SS (ed) Oceanology of the Antarctic Continental Shelf, Ant Res Ser 43. AGU, Washington, pp 87-107

19. Jacobs SS (1985) Oceanographic evidence for land ice/ocean interactions in the Southern Ocean. In: Glaciers, Ice Sheets, and Sea Level, Effects of a CO_2 Induced Climatic Change. Nat Acad Press, Washington, pp 116-128

20. Tressler WL, Ommundsen AM (1962) Seasonal oceanographic studies in McMurdo Sound, Antarctica. Tech Rep 125. US Navy Hydrographic Office, Washington, 144 pp

21. Foldvik A, Gammelsrod T, Torresen T (1985) Circulation and water masses on the southern Weddell Sea shelf. In: Jacobs SS (ed) Oceanology of the Antarctic Continental Shelf, Ant Res Ser 43. AGU, Washington, pp 5-20

22. NODC (1994) World Ocean Atlas, CD-ROM Data Set Documentation. Ocean Clim Lab, National Oceanographic Data Center IR13, Washington, 30 pp.

23. Stocker TF, Wright DG, BroeckerWS (1992) The influence of high-latitude surface forcing on the global thermohaline circulation. Paleoceanography 7(5):529-541

24. Toggweiler JR, Samuels AM (1995) Effect of sea ice on the salinity of Antarctic Bottom Water. J Phys Ocean 25:1980-97

25. Levitus S (1982) Climatological Átlas of the World Ocean. NOAA Prof Paper 13, Rockville,173 pp

26. Jacobs SS (1991) On the nature and significance of the Antarctic Slope Front. In: Treguer P, Queguiner B (eds) Biochemistry and Circulation of Water Masses in the Southern Ocean. Mar Chem 35:9-24

27. Lozier MS, McCartney MS, Owens WB (1994) Anomalous anomalies in averaged hydrographic data. J Phys Ocean 24:2624-2638

28. Grumbine RW (1991) Model of the formation of high-salinity shelf water on polar continental shelves. J Geophys Res 96(C12):22049-22062

29. Carmack EC (1977) Water characteristics of the Southern Ocean south of the Polar Front. In: Angel M (ed) A Voyage of Discovery, G. Deacon 70th Anniv Vol Suppl to Deep Sea Res. Pergamon, New York, pp 15-42

30. Fofonoff NP (1956) Some properties of seawater influencing the formation of Antarctic bottom water. Deep Sea Res 4:32-66

31. Foldvik A, Kvinge T (1974) Conditional stability of sea water at the freezing point. Deep Sea Res 21(3):169-174

32. Jacobs SS, Hellmer HH, Doake CSM, Jenkins A, Frolich R (1992) Melting of ice shelves and the mass balance of Antarctica. J Glaciol 38:75-387

33. Williams RT, Robinson ES (1980) Ocean tide in the southern Ross Sea. J Geophys Res 85(C11):6689-6696

34. MacAyeal DR (1985) Evolution of tidally triggered meltwater plumes below ice shelves. In: Jacobs SS (ed) Oceanology of the Antarctic Continental Shelf, Ant Res Ser 43. AGU, Washington, pp 133-143

35. MacAyeal DR (1985) Tidal rectification below the Ross Ice Shelf, Antarctica. In: Jacobs SS (ed) Oceanology of the Antarctic Continental Shelf, Ant Res Ser 43. AGU, Washington, pp 109-132

36. Scheduikat M, Olbers DJ (1990) A one-dimensional mixed layer model beneath the Ross Ice Shelf with tidally induced vertical mixing. Antarct Sci 2:29-42

37. Nost OA, Foldvik A (1994) A model of ice shelf-ocean interaction with application to the Filchner-Ronne and Ross Ice Shelves. J Geophys Res 99(C7):14243-14254

38. Hellmer HH, Jacobs SS (1995) Seasonal circulation under the eastern Ross Ice Shelf, Antarctica. J Geophys Res 100(C6):10873-10885

39. Zwally HJ, Comiso JC, Gordon AL (1985) Antarctic offshore leads and polynyas and oceanographic effects. In: Jacobs SS (ed) Oceanology of the Antarctic Continental Shelf, Ant Res Ser 43. AGU, Washington, pp 203-226

40. Kurtz DD, Bromwich DH (1985) A recurring, atmospherically forced polynya in Terra Nova Bay. In: Jacobs SS (ed) Oceanology of the Antarctic Continental Shelf, Ant Res Ser 43. AGU, Washington, pp 177-201

41. Jeffries MO, Adolphs U (1997) Early winter ice and snow thickness distribution, ice structure and development of the western Ross Sea pack ice between the ice edge and the Ross Ice Shelf. Antarct Sci 9(2):188-200

42. White WB, Peterson RG (1996) An Antarctic circumpolar wave in surface pressure, wind, temperature and sea ice extent. Nature 380:699-702

43. Davey FJ (1995) Bathymetry, Seismic Stratigraphic Atlas of the Ross Sea, Antarctica. In: Cooper A, Barker P, Brancolini G (eds) Geology and Seismic Stratigraphy of the Antarctic Margin. Ant Res Ser 68. AGU, Washington, Plate 1, Map 1b

44. Biggs DC, Amos AF (1983) Oceanographic data from the southwestern Ross Sea, January 1982, STD and nutrient chemistry programs. Ref 83-3-T Dept Ocean. Texas A&M Univ, College Station, 167 pp

45. El-Sayed SZ, Biggs DC, Holm-Hansen O (1983) Phytoplankton standing crop, primary productivity, and near surface nitrogenous nutrient fields in the Ross Sea, Antarctica. Deep Sea Res 30(8A):871-886

46. Giulivi CF, Jacobs SS, O'Hara ŚH, Ardai JL (1995) Ross Sea Polynya Project 1994, Oceanographic Data, NB Palmer Cruise 9406. TR LDEO-95-1 Lamont Earth Observatory, Palisades, 315 pp

47. Heath RA (1971) Circulation and hydrology under the seasonal ice of McMurdo Sound, Antarctica. NZ J Mar Freshw Res 5(3/4):497-515

48. Littlepage JL (1965) Oceanographic investigations in McMurdo Sound, Antarctica. In: Pawson DL (ed) Biology of the Antarctic Seas II, Ant Res Ser 5. AGU, Washington pp 1-37

Table 1. A chronological summary of ocean stations with temperature and salinity data on the Ross Sea continental shelf, from 1928-29 through 1996-97. In this compilation each season (year) begins on 01 June and the months are indicated numerically. Identified data sets for which the stations have yet to be merged with this file appear as blanks under # Stations. Most ship data is available from the National Oceanographic Data Center, and some also in data reports [e.g., 17,44,46].

Season	Months	Ship/Source	# St.	Season	Months	Ship/Source	# St.
1928-1929	12,1	Larson	8	1967-1968	1,2	Eltanin	32
1935-1936	1	Discovery	14		2	Burton Island	28
1954-1955	1	Atka	7	1968-1969	2	Burton Island	21
1955-1956	1,2	Edisto	7		2	Pelamida	12
	1,3	Glacier	3	1969-1970	2	Edisto	23
	3	*(Unknown)*	1	1970-1971	1	[47]	6
1956-1957	11,12	Glacier	7	1971-1972	2,3	Eltanin	11
	3	Northwind	2	1974-1975	9,10	Ice Island	8
1957-1958	12,2	Glacier	13	1976-1977	12	Northwind	42
	1	Burton Island	3	1976-1977		[45]	
	12,1	Atka	23	1977-1978	1,2	Burton Island	68
1958-1959	11,12	Glacier	18	1978-1979	2	Glacier	12
	12,1	Northwind	9	1981-1982	1	Glacier	36
	12,1,3	Staten Island	4	1982-1983	2,3	Glacier	17
1959-1960	12	Glacier	6	1982-1983		[7]	
	5	[20]	3	1983-1984	1,2	Polar Sea	107
1960-1961	6-2	[20]	24	1984-1985	1,2	Polar Star	35
	12	Staten Island	8	1985-1986	2	Vieze	2
1960-1961		[48]		1987-1988	2	Fedorov	1
1961-1962	1,2	Burton Island	28	1989-1990	12,1	Cariboo	27
	2	Eastwind	23		1,2	Polar Duke	26
	1,2	Glacier	9	1990-1991	12,1	Cariboo	17
1961-1962		[48]		1992		Polar Duke	
1962-1963	2,3	Edisto	101	1993-1994	2	Polar Sea	42
1963-1964	2,3	Atka	36		2	Palmer	2
1964-1965	2	Staten Island	24	1994-1995	11,12	Palmer	151
1965-1966	2	Atka	24	1995-1996	5	Palmer 9503	11
1966-1967	1	Eltanin	22			Palmer 9508	
	1,2	Glacier	13	1996-1997		Palmer (JGOFS)	
	2	Staten Island	26			Palmer (ROAVERRS)	

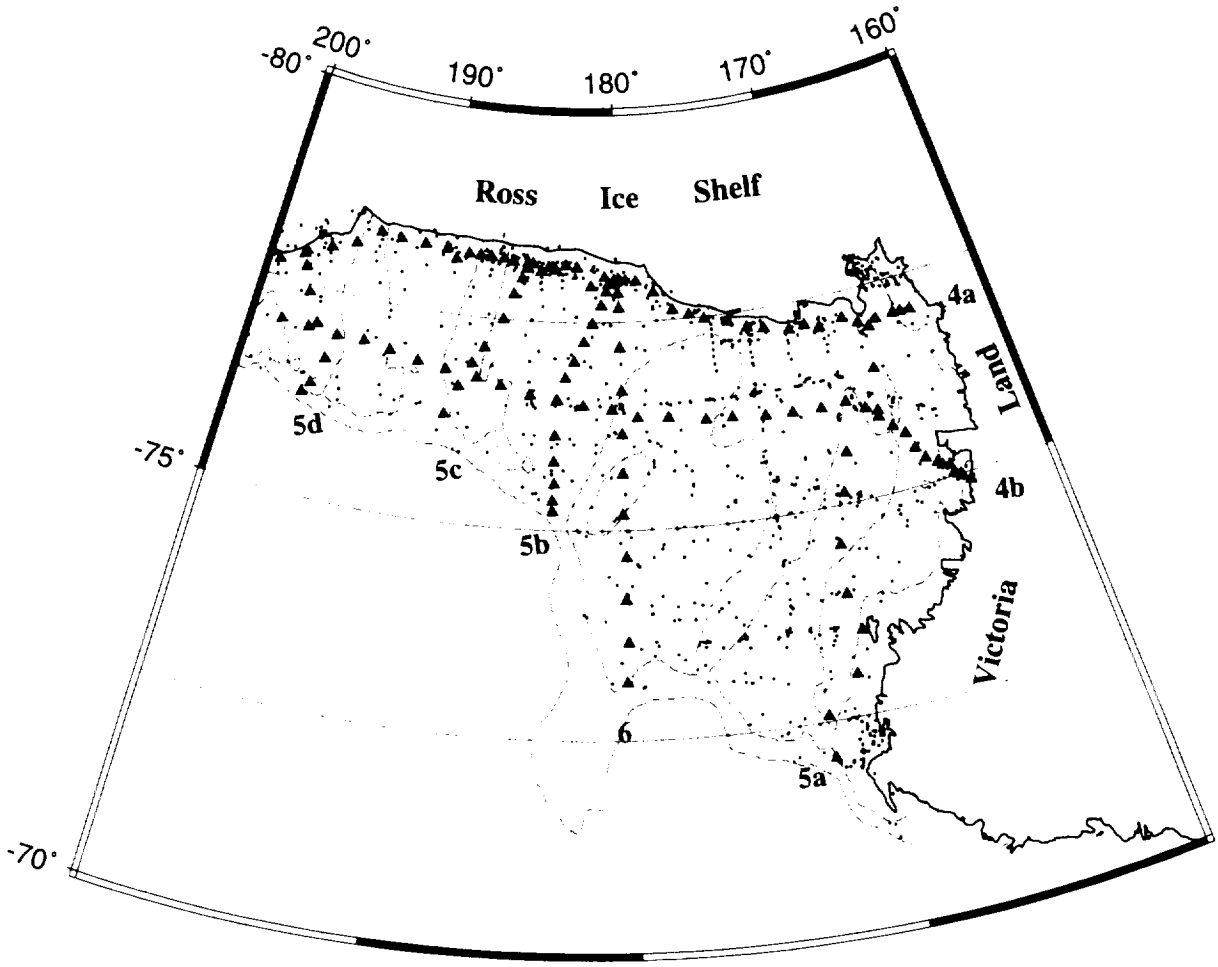

Fig. 1. Distribution of the ocean stations (small dots) summarized in Table 1, superimposed on 500 and 1000 m bathymetric contours. More detailed bathymetric data may be found in Davey [43]. Coordinates are negative south and positive east, with 190 and 200 equivalent to 170°W and 160°W.McMurdo Station, on the west side of McMurdo Sound and the SE end of Ross Island, is located near 77°51'S, 166°40'E. The larger symbols at the northern and western ends of the transects show the stations in Figures 4-6.

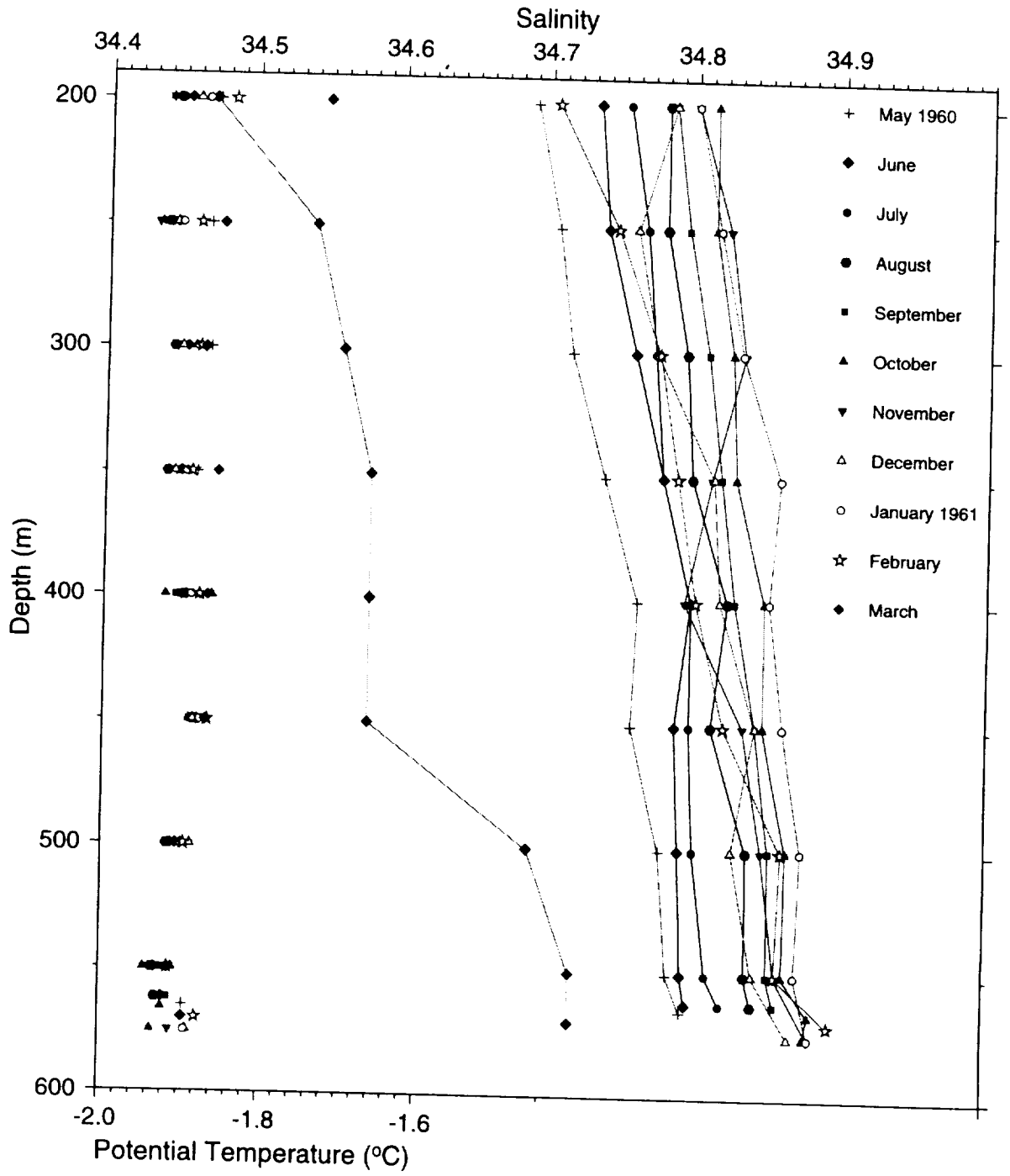

Fig. 2. Temperature (left, symbols only) and salinity (right, connected symbols) measurements through an ice hole at ~77°53'S, 166°53'E, in water ~575m deep in McMurdo Sound, from May 1960 through March 1961 [20]. For most months, the standard-depth observations have been averaged from 2 or 3 separate casts a week or two apart.

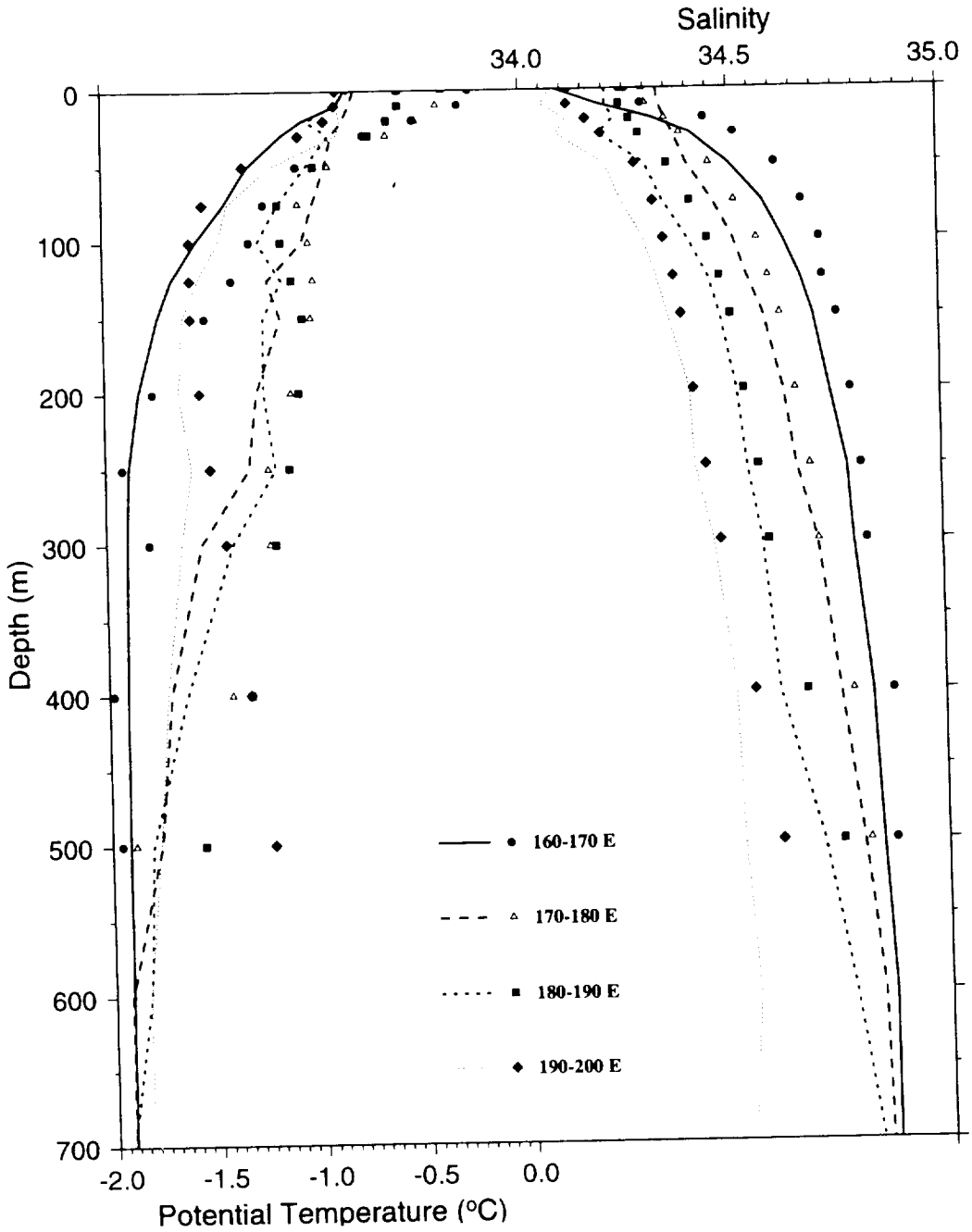

Fig. 3. Depth-averaged temperature (left) and salinity (right) from summer (DJF) stations in Table 1 (continuous lines), and from data objectively interpolated into one-degree grids at standard levels in the NODC World Ocean Atlas [22] (discrete symbols). Both data sets are divided into 10-degree meridional bands and restricted to summer stations/grids south of the continental shelf break. This figure has been truncated at 700m, below which measurements in the two western bands extend ~monotonically to 900 and 1200 m.

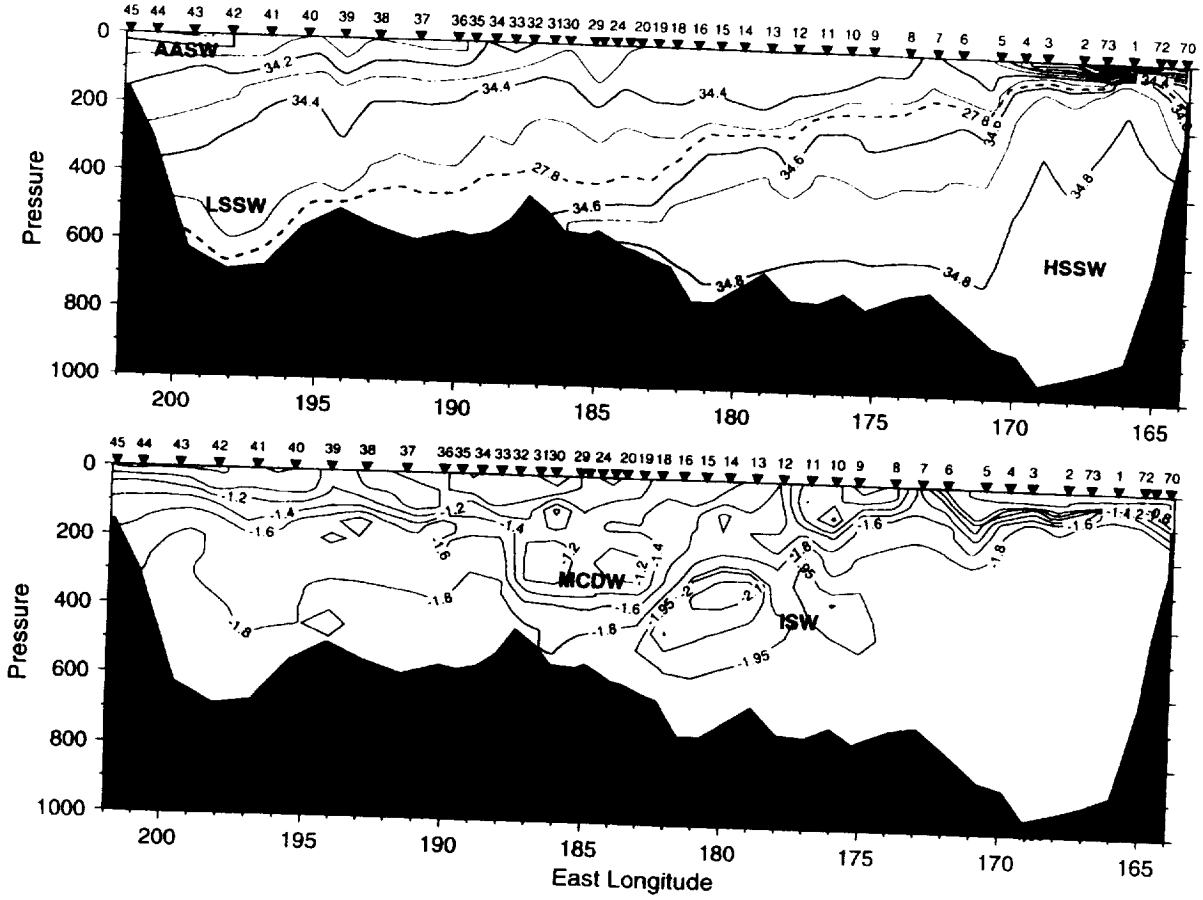

Fig. 4a. Salinity and potential temperature along the Ross Ice Shelf front and westward across McMurdo Sound (right) from ocean stations (numbers at the top; locations in Figure 1) in early February 1984. From the continuous vertical measurements at each CTD station, projected onto 77.5°S, a 50 dbar by 1° longitude grid was derived and machine-contoured, removing some of the spatial variability. Pressure (in decibars) is roughly equal to depth in meters; potential temperature (°C) is within 0.03 of the in-situ temperature at these depths; salinity is in practical salinity units. The 27.8 σ_θ isopycnal illustrates the similarity between the density and salinity fields.

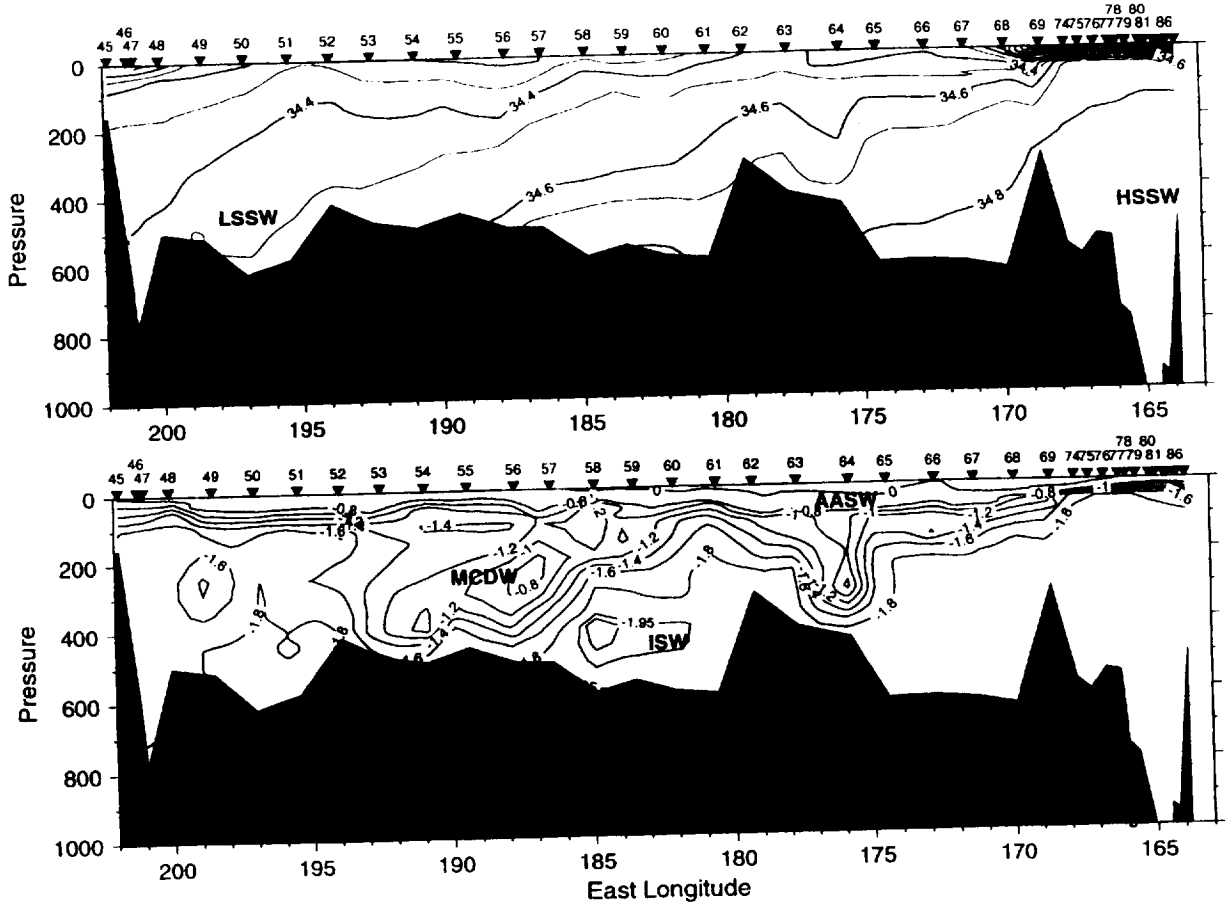

Fig. 4b. East-west section as in Figure 4a, but further north (Figure 1) extending northwest at the right end into Terra Nova Bay (74°50'S, 164°30'E).

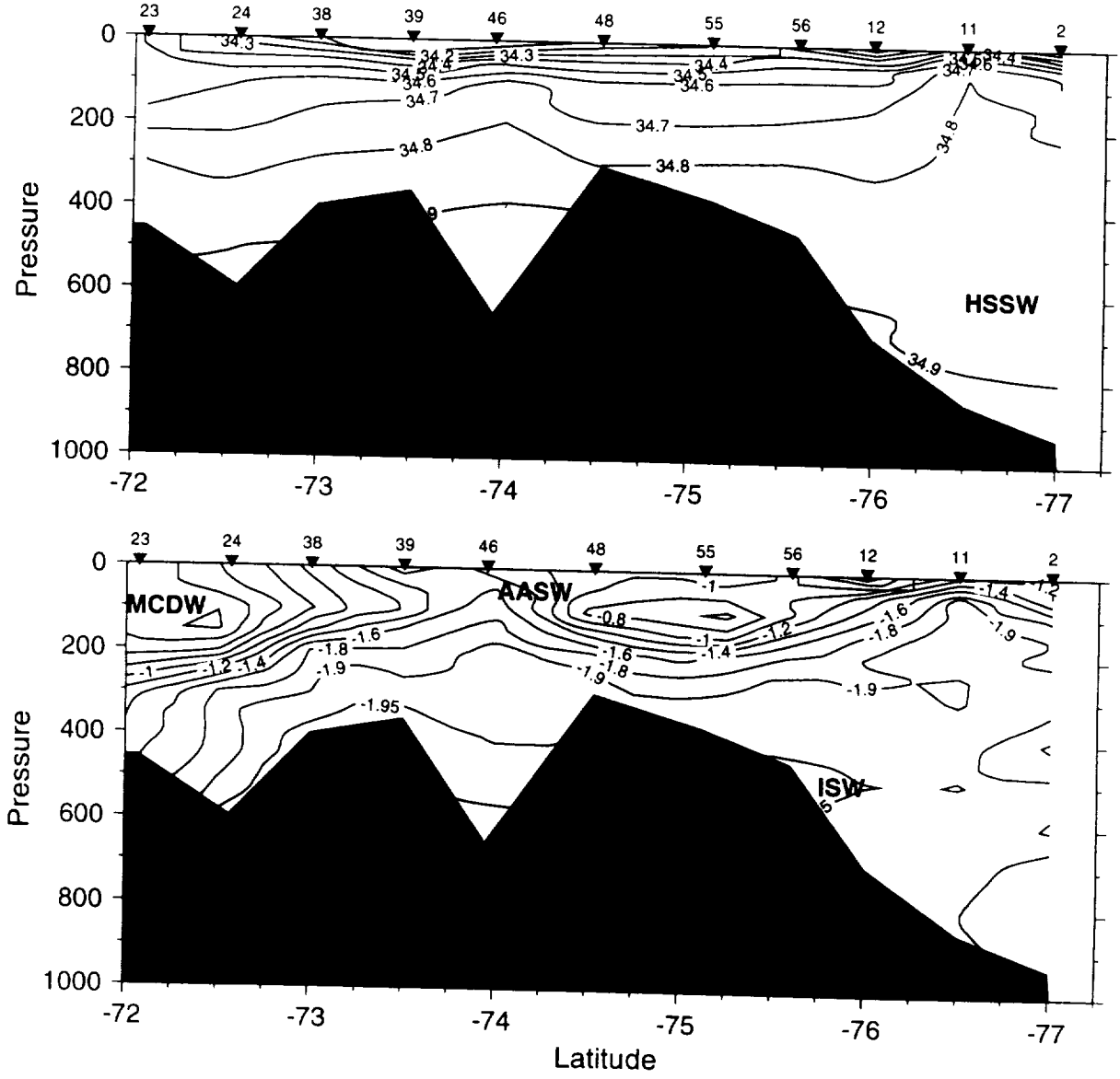

Fig. 5a. As in Figure 4a, but constructed from bottle measurements made in February 1963, and projected along a constant longitude. This western Ross Sea section extends from just south of the continental shelf break at left to the vicinity of Ross Island at right (Figure 1).The horizontal contouring grids were 0.25°and 0.5° in latitude for temperature and salinity.

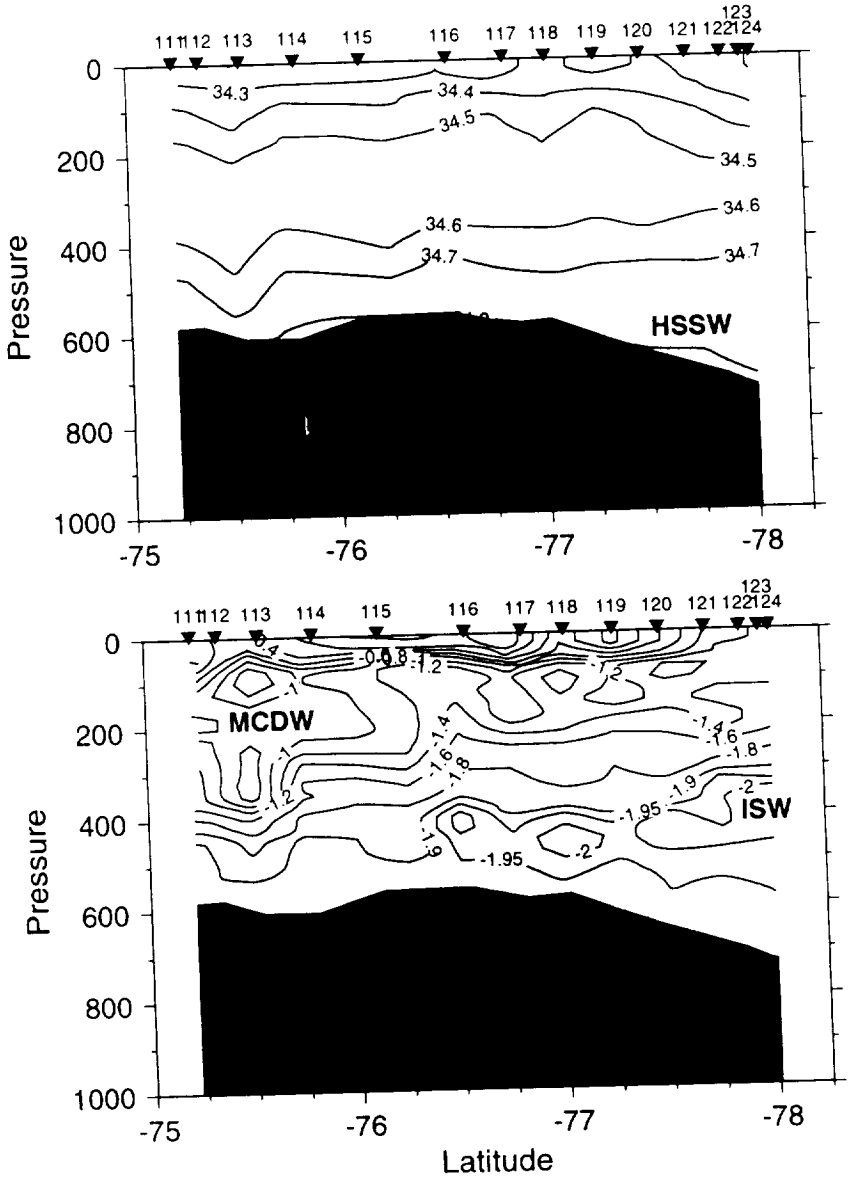

Fig. 5b. As in Figure 4a, from CTD data taken in February 1984 between the continental shelf break at left and the Ross Ice Shelf at right (Figure 1). Projected on constant longitude with 25 dbar and 0.25°latitude gridding.

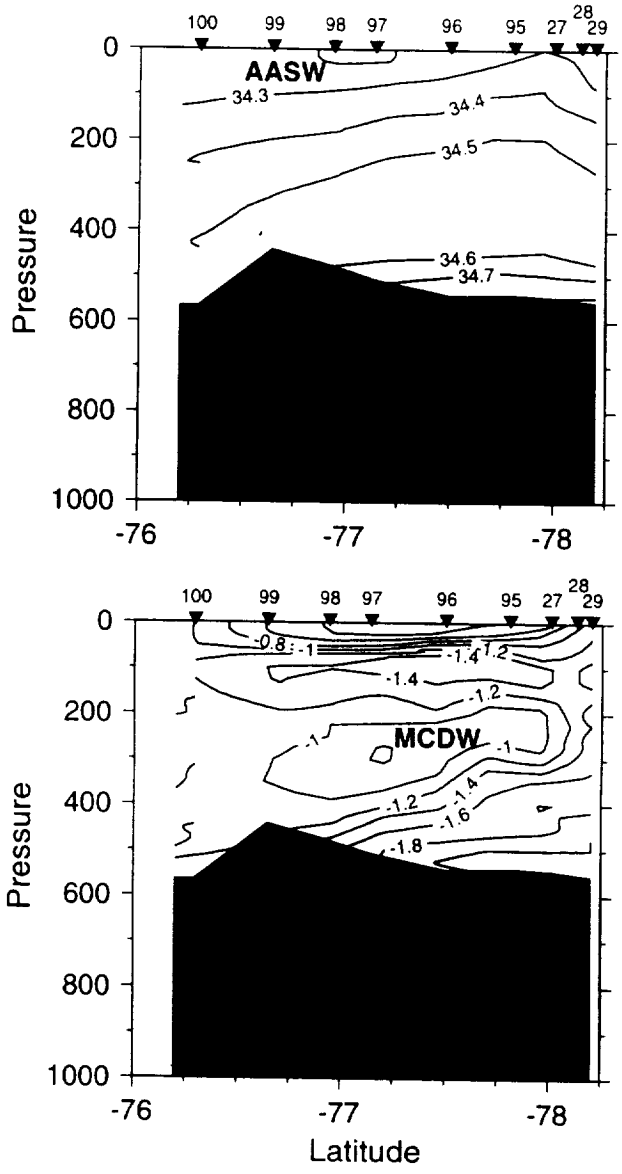

Fig. 5c. As in Figure 5b, from CTD data taken in February 1984 between the continental shelf break and the Ross Ice Shelf (Figure 1).

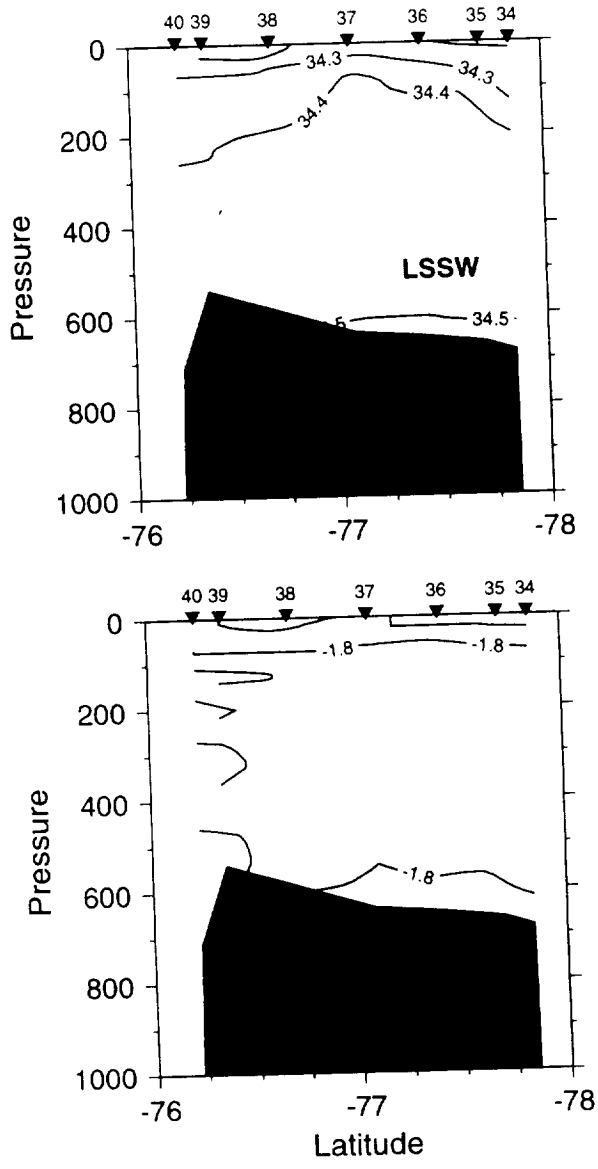

Fig. 5d. As in Figure 5b, from CTD data taken in late December 1976 between the continental shelf break and the Ross Ice Shelf (Figure 1).

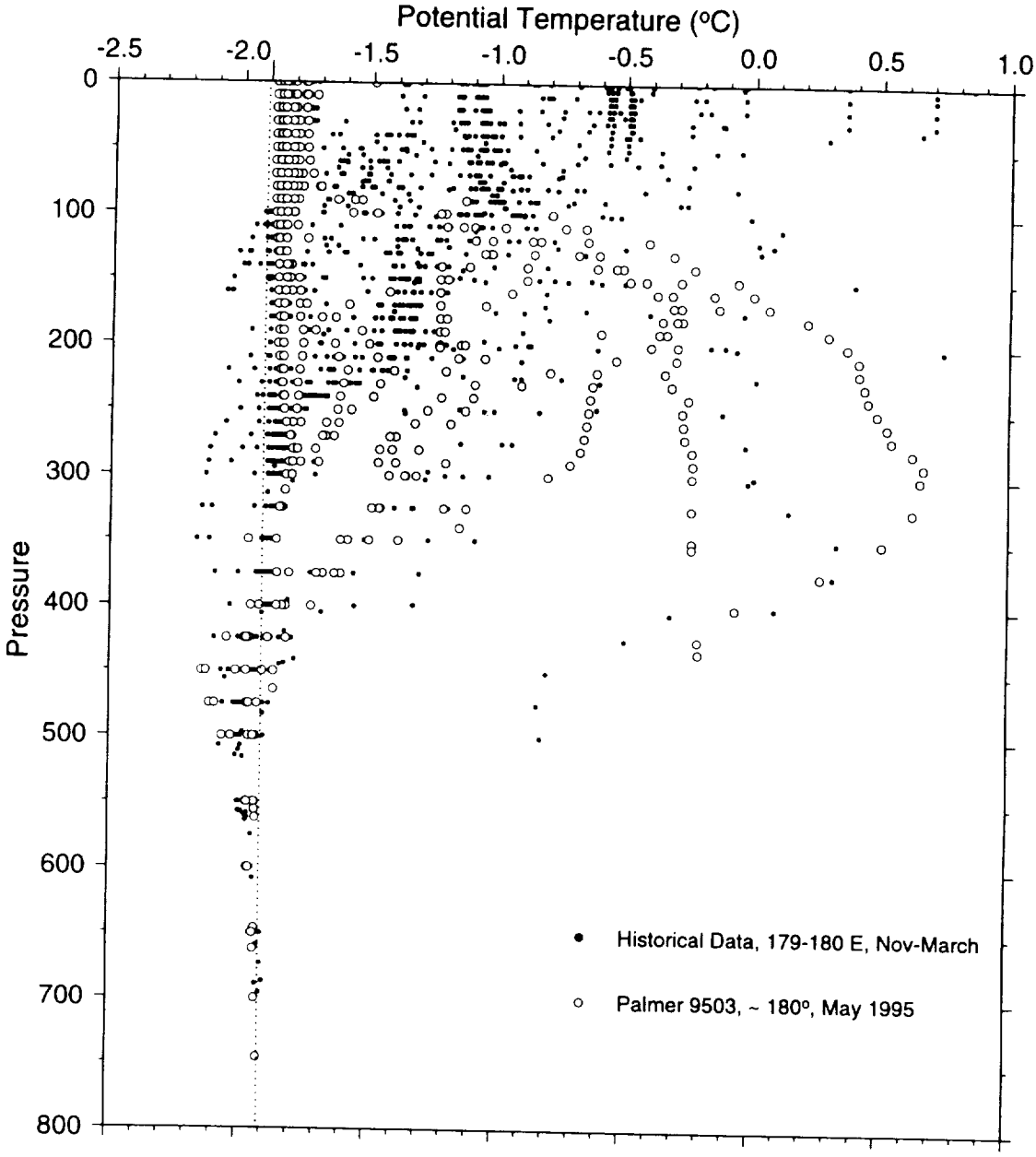

Fig. 6. Potential temperature vs pressure (in dbar) near the dateline in Figure 1. May 1995 stations from the *N.B. Palmer* appear against a background of historical summer data from the same meridional band. The vertical dotted line is the sea surface freezing point.

INTERANNUAL OCEAN AND SEA ICE VARIABILITY IN THE ROSS SEA

Stanley S. Jacobs and Claudia F. Giulivi

Lamont-Doherty Earth Observatory of Columbia University, Palisades, NY

In the context of reported environment and ecosystem changes in the McMurdo Sound region of Antarctica, we investigate evidence for interannual variability of ocean properties and circulation on the Ross Sea continental shelf. High Salinity Shelf Water, the densest water mass in the Southern Ocean, has varied by 0.15 in salinity to depths exceeding 900 m near Ross Island since the early 1960's. Temperature and salinity sections reveal similar changes along the Ross Ice Shelf front from the late 1960's through 1994, and fluctuations in the properties of Ice Shelf Water and Modified Circumpolar Deep Water. In addition to seasonal signals and semiannual oscillations characteristic of many regional atmospheric records, multiyear records of temperature and current velocities at 225-meter depths near the ice shelf display substantial changes from one year to the next. Sea ice extent in the Ross Sea oscillates at a period of 4-5 years, with summer minima roughly in phase with winter maxima. This results in large interannual cycles of sea ice range that can be correlated with meridional winds, regional air temperatures and shelf water salinities. Those temperatures have increased by 0.25°C per decade and the salinities have decreased by 0.03 per decade since the late 1950's. The observed sea ice and shelf water variability will influence the sub-ice shelf circulation and bottom water formation.

INTRODUCTION

A growing interest in climate-related issues and a lengthening record of observations have led to several reports of environment and ecosystem change in the southwest Ross Sea (Figure 1). Interdecadal variations in a sponge/predator population and in anchor/platelet ice at depths above 30 m in McMurdo Sound were attributed by *Dayton* [1989] to ocean climate shifts reflected in alterations of regional currents. *Blackburn et al.* [1991] suggested that a dramatic increase since 1980 in the number of Adelie penguins breeding in the Ross Sea region was probably the result of a recent warming in the Ross Sea climate. Weddell seals in the Sound have undergone fluctuations in reproductive rate every 4-6 years [*Testa et al.*, 1991]. For the 1958-87 period, *Weatherly et al.* [1991] found rising autumn (AMJ) temperatures of 0.8°C per decade at Scott Base. A small ice tongue in southwest McMurdo Sound has retreated significantly during the past 80 years [*Gow and Govoni*, 1994]. In the nearby Dry Valleys (~77°30'S, 122°E), *Lindner et al.* [1993] reported a steady rise since 1971 in most lake levels, which respond to glacial meltwater influx, and a general trend toward thinner lake ice. Last if not least, *Jacobs* [1985] noted a salinity decrease over two decades at ocean stations north of Ross Island.

Such changes could be caused by an evolving circulation of the atmosphere or ocean, their properties and sea-ice modulated interactions. Apparent fluctuations could also result from multiyear periodicity in combination with uneven temporal or spatial sampling. That uncertainty provided the motivation for this study of variability during recent decades in this regional hydrosphere, and in the atmosphere and cryosphere with which it interacts. We begin by describing the general ocean circulation on the Ross Sea continental shelf, and our data sources. That is followed by a consideration of evidence for interannual changes in the shelf waters and sea ice extent, particularly along the Ross Ice Shelf front. We then evaluate atmospheric variability revealed by gridded wind fields and station air temperatures, in relation to observed changes in the shelf waters. Near the end we discuss potential causes of recently fresher shelf water and apparent correlations between several of the parameters.

GENERAL CIRCULATION

The large-scale ocean circulation on the Ross Sea continental shelf is broadly known from the studies of *Killworth* [1974], *Jacobs et al.* [1985 and references therein], *Trumbore et al.* [1991], *Locarnini* [1994], and *Jacobs and Giulivi* [1998]. Surface water, low-salinity shelf water and 'Modified' Circumpolar Deep Water (MCDW; Figure 2; see also *Whitworth et al.* [this vol-

ume]) enter this shelf region from the north and east and are seasonally cooled, warmed, salinized by sea ice formation and evaporation, and freshened by meltwater and precipitation. Surface circulation on the open shelf is generally to the west and north, and is bounded by strong, narrow currents along the Ross Ice Shelf and near the Antarctic Slope Front over the upper continental slope [*Keys et al.*, 1990; *Jacobs,* 1991]. Intense winter sea ice formation is accompanied by the production of salty, nearly isothermal High Salinity Shelf Water (HSSW; Figure 2), as in the Weddell Sea [*Carmack,* 1977; *Grumbine,* 1991]. Coastal upwelling is consistent with the large-scale density field [*Killworth,* 1974], and with predominantly offshore winds and the production of ice crystals in the water column as the rising water becomes supercooled [*Foldvik and Kvinge,* 1974; *Lewis and Perkin,* 1985]. Ocean current time series at several locations on the shelf have revealed the dominant tidal and seasonal cycles, along with typical velocity ranges [e.g., *Gilmour et al.*, 1960; *Heath,* 1971; *Lewis and Perkin,* 1988; *Pillsbury and Jacobs,* 1985; *Barry and Dayton,* 1988; *Jacobs,* 1989; *Dunbar and Leventer,* 1991; *Jaeger et al.*, 1996].

The continental shelf region north of the Ross Ice Shelf is covered by sea ice in various concentrations during most of the year, with both growth and decay starting near the ice shelf in late February and in October-November, respectively. From 1979-87, the length of the summer 'open water' season on the shelf varied by about a month, with little apparent interannual change in winter ice concentration [*Jacobs and Comiso,* 1989]. The strongest northward transport of sea ice occurs in the western sector, where barrier and katabatic winds maintain the large Ross Sea Polynya adjacent to the ice shelf front [*Zwally et al.*, 1985; *Bromwich et al.*, this volume] and a small, persistent polynya near 75°S on the Victoria Land coast [*Kurtz and Bromwich,* 1985]. The volume of sea ice exported from the shelf each year has been estimated by *Zwally et al.* [1985], but satellite passive microwave data are of limited use for obtaining Antarctic sea ice thickness, direct measurements are scarce [*Jeffries and Adolphs,* 1997], and satellite radar observations are only beginning to yield comprehensive records of ice transport [*Emery et al.*, 1997].

The Antarctic continental shelf plays a significant role as a production and temporary storage site for dense shelf water. Some of that water contributes directly to bottom water formation near the continental shelf break, providing the cold, high-oxygen end member by which recent deep ocean ventilation can be identified. Salinity (density) gradients in the shelf water drive the thermohaline circulation, which is enhanced by a strong wind-driven circulation. Most HSSW, the densest water mass in the Southern Ocean, probably drains southward beneath the Ross Ice Shelf, which covers the southern half of this continental shelf. Circulation, melting and freezing under the ice shelf has been inferred from measurements near the ice front, at locations on and beneath

the ice, and from models of the thermohaline circulation [*Jacobs et al.*, 1979, 1985, 1992; *Williams and Robinson*, 1980; *MacAyeal*, 1985a,b; *Nost and Foldvik*, 1993]. Both high and low-salinity shelf waters flow into this cavity and are transformed into Ice Shelf Water (ISW; Figure 2) deep beneath the ice. The main ISW outflow extends northward to at least the continental shelf break [fig. 6a in *Jacobs et al.*, 1985]. Circumpolar Deep Water evolves rapidly into MCDW near the shelf break, and intrudes year-round at intermediate depths onto the shelf. A persistent inflow occurs near a submarine rise around 172°W, and presumably extends beneath the ice shelf before recirculating into the open Ross Sea [*Pillsbury and Jacobs*, 1985; *Keys et al.*, 1990]. Counterclockwise flow of shelf water around Roosevelt Island (79°25'S, 162°00'W) has been simulated by a 2-D numerical model, in agreement with ocean measurements in that vicinity [*Hellmer and Jacobs*, 1995].

The large-scale ocean circulation in the Ross Sea is analogous to that in the Weddell Sea, with the westward to northwestward flow on the continental shelves extending the reach of the large, deep-ocean cyclonic gyres to the north. Similar water masses exist in these large embayments, with shelf water salinities increasing from east to west adjacent to large (~500,000 km^2) ice shelves. The Ross Sea shelf regime is warmer than that in the Weddell Sea due to warmer MCDW intrusions and greater radiational heating of the more exposed summer sea surface. Less ISW is produced in the Ross Sea, a probable consequence of a thinner ice shelf (427 m average vs. 650 m for the Filchner-Ronne [*Drewry et al.*, 1982]), that is less able to exploit the pressure dependent seawater freezing point. Another factor may be a stronger tidal regime in the Weddell Sea [*St. Pierre*, 1989], where the tidal currents are typically larger than mean flows resulting from wind and thermohaline forcing [*Robertson et al.*, this volume]. The Ross Sea continental shelf has historically contained the saltiest HSSW, a likely consequence of its better-developed polynyas. A generally divergent pack and open water during summer facilitated its early exploration, and has allowed the occupation of numerous oceanographic stations on the shelf since the mid-1950's.

DATA SOURCES

Temperature and salinity data were obtained from the National Oceanographic Data Center and supplemented by more recent observations [e.g., *Giulivi et al.*, 1995; *Giulivi and Jacobs*, 1997]. Only stations south of the 600-meter isobath near the continental shelf break were utilized, after the removal of doubtful values. Most measurements were made from December through February, and have a spatial distribution that is tilted toward the southern and western sectors (Figure 1). Current and temperature data from Aanderaa RCM-4 instruments bottom-moored near the central ice shelf front

were provided by Oregon State University from recordings at 1-hr intervals during 1983 [*Pillsbury and Jacobs,* 1985] and 1984, and at 2-hr intervals in 1985 and 1986 [*Pillsbury,* unpublished]. Monthly average sea ice extents derived from satellite passive microwave data were generously provided by J. Comiso [e.g., *Comiso et al.,* 1997] and supplemented by information in *Naval Oceanography Command* [1985]. Surface air temperatures and related meteorological data were taken from *Jones and Limbert* [1987], with an update from the New Zealand National Institute of Water and Atmospheric Research, and from automatic weather station reports [e.g., *Keller et al.,* 1991]. Winds are from a National Center for Environmental Prediction - National Center for Atmospheric Research (NCEP-NCAR) reanalysis project. Both wind and Southern Oscillation Index data were obtained from the Lamont Climate Group Data Library (http://rainbow.ldeo.columbia.edu).

HIGH SALINITY SHELF WATER NEAR ROSS ISLAND

The most distinctive water mass in the Ross Sea, HSSW is concentrated in the western sector with temperatures near the sea surface freezing point. Salinities in this water mass were lower in the early 1980's than in the late 1960's, perhaps due to decreased sea ice formation or shorter shelf water residence time [*Jacobs,* 1985]. The implied change in annual sea ice formation rate could not be accounted for by the invariable winter ice concentrations noted above, and the unknown ice volume flux. The amount of brine and freshwater that are added to the HSSW during subsurface melting and freezing might be altered, but those processes could be expected to be less variable than sea surface forcing. *Hellmer and Jacobs* [1994] noted that shelf water salinity changes might also be related to fresher surface waters or weaker MCDW intrusions.

Vertical temperature profiles in the HSSW north of Ross Island (Figure 3) display a narrow range of ~ -1.90 to -1.92°C. Those temperatures are acquired at the winter sea surface, and illustrate the weak dependence of the seawater freezing point on salinity. Deep salinity at this location has varied by 0.12 to 0.15, well above the measurement accuracy over the 1963-95 period. The salinity/depth profiles can be divided into two groups, with a reduced vertical gradient (darker symbols) more common at depth on the recent stations. Although this lessened static stability should facilitate deep convection, the relatively fresher recent salinities suggest less active renewal by dense water. The highest deep salinities were measured in 1967 and the lowest in 1994, but the oldest profile (ED-03 in 1963) has intermediate values, and PS-02-03 in 1984 is saltier at most depths than GL-28 two years earlier. Any progression over time is therefore not monotonic toward lower salinity, but includes interannual variability.

The possibility of a seasonal signal within the summer data of Figure 3 is suggested by a similar salinity range measured during a year-round series of casts beneath the sea ice in McMurdo Sound (Figure 4). The column-average salinity there peaked in early November before decreasing to very low values the following March. From other information in *Tressler and Ommundsen* [1962], we infer that the last cast in March could well have resulted in erroneous data [*Jacobs and Giulivi,* 1998]. The remaining salinity range of ~0.1 at depth might be caused by peculiarities in the McMurdo Sound circulation [*Lewis and Perkin,* 1985], or by seasonal cycles advected under the ice shelf [*Hellmer and Jacobs,* 1995; see also *Nicholls and Makinson,* this volume] and then back into the open Ross Sea. Because the Figure 4 record suggests that spurious interannual variability could be inferred from persistent transients in the shelf circulation, coupled with ill-timed sampling at a particular location, it is important that evidence of interannual salinity changes be sought over a wider region.

SALINITY AND TEMPERATURE NEAR THE ROSS ICE SHELF

Vertical sections of salinity and temperature along the ice shelf front over the past three decades also reveal substantial changes in the ocean stratification (Figure 5). Stations occupied there in the late 1950's were widely spaced with large density inversions, so we begin with a 1967-68 composite of *Eltanin* and *Staten Island* bottle data. Subsequent transects are derived from continuous conductivity-temperature-depth profiles made during cruises on the *Northwind* in 1976 and the *Polar Sea* in 1984 and 1994. Water saltier than 34.9 in the late 1960's had disappeared by 1976, and the apparent volume saltier than 34.8 had fluctuated to a low point by 1994 (Figures 5a-d). This brought HSSW characteristics closer to those of the analogous Western Shelf Water in the Ronne Depression of the southwest Weddell Sea [*Gammelsrod et al.,* 1994]. On the later Ross Sea transects, a double dome of salty water occurs beneath a fresh surface layer west of ~171°E. The western dome corresponds to the inflowing limb of the cyclonic circulation in northern McMurdo Sound [*Lewis and Perkin,* 1985], with an outflow of lower-salinity water along the Victoria Land coast. Steep isohalines east of the other dome suggest flow into the sub-ice shelf cavity on the east side of Ross Island, perhaps consistent with the greater local basal melting inferred by *Bamber and Bentley* [1994] from increased ice elevation gradients in that vicinity. Lower salinity water appears across the entire Ross Ice Shelf front on the more recent sections, with isohalines ~0.1 fresher at most depths causing similar decreases in the density field. A dominant mode in the salinity interval 34.5 to 34.6 in Figures 5a and 5b has been replaced by a mode between 34.4 and 34.5 in Figure 5d. Fresher surface water on the western (right) side

in 1984 and 1994 may result from measurements later in the melt season. Near-bottom conditions (Figure 6) show a slightly larger salinity decrease in the western than in the eastern Ross Sea, and little change in salinity gradient strength on the western flank of the submarine rise near 187°E.

The temperature sections in Figure 5 (e-h) reveal more subtle changes with time, since temperature is set by the sea surface freezing point thoughout much of the deep domain. The primary ISW outflow (T<-1.95°C) is located between 300 and 500 dbar near 180°E, and occupies a somewhat smaller area on the later sections. Minor outflows appear at the eastern end of the 1960's transect and at scattered locations on the other sections, often on individual stations that are not obvious from the contoured grid. *Jacobs et al.* [1992] showed that ISW outflow volume and salinity can be used to infer the basal melt rate deep beneath the ice shelf. A comparison of the temperature and salinity panels of Figure 5 reveals that the ISW salinity is more variable than its temperature or area, lower when salinity is lower in the HSSW from which it is formed. To the extent that ISW participates in deep ocean ventilation north of this region [*Jacobs et al.*, 1985], that could influence the properties and volume of bottom water formed near the continental shelf break. Bottom temperature along the ice shelf front (Figure 6) displays a less coherent bottom shift than does bottom salinity, and a greater variability in the eastern sector.

MODIFIED CIRCUMPOLAR DEEP WATER VARIABILITY

The MCDW in Figure 5 is best developed over the topographic high near 187°E, with temperatures ranging from -1.0 to -1.5°C near the ice shelf front. Some of the apparent temporal changes in temperature and volume may result from the narrow width of this high latitude flow, in combination with the wider and more variable station spacing on the earlier transects. Closer spacing on the 1984 section (Figure 5g) resolved the MCDW into two distinct features, and accompanying current measurements revealed southward flow in the eastern core and recirculating northward flow to the west. MCDW occurs above the submarine rise on all transects, in spite of the salinity changes over time (Figure 5a-d), supporting the idea that its position is controlled by the bathymetry of the sea floor [*Visser and Jacobs*, 1987], and perhaps locally by the inverted topography of the ice shelf base. The cooler MCDW encountered in 1994 (Figure 5h) would likely have lowered the melt rate at the outer ice shelf base. West of its primary location near the ice front, MCDW inflows override the denser HSSW. For example, in the 1967-68 transects MCDW is centered at a salinity just above 34.5, an isohaline that approaches the sea surface around 172°E and outcrops at the western end of the section. Thermohaline data alone are insufficient to determine the ori-

gin of late-summer surface water, but the westward shoaling isohalines (isopycnals) in Figures 5a-d and a generally cyclonic near-surface circulation indicate that upwelling MCDW will influence surface water properties in the southwest Ross Sea.

Most time-series records obtained on the Ross Sea continental shelf from ice- and bottom-moored instruments include current velocity for periods of up to one year. Many also include temperature, but salinity measurements have typically been degraded by sensor drift. Velocity and temperature records 3.75 years in length can be assembled from three Aanderaa RCM-4 current meters moored at about the same location near the ice front from early 1983 to early 1987 (Figures 1 and 5g). Monthly average meridional velocities at that site show the dominant southward flow of MCDW, stronger during winter when atmospheric forcing and brine release are greater (Figure 7a). Seawater temperature also displays a regular annual cycle (Figure 7b), with most cooling from March through May, as variable amounts of near-freezing surface water reach these intermediate depths, followed by warming from October through January. Seawater temperature lags the air temperature (Figure 7c) by about a month throughout the year. The water temperature and most velocity curves show an early winter reversal or plateau followed by late winter cooling, similar to air temperature records at nearby sites on the ice shelf. This semiannual oscillation appears in many high southern latitude atmospheric records [*Van Loon,* 1967], and in other subsurface temperature records near the ice shelf front [*Jacobs and Comiso,* 1989]. Monthly average water temperatures at these 211-240 m depths remained above the sea surface freezing point year-round, an indication that the MCDW supplies sensible heat to the Ross Sea Polynya and influences its sea ice formation rate.

MCDW obtains its characteristic temperature signal near the continental slope from the massive Circumpolar Deep Water reservoir. The properties of that reservoir will change relatively slowly with time, but MCDW may be drawn onto the shelf from different deep or slope water strata at different times in response to the shifting density field on the continental shelf. The lower shelf water densities in 1994 may thus account for the relatively weak MCDW signal in 1994 (Figure 5h). The volume and properties of MCDW may also vary in response to changes in the export of lighter surface and denser shelf waters, and to vertical mixing driven by winds and seasonal brine release. At the MCDW mooring site, year-to-year changes in temperature and current velocity were largest during autumn and early winter (Figure 7). Relatively low temperatures during early 1983 were offset by high velocities for most of that year, resulting in 75% higher southward heat transport that year than in 1984. At the surface, however, 1984 was a relatively warm year compared with 1987-91 (Figure 7c). February-October water temperatures were

0.1-0.2°C warmer in 1985-86 than in 1983-84, opposite the Scott Base air temperature pattern discussed below.

In summary, temporal or spatial changes in MCDW volume cannot be determined from the records at a single mooring site. While the temperature and current variability could result from shifts in ocean characteristics or circulation strength, the instruments were located on the eastern edge of the MCDW inflow (Figure 5g), and could as well have recorded meandering of this narrow current. Ocean station data also do not reveal consistent interannual patterns near the MCDW temperature maximum, probably because the thin, intermediate depth intrusions are poorly sampled and strongly influenced by surface variability. These brief mooring records give us a sense of the seasonal and interannual variability of subsurface temperature and velocity in the south-central Ross Sea, but are inadequate to determine quantitative temporal changes in MCDW flow onto the shelf.

SEA ICE EXTENT

Sea ice integrates a variety of small- to large-scale atmospheric and oceanic processes. The satellite passive microwave record of monthly average ice extent (area of pixels with >15% ice concentration) now exceeds two decades in the Ross Sea (Figure 8). Ice extent fluctuations in this sector reflect forcing over a larger region than our study area. However, sea ice formed on the Ross Sea continental shelf is exported to a much wider area, and most regional ice that survives the summer season drifts over or toward the shelf. In this regime both the winter and summer extremes undulate over periods of several years (Figure 8). The winter maxima are roughly in phase with the summer minima, and vice-versa, as has been noted previously for shorter records in other sectors [*Zwally et al.*, 1983; *Jacobs and Comiso*, 1997]. Winter maxima lead the following summer minima in a table of daily extremes in the Weddell Sea [*Comiso and Gordon*, 1998], but such a relationship is not always present in these monthly averaged Ross Sea records. In addition, at the summer minimum the Ross Sea monthly ice extents appear to be more variable than the Weddell Sea daily ice cover.

The seasonal sea ice range for each year, i.e., the difference between the 3-month averages of the highest and lowest (always JFM) ice extents, fluctuates with a period of 4-5 years (Figure 9a). That is slightly longer than the expected passage through this sector of a regular wave in the northward sea ice edge [fig. 1 in *White and Peterson*, 1996], perhaps due to the different sea ice indices used. Since summer minima tend to balance winter maxima in Figure 8, the annual average ice extent will vary less than might be inferred from changing positions of the northern ice edge. A northern ice edge index could also differ substantially from actual ice area or extent when there are large and variable coastal polynyas. In any case, the near-coincidence of winter maxima

and summer minima are presumably associated with periods of stronger northward meridional winds and currents, which would advect more ice and surface water from the continental shelf. That would leave behind on the shelf thinner ice that is more easily melted during summer, and a thinner surface layer that is more readily penetrated during winter. Conversely, lower winter and higher summer ice extents should correspond to periods of thicker ice, but weaker atmospheric and oceanic circulations.

WIND

Instrumental wind records from this region are less continuous than the satellite sea ice record, or relatively short or characteristic of local conditions near the stations. Gridded wind analyses by the European Center for Medium-range Weather Forecasting date from 1985 and are subject to changes in model technique over time [*Bromwich and Robasky,* 1993]. Here we utilize an NCEP-NCAR product that provides monthly average wind components on a 2.5° grid beginning in January 1974. Annual average near-surface meridional wind speeds from 160-230°E and 60°-80°S are predominantly northward, with a range of ~1 m s^{-1} and a periodicity similar to that of the sea ice range (Figure 9a). The wind and ice fluctuations appear to be roughly in phase, with a high ice range corresponding to stronger northward winds. Notable exceptions occurred in 1980 and 1992, years that are also anomalous in other sectors [*Jacobs and Comiso,* 1997; *Comiso and Gordon,* 1998]. An annual average of the Southern Oscillation Index, the difference between the standardized Tahiti and Darwin sea level pressures, appears more negative over the period for which sea ice and wind analyses are shown in Figure 9a. The similar cycles in these three records suggests coupling between the high and low latitude atmospheric circulations in the South Pacific (see also *Smith et al.* [1996], *Ledley and Huang* [1997] and references therein).

The correlation between meridional winds and sea ice range the same year is positive, but not very strong (Figure 10a). Of course other factors than the meridional wind stress will influence sea ice extent, which seasonally covers a smaller area than the sector-average winds we have utilized. For example, two record-warm months in 1988 may have contributed to an observed ice extent lower than would be inferred from the average winds that year (Figures 10a and 10b). In addition, stronger southerly winds over the western shelf could lead to more compact ice in the Victoria Land embayment, at the expense of greater ice expansion. The zonal wind component (not shown here) also displays considerable interannual variability. Stronger westerly winds north of the central Ross Sea Gyre would increase sea ice extent, as in *Fletcher* [1969], but stronger easterlies to its south and over the continental shelf would have the opposite effect.

AIR TEMPERATURE

Air temperatures have been regularly logged in the Ross Sea since the late 1950's. A four-decade annual average record from Scott Base in southeastern McMurdo Sound (Figure 9b) indicates a trend of +0.25°C/decade [see also table 1 in *Jones*, 1995]. Over this period the large autumn (AMJ) trend noted in the Introduction dropped to 0.3°C/decade, as more cool years have been experienced since 1988. The interannual variability at this site is also high [*Sansom*, 1989] and has a bimodal character with a range of ~2°C. The moving mean over four years shows gradual rises interrupted by brief reversals, and hints of interdecadal periodicity. The Scott Base data are coherent with shorter-term observations from Franklin Island (Figure 1) and the air temperature cycles appear to correlate positively with sea ice range, at least through the mid-1980's. This may seem counter-intuitive, if not contrary to observations in the Southeast Pacific showing higher air temperature coincident with lower ice extent [*Weatherly et al.*, 1991; *Smith et al.*, 1996; *Jacobs and Comiso*, 1997]. However, greater sea ice range corresponds to less sea ice cover during summer. In addition, *Bromwich et al.* [this volume] indicate that warmer maritime air from atmospheric lows is entrained into katabatic surge events. Those events open the Ross Sea Polynya, but that will in turn lead to overall ice growth in this offshore-wind environment. The phasing in Figure 9 appears to shift in the late 1980's, perhaps similar to a pattern between derived ice sheet accumulation and the Southern Oscillation Index [*Cullather et al.*, 1996].

Annual average air temperature vs. sea ice range (Figure 10b) bears out the positive relationship noted above. The 1988 year is again an outlier, as in Figure 9, and 1976 included two months of record-low air temperatures. A weak correlation may indicate a stronger continental than maritime influence on the Scott Base winds, a possible factor in the lack of a strong connection between air temperature and sea ice concentration over this shelf region from 1979-87 [*Jacobs and Comiso*, 1989]. As longer ice and atmospheric records become available, more open water in the southern Ross Sea may be found to correlate with increased cyclonic activity. Certainly greater sea to air heat flux over the shelf and slope region could be expected when the sea ice is thinner or more dispersed, increasing air temperature at times of large ice range.

SALINITY OF THE HIGH SALINITY SHELF WATER

The salinity and volume of HSSW should increase in response to stronger winter surface forcing, coincident with the more rapid removal of newly formed sea ice. At these times more brine would drain into the HSSW, some of it well north of the southern coastal regions de-

picted in Figures 3-7. To evaluate this response, we averaged summer (DJF) ocean station data from 450-550 m throughout the western Ross Sea (Figure 9c). Most sampled years have data in both the 160-170°E and 170-180°E meridional bands, allowing a correction for the zonal salinity gradient when that was not the case. Large time gaps in the ocean data set confound pattern matching with the ice and wind records, but it is apparent that HSSW salinity displays considerable interannual variability, along with a salinity trend of -.03 per decade. Given the discontinuous nature of the ocean data and the large short-term changes, this decrease is of doubtful significance. HSSW salinity was higher in 1990 and 1991, e.g., than in 1958 and 1959. However, understanding the apparent drift toward lower salinities on the Ross Sea continental shelf over nearly four decades (see also Figure 5) could provide insight into the observed variability of shelf and deeper water in other sectors [e.g., *Nost and Osterhus*, this volume; *Gordon*, this volume]. In the next paragraphs we expand on earlier comments concerning possible causes for a decrease in shelf water salinity.

Freshening of HSSW could result from several processes, acting separately or in tandem, the most obvious being a decrease in brine drainage due to less sea ice formation. A salinity decrease of 0.12 in a 500 m-thick layer of HSSW with a 4-year residence time [*Trumbore et al.*, 1991] would correspond to 50 cm less sea ice now being formed each year in the southwest Ross Sea vs. 40 years ago. A change in that direction is consistent with the observed Scott Base temperature rise in Figure 9b, i.e., higher air temperatures could be expected to result in less sea ice formation and brine drainage into the HSSW. Related evidence might also be inferred from whaling data, which reportedly suggest an abrupt decrease in sea ice extent prior to the mid-1970's [*de la Mare*, 1997]. While the apparent multidecadal freshening of HSSW in Figure 9c depends on the higher salinities prior to 1973, annual average sea ice extent in the Ross Sea since that first year of routine satellite coverage has varied by as much as 20% from the mean, with no significant upward or downward trend.

A second parameter that will influence HSSW salinity is freshwater added at the sea surface or below. The additional precipitation and/or runoff that would be required to effect the measured salinity decrease seems unlikely without larger air temperature increases. In particular, a substantial proportion of snow, including that blown off the ice sheet, will land on the sea ice and, if not converted into snow ice [*Jeffries and Adolphs*, 1997], will be transported off the continental shelf. A connection with increased subsurface melting of the Ross Ice Shelf seems improbable, as lower salinity (density) HSSW would reduce the strength of the thermohaline circulation beneath the ice. That should also reduce the rate of basal melting [e.g., *Nicholls and Makinson*, this volume]. Any corresponding increase in basal freezing, or in the formation of ice platelets in water

north of the ice shelf [e.g., *Bombosch,* this volume], would produce a salinity change opposite in direction to that observed.

Freshening could also result from a stronger shelf circulation, since a shorter residence time would decrease the amount of brine that HSSW could accumulate. However, the lower salinities in recent years would tend to weaken the thermohaline circulation, as noted above, and we have no evidence that wind strengths have increased over this period. HSSW evolves from fresher surface and shelf waters, and from MCDW, the properties of which may also change on decadal time scales. For example, higher air temperature and more open water should increase runoff and precipitation into the AASW, which would then soak up more of the winter brine that would otherwise penetrate into the HSSW. Other potential factors even include the variable shape and position of the Antarctic coastline. That is, brine production in coastal polynyas is likely to vary with the dimensions of upstream ice tongues, icebergs [*Kurtz and Bromwich,* 1985; *Nost and Osterhus,* this volume], and ice fronts. The steady northward advance of the western side of the Ross Ice Shelf front over recent decades [*Jacobs et al.,* 1986; *Keys et al.,* 1998] may have gradually reduced the size or intensity of the Ross Sea Polynya. To cause a net HSSW salinity decrease, this would have had to exceed the effect of any contemporary increase in the size of the Terra Nova Bay Polynya, which is protected by the Drygalski Ice Tongue near 75°S on the Victoria Land coast [*Frezzotti and Mabin,* 1994]. Some coastline changes will also move their adjacent low-salinity coastal currents, and could alter the nature and position of the quasi-permanent gyres or upwelling regions that are suggested by the HSSW domes near Ross Island.

Returning to interannual HSSW salinity changes, a positive correspondence between shelf water salinity and sea ice range the preceding winter is illustrated in Figure 10c. This seems consistent with a scenario of stronger atmospheric forcing at times of greater sea ice range and higher salinity. The scattered station locations, salinity measurement accuracy and inclusion of time-lagged, lower-salinity ISW in the 450-550 m depth interval will contribute to the scatter. Calculating salinity range between the two extreme months each year does not improve the fit, nor does a weighted averaging of sea ice range up to four years prior to the salinity measurements. Unfortunately, the 4-year HSSW residence time of *Trumbore et al.* [1991] now appears similar to the periodicity in surface forcing.

In Figure 11 the zonal salinity gradient is roughly correlated with the mean salinity at 500 ± 50 m. The regression slope implies a stronger geostrophic circulation when the zonal gradient is high and mean salinity is low. This is out of phase with the surface forcing, but could result from a time-lagged ISW outflow or spatially variable HSSW loss from the shelf. Alternatively, more active recharging of the eastern side of the HSSW

reservoir would decrease the zonal gradient. That is, stronger surface forcing may increase HSSW salinity and/or volume in the 170-180°E band, which includes the Ross Sea Polynya, more than it does the 160-170°E band that includes polynyas along the Victoria Land coast.

CONCLUSIONS

The annual range of sea ice extent in the Ross Sea and annual average air temperature in its southwestern sector vary over interannual cycles of several years duration. Higher winter and lower summer ice extents are roughly in phase, are accompanied by stronger northward winds and higher local air temperatures, and are followed by higher shelf water salinities. The thermohaline circulation strength on the open continental shelf should respond on a similar cycle and cause sympathetic fluctuations in the sub-ice shelf regime. The salinity of the ISW outflow appears to correlate positively with changes in the HSSW salinity. MCDW brings salt and heat onto the continental shelf year-round, and will thus contribute to shelf water salt budgets and to polynya maintenance. Changes in shelf water salinity have altered the density but not the location of the primary MCDW intrusion near the central ice shelf front.

A four-decade trend toward fresher HSSW, while similar to the large interannual variability, is comparable in magnitude to the "Great Salinity Anomaly" in the North Atlantic Ocean [*Dickson et al.*, 1988]. The salinity decrease parallels increasing air temperatures in the southwest Ross Sea over the same period and could imply regionally thinner sea ice. Because HSSW evolves into other key water masses, temporal changes are also likely in the characteristics or volume of bottom water that issues from the Ross Sea, with implications for the interpretation of oceanographic data in downstream locations [e.g., *Rintoul*, this volume]. This suggests that similar changes in shelf waters related to sea ice cycles [*Drinkwater*, personal communication, 1997; *Comiso and Gordon*, 1998] might account for recently fresher bottom water in the Weddell Sea [*Gordon*, this volume].

Sponges and penguins may well be insensitive to 0.1-0.2 salinity changes in the deep shelf waters, but associated shifts in sea ice cover or thickness or other near-surface parameters [*Murphy et al.*, 1995] could be important. If changes in ocean currents bathe new areas of the sea floor in near-freezing water, forming anchor ice or ice crystals that subsequently rise through the water column, that could be a liability for some benthic species. If circulation changes include greater upwelling and intrusion of deep water onto the shelf, a fresher and more stable mixed layer or stronger ocean fronts, that could be an asset to other components of the ecosystem. The idea that Adelie penguins could benefit from a warmer climate may be questionable for the Antarctic Peninsula region [*Kaiser*, 1997], but Weddell Seal pupping cycles

appear to reflect some of the interannual fluctuations we have noted here.

Much work remains to confirm, refine and extend the cycles and connections outlined above. Particular efforts should be made to acquire long time-series salinity measurements in the deep southwest Ross Sea, determine the volume of sea ice exported from the continental shelf, and investigate relationships between MCDW and shelf water variability. Longer records will be needed to assess the significance of apparent trends in the regional air temperature and HSSW over recent decades.

Acknowledgments. We thank J. Ardai, P. Catanzaro, J. Comiso, S. O'Hara, S. Peng and others for assistance with data acquisition, reduction and presentation, R. Weiss for editorial control, and K. Aagaard, S. Levitus, R. Locarnini and anonymous reviewers for helpful comments on the manuscript. This work was supported by the NASA Polar Research Program (NAGW 3362) and the National Science Foundation (OPP-94-18151). Lamont-Doherty Earth Observatory contribution # 5728.

REFERENCES

Bamber, J. and C. R. Bentley, A comparison of satellite-altimetry and ice-thickness measurements of the Ross Ice Shelf, Antarctica. *Ann. Glaciol.*, 20, 357-364, 1994.

Barry, J. P. and P. K. Dayton, Current patterns in McMurdo Sound, Antarctica, and their relationship to local biotic communities, *Polar Biol.*, 8, 367-376, 1988.

Blackburn, N., R. H. Taylor and P. R. Wilson, Interpretation of the growth of the Adelie penguin rookery at Cape Royds, 1955-1990, *N.Z. J. Ecol.*, 15(2), 117-121, 1991.

Bombosch, A., Interactions between floating ice platelets and ocean water in the southern Weddell Sea, this volume.

Bromwich, D. H., and F. M. Robasky, Recent precipitation trends over the polar ice sheets, *Meteorol. Atmos. Phys.*, 51, 259-274, 1993.

Bromwich, D. H., Z. Liu, M. L. Van Woert and A. Rogers, Winter atmospheric forcing of the Ross Sea Polynya, this volume.

Carmack, E. C., Water characteristics of the Southern Ocean south of the Polar Front, in *A Voyage of Discovery*, G. Deacon 70th anniv. vol., Suppl. to Deep-Sea Res., edited by M. Angel, pp 15-41, Pergamon, Oxford, 1977.

Comiso, J. C., D. J. Cavalieri, C. L. Parkinson and P. Gloersen, Passive microwave algorithms for sea ice concentration : A comparison of two techniques, *Remote Sens. Environ.*, 60, 357-384, 1997.

Comiso, J. C. and A. L. Gordon, Interannual variability in summer sea ice minimum, coastal polynyas and bottom water formation in the Weddell Sea, in *Antarctic Sea Ice: Physical Processes, Interactions and Variability, Antarct. Res. Ser.* vol. 74, edited by M. Jeffries, pp 293-316, AGU, Washington, DC, 1998.

Cooper, A. K., P. F. Barker and G. Brancolini (editors), *Geology and Seismic Stratigraphy of the Antarctic Margin, Antarct. Res. Ser.* vol. 68, 301 pp, Atlas, CD-ROMS, AGU, Washington, DC, 1995.

Cullather, R. I., D. H. Bromwich and M. L. Van Woert, Interannual variations in Antarctic precipitation related to El Nino Southern Oscillation, *J. Geophys. Res.*, 101(D14), 19109-19118, 1996.

Dayton, P. K., Interdecadal variation in an Antarctic sponge and its predators from oceanographic climate shifts, *Science*, 245, 1484-1486, 1989.

de la Mare, W. K., Abrupt mid-twentieth-century decline in Antarctic sea-ice extent from whaling records, *Nature*, 389, 57-60, 1997.

Dickson, R. R., J. Meincke, S-A. Malmberg and A. J. Lee, The "Great Salinity Anomaly" in the northern North Atlantic 1968-1982, *Prog. Oceanog.*, 20, 103-151, 1988.

Drewry, D. J., S. R. Jordan and E. Jankowski, Measured properties of the Antarctic ice sheet: Surface configuration, ice thickness, volume and bedrock characteristics, *Ann. Glaciol.*, 3, 83-91, 1982.

Dunbar, R. B. and A. Leventer, Circulation in eastern McMurdo Sound, Antarctica, January through November 1990, *Ant. J. of the U.S.*, 26(5), 117-120, 1991.

Emery, W. J., C. W. Fowler and J. A. Maslanik, Satellite-derived maps of Arctic and Antarctic sea ice motion: 1988 to 1994, *Geophys. Res. Lett.*, 24(8), 897-900, 1997.

Fletcher, J., Ice extent on the Southern Ocean and its relation to world climate, RM-5793-NSF, 119 pp, Rand Corp., Santa Monica, CA, 1969.

Foldvik, A. and T. Kvinge, Conditional stability of sea water at the freezing point, *Deep-Sea Res.*, 21(3), 169-174, 1974.

Frezzotti, M. and M. C. G. Mabin, 20th century behavior of the Drygalski Ice Tongue, Ross Sea, Antarctica, *Ann. Glaciol.*, 20, 397-400, 1994.

Gammelsrod, T., A. Foldvik, O. A. Nost, O. Skagseth, L. G. Anderson, E. Fogelqvist, K. Olsson and T. Tanhua, Distribution of water masses on the continental shelf in the southern Weddell Sea, in *The Polar Oceans and their Role in Shaping the Global Environment, Geophys. Mono. Ser.* vol. 85, edited by O. Johannessen, R. Muench and J. Overland, pp. 159-176, AGU, Washington, DC, 1994.

Gilmour, A. E., W. J. MacDonald and F. G. Van der Hoeven, Ocean currents in McMurdo Sound, *Nature*, 187, 867, 1960.

Giulivi, C. F, S. S. Jacobs, S. H. O'Hara and J. L. Ardai, Ross Sea Polynya Project, 1994: Oceanographic data on NB Palmer cruise 9406, Tech. Rept. 95-1, 315 pp, Lamont-Doherty Earth Observatory, Palisades, NY, 1995.

Giulivi, C. F. and S. S. Jacobs, A zonal oceanographic section in the southern Ross Sea: USCGC Polar Sea, February 1994, Tech. Rept. 97-2, 90 pp, Lamont-Doherty Earth Observatory, Palisades, NY, 1997.

Gordon, A. L., Western Weddell Sea thermohaline stratification, this volume.

Gow, A. J. and J. W. Govoni, An 80-year record of retreat of the Koettlitz Ice Tongue, McMurdo Sound, Antarctica, *Ann. Glaciol.*, 20, 237-241, 1994.

Grumbine, R. W., Model of the formation of high-salinity shelf water on polar continental shelves, *J. Geophys. Res.*, 96(C12), 22049-22062, 1991.

Heath, R. A., Circulation and Hydrology under the seasonal ice in McMurdo Sound, Antarctica, *N. Z. J. Mar. Freshwater Res.*, 5(3,4), 479-515, 1971.

Hellmer, H. H. and S. S. Jacobs, Temporal changes in shelf water of the southern Ross Sea, *Ant. J. of the U. S.*, 29(5), 123-124, 1994.

Hellmer, H. H. and S. S. Jacobs, Seasonal circulation under the eastern Ross Ice Shelf, Antarctica, *J. Geophys. Res.*, 100(C6), 10873-10885, 1995.

Hofmann, E. E. and J. M. Klinck, Hydrography and circulation of the Antarctic continental shelf: 150°E to the Greenwich Meridian, Chapter 35 in *The Sea, The Global Ocean, Regional Studies and Synthesis*, vol. 11, edited by K. Brink and A. Robinson, Wiley, in press, 1998.

Jacobs, S. S., Oceanographic evidence for land ice/ocean interactions in the Southern Ocean, in *Glaciers, Ice Sheets, and Sea Level: Effects of a CO_2 Induced Climatic Change*, Report of a Workshop, Seattle, 13-15 Sept. 1984, pp 116-128, Nat. Acad. Press, Washington, DC, 1985.

Jacobs, S. S., Marine controls on modern sedimentation on the Antarctic continental shelf, *Mar. Geol.*, 85, 121-153, 1989.

Jacobs, S. S., On the nature and significance of the Antarctic Slope Front, in Biochemistry and Circulation of Water Masses in the Southern Ocean, edited by P. Treguer and B. Queguiner, *Mar. Chem.*, 35, 9-24, 1991.

Jacobs, S. S. and J. C. Comiso, Sea ice and oceanic processes on the Ross Sea continental shelf, *J. Geophys. Res.*, 94, 18195-18211, 1989.

Jacobs, S. S. and J. C. Comiso, Climate variability in the Amundsen and Bellingshausen Seas, *J. Clim.*, 10(4), 697-709, 1997.

Jacobs, S. S. and C. F. Giulivi, Thermohaline data and ocean circulation on the Ross Sea continental shelf, in *Oceanography of the Ross Sea - Antarctica*, edited by G. Spezie and G. Manzella, Springer-Verlag, Heidelberg, in press, 1998.

Jacobs, S. S., A. L. Gordon and J. L. Ardai, Jr., Circulation and melting beneath the Ross Ice Shelf, *Science*, 203, 439-442, 1979.

Jacobs, S. S., R. G. Fairbanks and Y. Horibe, Origin and evolution of water masses near the Antarctic continental margin: Evidence from $H_2{}^{18}O/H_2{}^{16}O$ ratios in seawater, in *Oceanology of the Antarctic Continental Shelf, Ant. Res. Ser.* vol. 43, edited by S. Jacobs, pp 59-85, AGU, Washington, DC, 1985.

Jacobs, S. S., D. R. MacAyeal and J. L. Ardai, Jr., The recent advance of the Ross Ice Shelf, Antarctica, *J. Glaciol.*, 32, 464-474, 1986.

Jacobs, S. S., H. H. Hellmer, C. S. M. Doake, A. Jenkins and R. Frolich, Melting of ice shelves and the mass balance of Antarctica, *J. Glaciol.*, 38, 375-387, 1992.

Jaeger, J. M., C. A. Nittrouer, D. J. DeMaster, C. Kelchner and R. B. Dunbar, Lateral transport of settling particles in the Ross Sea and implications for the fate of biogenic material, *J. Geophys. Res.*, 101(C8), 18479-18488, 1996.

Jeffries, M. O. and U. Adolphs, Early winter ice and snow thickness distribution, ice structure and development of the western Ross Sea pack ice between the ice edge and the Ross Ice Shelf, *Antarct. Sci.*, 9(2), 188-200, 1997.

Jones, P. D., Recent variations in mean temperature and the diurnal temperature range in the Antarctic, *Geophys. Res. Lett.*, 22(11), 1345-1348, 1995.

Jones, P. D. and D. W. S. Limbert, *A data bank of Antarctic surface temperature and pressure data*, DOE-ER-60397-H2, 52 pp, U.S. Dept. of Energy, 1987.

Kaiser, J., Is warming trend harming penguins?, *Science*, 276, 1790, 1997.

Keller, L. M., G. A. Weidner and C. R. Stearns, *Antarctic Automatic Weather Station data for the calendar year 1990*, 383 pp, Dept. Meteor., Univ. Wisc., Madison, WI, 1991.

Keys, H. J. R., S. S. Jacobs and D. Barnett, The calving and drift of iceberg B-9 in the Ross Sea, Antarctica, *Antarct. Sci.*, 2(3), 243-257, 1990.

Keys, H. J. R., S. S. Jacobs and L. W. Brigham, Continued northward expansion of the Ross Ice Shelf, *Ann. Glaciol.*, 27, in press, 1998.

Killworth, P. D., A baroclinic model of motions on Antarctic continental shelves, *Deep-Sea Res.*, 21(10), 815-838, 1974.

Kurtz, D. D. and D. H. Bromwich, A recurring, atmospherically forced polynya in Terra Nova Bay, in *Oceanology*

of the Antarctic Continental Shelf, Ant. Res. Ser. vol. 43, edited by S. Jacobs, pp 177-201, AGU, Washington, DC, 1985.

Ledley, T. S. and Z. Huang, A possible ENSO signal in the Ross Sea, *Geophys. Res. Lett.*, 24(24), 3253-3256, 1997.

Lewis, E. L. and R. G. Perkin, The winter oceanography of McMurdo Sound, Antarctica, in *Oceanology of the Antarctic Continental Shelf, Ant. Res. Ser.* vol. 43, edited by S. Jacobs, pp 145-166, AGU, Washington, DC, 1985.

Lindner, B. L., C. P. McKay, G. D. Clow and R. A. Wharton, Jr., Global change implications for Antarctic lakes, in *4th Symposium on Global Change Studies*, Anaheim, CA, 17-22 Jan 1993, pp 276-279, Amer. Meteorol. Soc., Boston, MA, 1993.

Locarnini, R. A., Water masses and circulation in the Ross Gyre and environs, PhD thesis, 86 pp, Dept. of Oceanography, Texas A&M Univ., College Station., TX, 1994.

MacAyeal, D. R., Tidal rectification below the Ross Ice Shelf, Antarctica, in *Oceanology of the Antarctic Continental Shelf, Ant. Res. Ser.* vol. 43, edited by S. Jacobs, pp 109-132, AGU, Washington, DC, 1985a.

MacAyeal, D. R., Evolution of tidally triggered meltwater plumes below ice shelves, in *Oceanology of the Antarctic Continental Shelf, Ant. Res. Ser.* vol. 43, edited by S. Jacobs, pp 133-143, AGU, Washington, DC, 1985b.

Murphy, E. J., A. Clarke, C. Symon and J. Priddle, Temporal variation in Antarctic sea-ice: analysis of a long term fast-ice record from the South Orkney Islands, *Deep-Sea Res.*, 42(7), 1045-1062, 1995.

Naval Oceanography Command, *Sea Ice Climatic Atlas: Vol. I Antarctic*, NAVAIR 50-1C-540, 132 pp, Naval Oceanography Command, Asheville, NC, 1985.

Nicholls, K. W. and K. Makinson, Ocean circulation beneath the western Ronne Ice Shelf, as derived from in situ measurements of water currents and properties, this volume.

Nost, O. A. and A. Foldvik, A model of ice shelf-ocean interaction with application to the Filchner-Ronne and Ross Ice Shelves, *J. Geophys. Res.*, 99(C7), 14243-14254, 1994.

Nost, O. A. and S. Osterhus, Impact of grounded icebergs on the hydrographic conditions near the Filchner Ice Shelf, this volume.

Pillsbury, R. D. and S. S. Jacobs, Preliminiary observations from long-term current meter moorings near the Ross Ice Shelf, Antarctica, in *Oceanology of the Antarctic Continental Shelf, Ant. Res. Ser.* vol. 43, edited by S. Jacobs, pp 87-107, AGU, Washington, DC, 1985.

Rintoul, S., On the origin and influence of Adelie Land Bottom Water, this volume.

Robertson, R., L. Padman and G. D. Egbert, Tides in the Weddell Sea, this volume.

St. Pierre, D. B., On the effectiveness of the production of Antarctic bottom Water in the Weddell and Ross Seas, Master's Thesis, 123 pp, Naval Postgraduate School, Monterey, CA, 1989.

Sansom, J., Antarctic surface temperature time series, *J. Clim.*, 2, 1164-1172, 1989.

Smith, R. C., S. E. Stammerjohn and K. S. Baker, Surface air temperature variations in the western Antarctic Peninsula region, in *Foundations for Ecological Research west of the Antarctic Peninsula, Ant. Res. Ser.* vol. 70, edited by R. Ross, E. Hofmann and L. Quetin, pp 105-121, AGU, Washington, DC, 1996.

Testa, J. W., G. Oehlert, D. G. Ainley, J. L. Bengston, D. B. Siniff, R. M. Laws and D. Rounsevell, Temporal variability in Antarctic marine ecosystems: Periodic fluc-

tuations in the phocid seals, *Can. J. Fish. Aquat. Sci.*, 48, 631-630, 1991.
Tressler, W. L. and A. M. Ommundsen, Seasonal oceanographic studies in McMurdo Sound, Antarctica, Tech. Rep. 125, 144 pp, U. S. Navy Hydrographic Office, Washington, DC, 1962.
Trumbore, S., S. S. Jacobs and W. Smethie, Jr., Chlorofluorocarbon evidence for rapid ventilation of the Ross Sea, *Deep-Sea Res.*, 38(7), 845-870, 1991.
Van Loon, H., The half-yearly oscillations in middle and high southern latitudes and the coreless winter, *J. Atmos. Sci.*, 24, 472-486, 1967.
Visser, A. and S. S. Jacobs, Annual mean estimates of heat transport into the Ross Sea sub-ice cavity, p 1022 in Abstract vol. 3, Int'l Un. Geodesy and Geophys., 19th Genl. Assembly, Aug 9-22, 1987, Vancouver, BC, 1987.
Weatherly, J. W., J. E. Walsh and H. J. Zwally, Antarctic sea ice variations and seasonal air temperature relationships, *J. Geophys. Res.*, 96, 15119-15130, 1991.
White, W. B. and R. G. Peterson, An Antarctic circumpolar wave in surface pressure, wind, temperature and sea ice extent, *Nature*, 380, 699-702, 1996.
Whitworth, T. III, A. H. Orsi, S. -J. Kim, W. D. Nowlin and R. A. Locarnini, Water masses and mixing near the Antarctic Slope Front, this volume.
Williams, R. T., and E. S. Robinson, Ocean tide in the southern Ross Sea, *J. Geophys. Res.*, 85(C11), 6689-6696, 1980.
Zwally, H. J., C. L. Parkinson and J. C. Comiso, Variability of Antarctic sea ice and changes in carbon dioxide, *Science*, 220, 1005-1012, 1983.
Zwally, H. J., J. C. Comiso and A. L. Gordon, Antarctic offshore leads and polynyas and oceanographic effects, in *Oceanology of the Antarctic Continental Shelf, Ant. Res. Ser.* vol. 43, edited by S. Jacobs, pp 203-226, AGU, Washington, DC, 1985.

C. Giulivi and S. Jacobs, Lamont-Doherty Earth Observatory, Columbia University, Palisades, NY 10964. (email: claudiag@ldeo.columbia.edu, sjacobs@ldeo.columbia.edu)

(Received January 2, 1997; accepted August 21, 1997.)

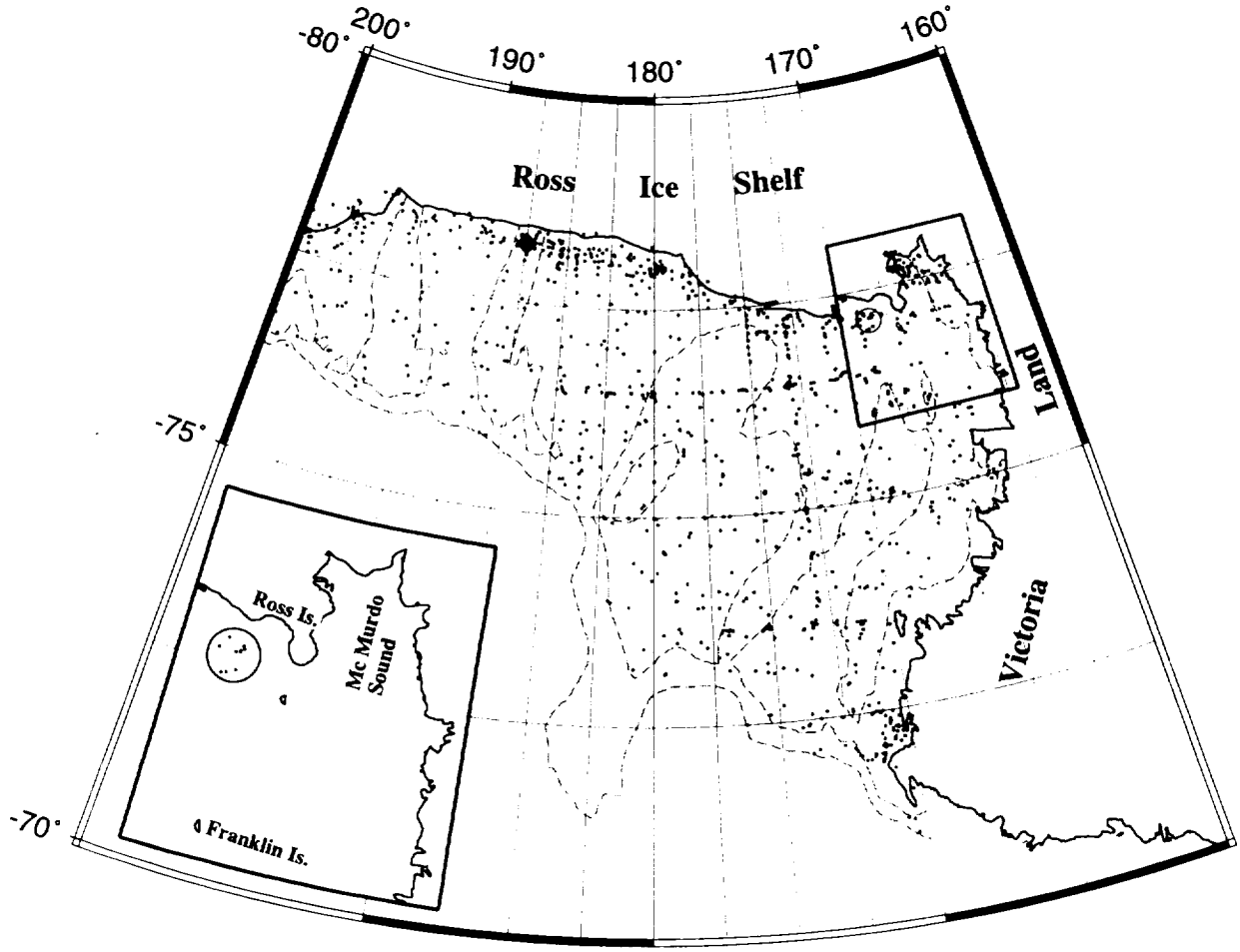

Fig. 1. Distribution of ocean stations (dots) used in this study, all south of the continental shelf break (~600 m) in the Ross Sea. Sea floor bathymetry (dashed 500 and 1000 m contours) has been interpolated from data on a CD-ROM that accompanies *Cooper et al.* [1995]. Temporal changes in the coastline account for some apparently anomalous station locations. Coordinates are negative south and positive east. The inset encompasses McMurdo Sound, where the salinities in Figure 4 were measured. The circle shows the locations of profiles in Figure 3, and the solid diamond near the ice shelf front sites the current meter records in Figure 7. Temperature data in Figure 9a were taken on Franklin Island and at Scott Base on the southwest end of Ross Island.

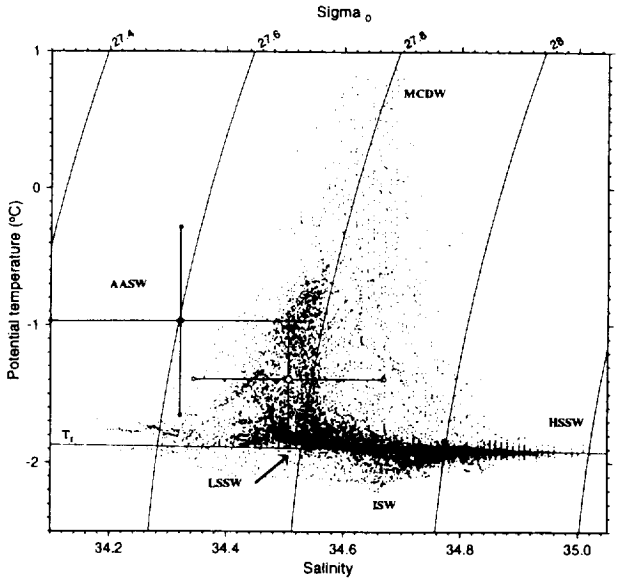

Fig. 2. Potential temperature/salinity characteristics of austral summer waters on the Ross Sea continental shelf, from standard levels at the stations in Figure 1. Antarctic Surface Water (AASW) points have been replaced here by bin averages, from 0-50 m and 51-200 m (closed and open symbols), with cross bars at one standard deviation. Actual values in the upper 200 m range from -2.08 to +2.58°C and 32.86 to 34.91 in salinity. 'Modified' Circumpolar Deep Water (MCDW) includes the cloud of points around -1°C and 34.52, and has previously been referred to as a 'Warm Core' in the Ross Sea. High Salinity Shelf Water (HSSW) has earlier been referred to as 'Ross Sea Shelf Water'. LSSW is Low Salinity Shelf Water. Ice Shelf Water (ISW) has temperatures colder than T_f, the sea surface freezing temperature. Most water on the shelf falls in the σ_0 isopycnal range of 27.4-28.2. The eastern and western parts of this shelf region are portrayed separately in T/S space by *Hofmann and Klinck* [1998].

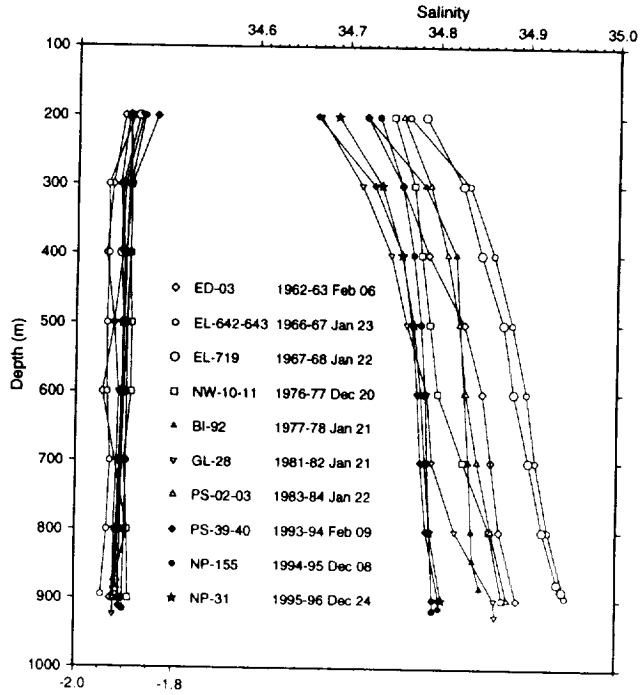

Fig. 3. Subsurface temperature and salinity vs. depth, from summer ocean stations (08 December - 09 February) taken over a 33-year period within a 15-km radius region north of Ross Island (Figure 1). The table identifies the profiles by ship code, station number, summer season, month and day; double station numbers are averages from adjacent profiles. Measurement accuracy over this period probably varied from .02 to .002 units.

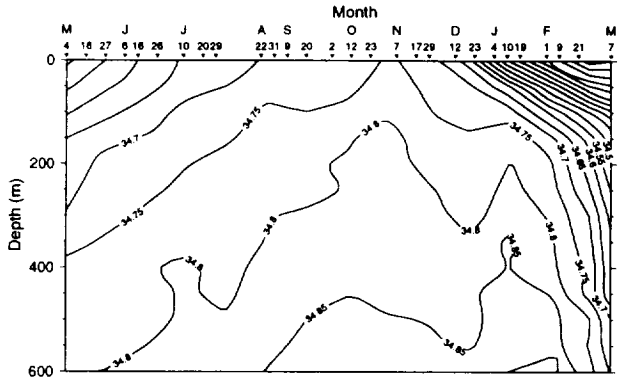

Fig. 4. Salinity vs. time from samples taken through an ice hole in McMurdo Sound at ~77° 53'S, 166° 53'E, from May 1960 through March 1961 [*Tressler and Ommundsen*, 1962]. Coincident temperatures varied little below 200m. Machine contoured from a 50-m, 22-day grid constructed from edited bottle samples at the dates (month and day) shown on the horizontal axis.

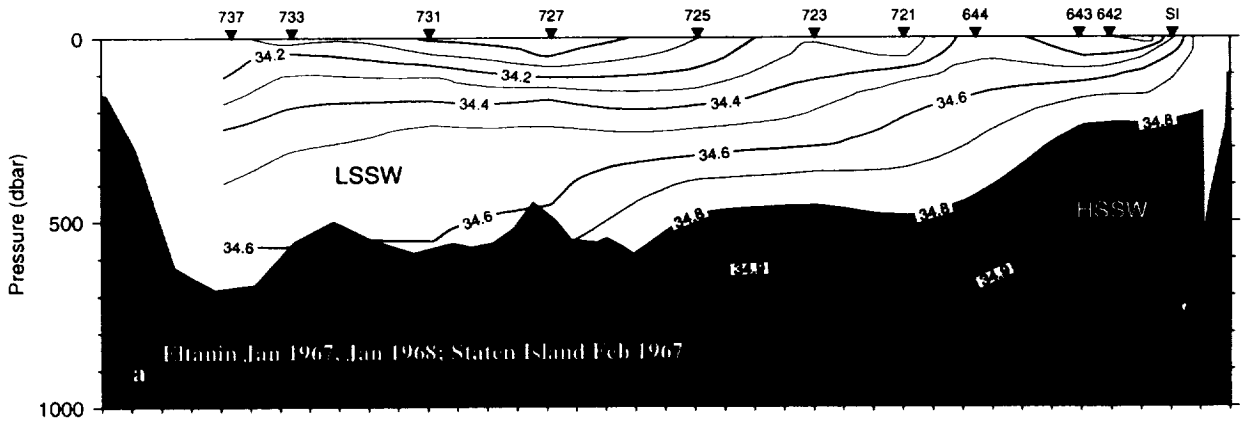

Fig. 5. Salinity (a-d) and potential temperature (e-h) sections at roughly decadal intervals near the front of the Ross Ice Shelf (Figure 1). Insets denote ship, month and year. East longitudes of original station numbers at the top of each panel are projected onto a constant latitude and bathymetry (black) from the 1984 traverse. The station data were machine contoured from a 50 decibar by 1° longitude grid, which removes some spatial variability. Pressure (decibars) ~ depth in meters: potential temperature is within .03°C of the in-situ temperature at these depths; salinity in practical salinity units. The 27.8 σ_0 dashed isopycnal on (c) illustrates the salinity control of the density field. The solid diamond on (g) shows the location of subsurface mooring data in Figure 7. Shading highlights HSSW salinity > 34.8, MCDW temperature > -1.2°C, ISW temperature < -1.95°C, and (on f) the adjacent ice shelf draft and Ross Island.

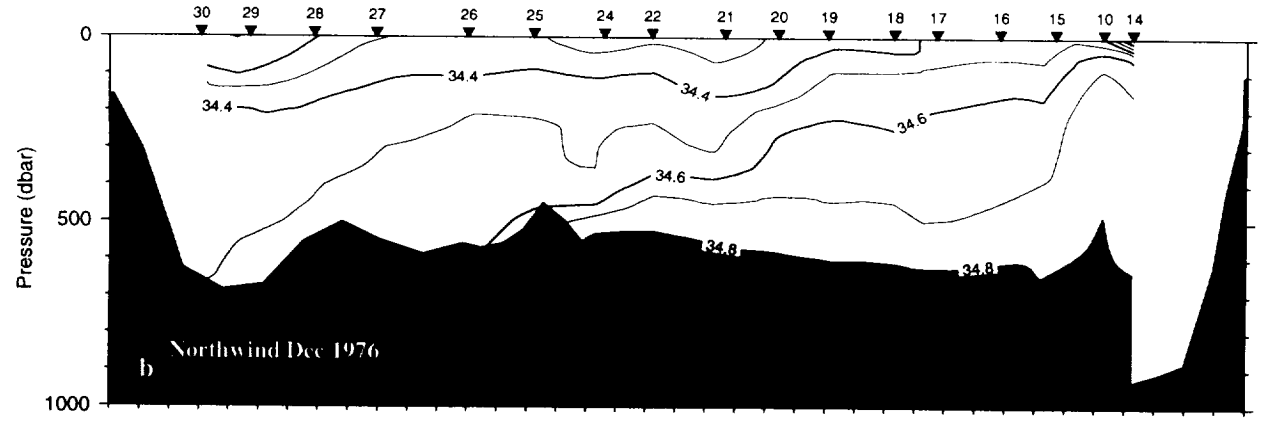
30 29 28 27 26 25 24 22 21 20 19 18 17 16 15 10 14
0
500
1000
Pressure (dbar)
34.4
34.4
34.4
34.6
34.6
34.8
34.8
b
Northwind Dec 1976

5b

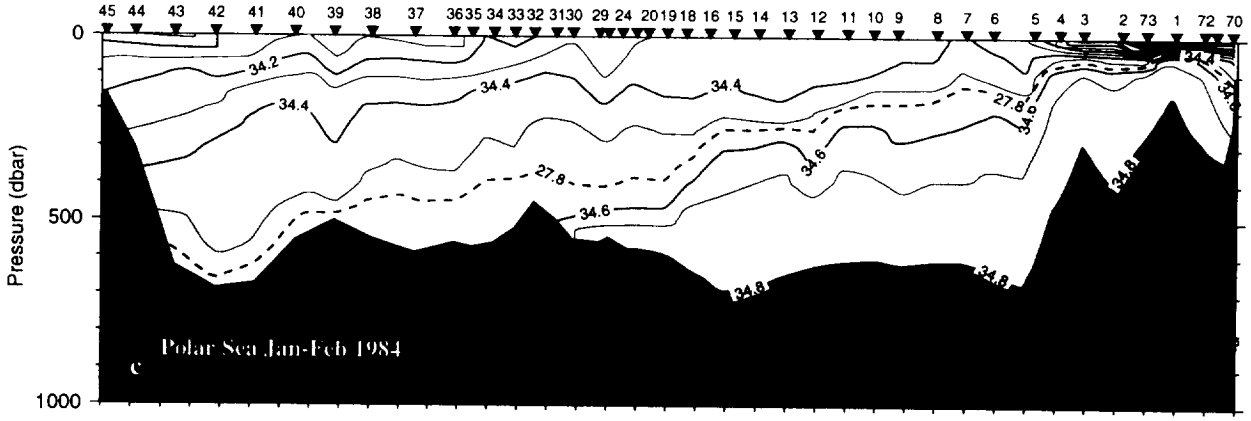
45 44 43 42 41 40 39 38 37 3635 34 33 32 3130 29 24 20 19 18 16 15 14 13 12 11 10 9 8 7 6 5 4 3 2 73 1 72 70
0
500
1000
Pressure (dbar)
34.2
34.4
34.4
34.4
27.8
27.8
34.6
34.6
34.6
34.8
34.8
34.8
c
Polar Sea Jan-Feb 1984

5c

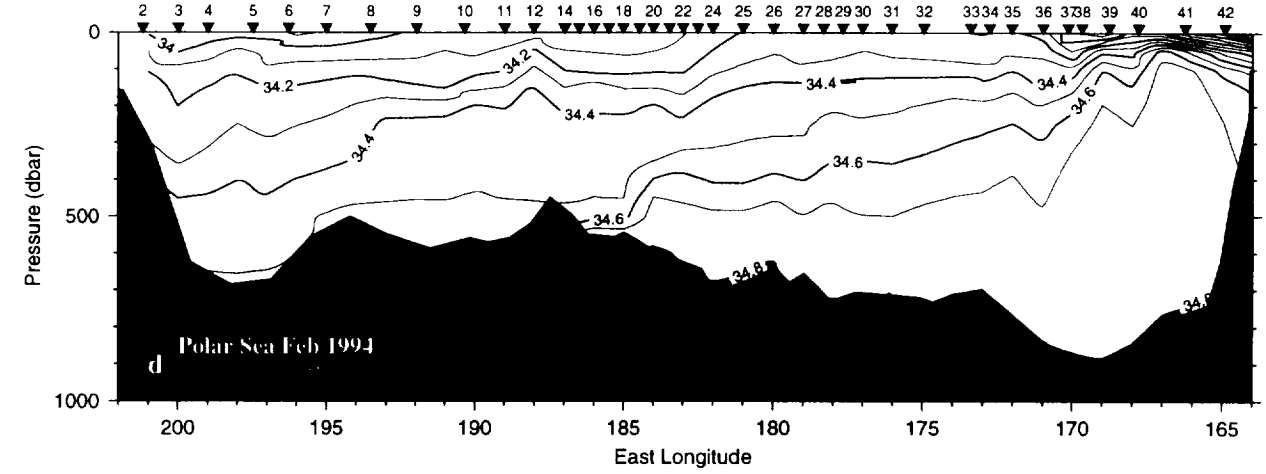
2 3 4 5 6 7 8 9 10 11 12 14 16 18 20 22 24 25 26 27 28 29 30 31 32 33 34 35 36 37 38 39 40 41 42
0
500
1000
Pressure (dbar)
34
34.2
34.2
34.4
34.4
34.4
34.4
34.6
34.6
34.6
34.8
34.8
d
Polar Sea Feb 1994
200
195
190
185
180
175
170
165
East Longitude

5d

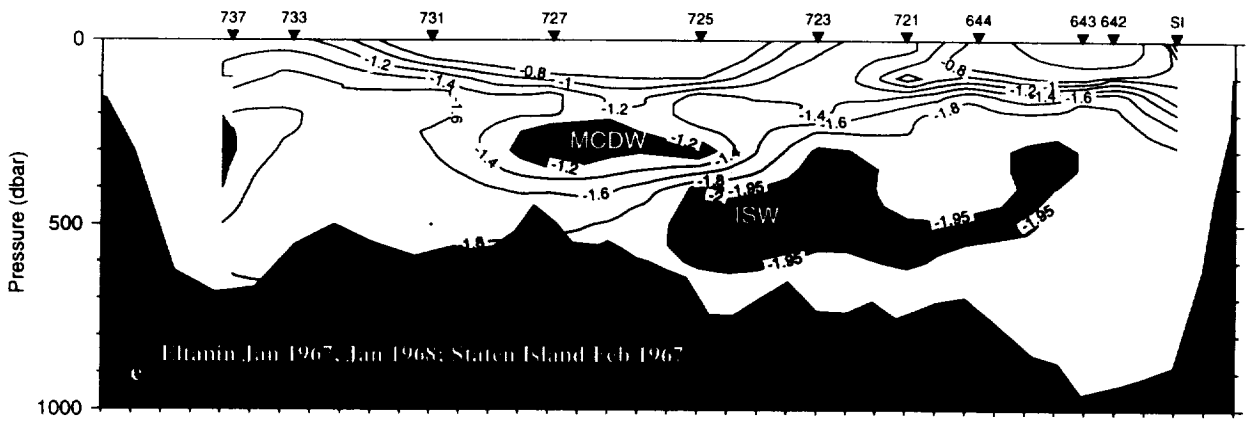
737 733 731 727 725 723 721 644 643 642 SI
0
500
1000
Pressure (dbar)
MCDW
ISW
-1.2
-1.4
-0.8
-1
-1.6
-1.8
-1.95
e Eltanin Jan 1967, Jan 1968; Staten Island Feb 1967

5e

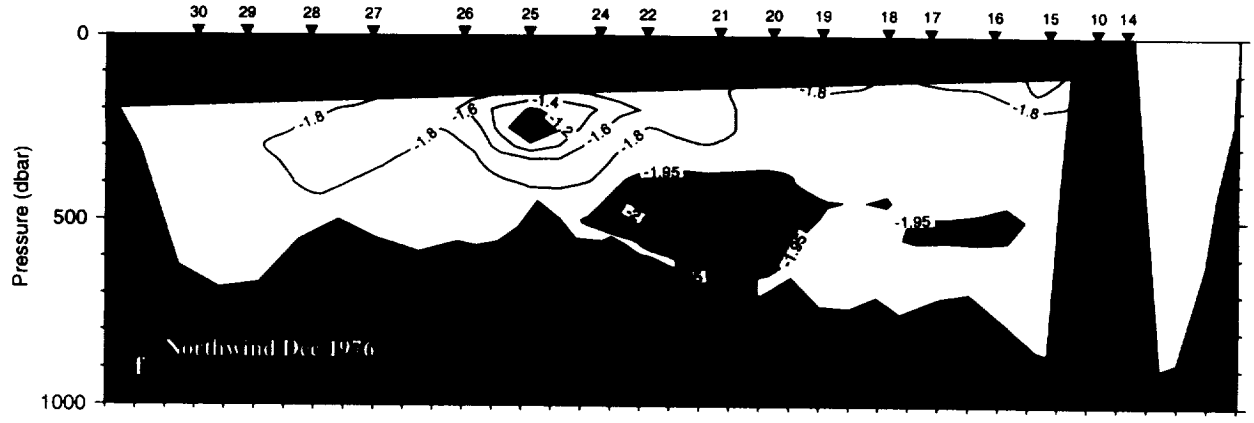
30 29 28 27 26 25 24 22 21 20 19 18 17 16 15 10 14
0
500
1000
Pressure (dbar)
-1.8
-1.6
-1.4
-1.95
f Northwind Dec 1976

5f

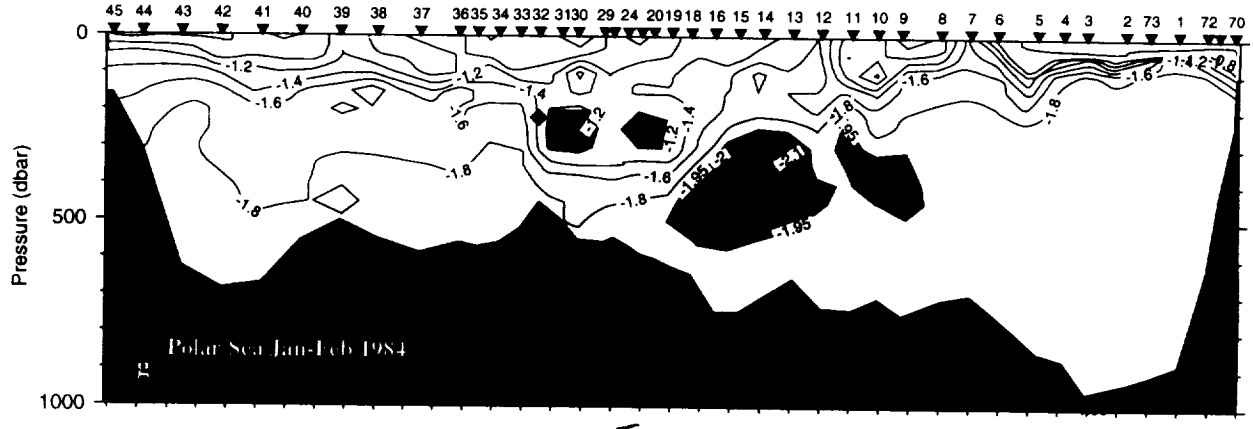
45 44 43 42 41 40 39 38 37 36 35 34 33 32 31 30 29 24 20 19 18 16 15 14 13 12 11 10 9 8 7 6 5 4 3 2 73 1 72 70
0
500
1000
Pressure (dbar)
-1.2
-1.4
-1.6
-1.8
-1.95
g Polar Sea Jan-Feb 1984

5g

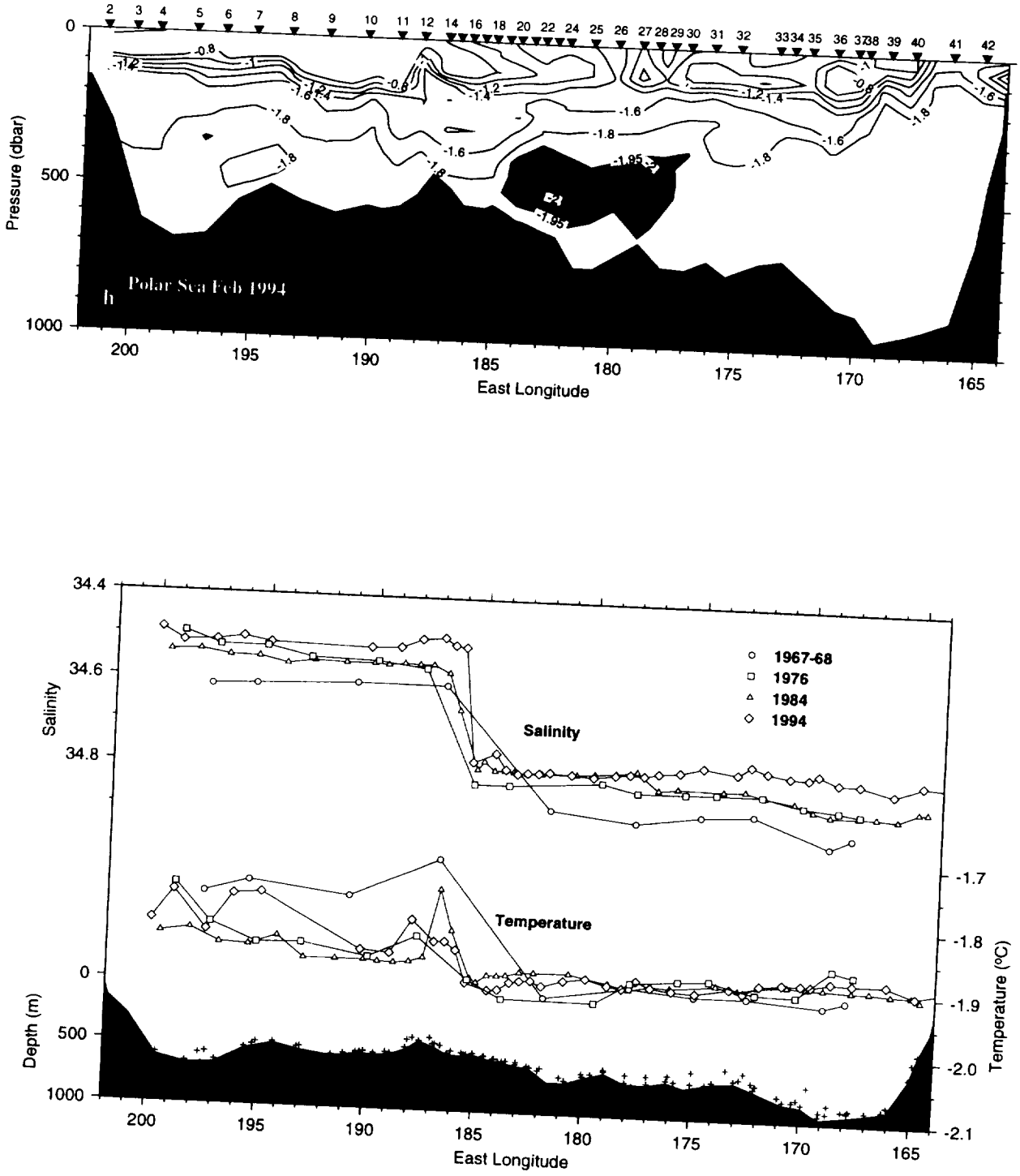

Fig. 6. Bottom salinity (note inverted scale) and temperature near the Ross Ice Shelf front, from the station transects in Figure 5. On average these measurements were made within 20 m of the sea floor, as indicated by crosses above the 1984 bathymetry (black).

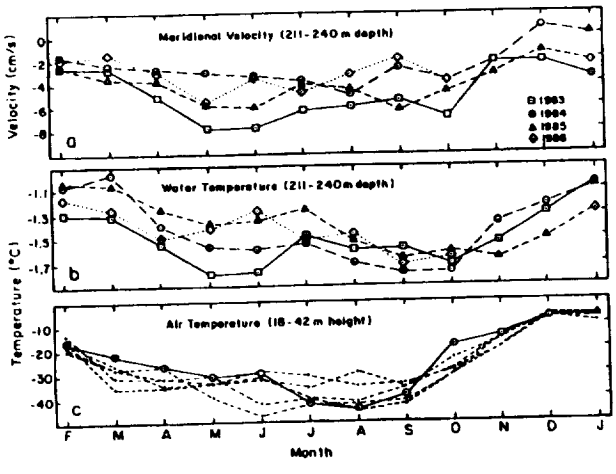

Fig. 7. (a,b) Monthly average northward current velocity and water temperature recorded by instruments moored at the solid diamonds in Figures 1 and 5g. The record years (1983-86) begin in February and end in January of the following year (October in 1986). The instruments were set at depths of 211 m in 1983, 215 m in 1984 and 240 m in 1985-86. At an in-situ salinity of ~34.5 (near 200m @ station 32 in Figure 5), surface freezing temperature would be -1.89°C. (c) Monthly average air temperature at automatic weather stations (172.5W and Martha I and II) on the Ross Ice Shelf within 40 km of the mooring site [e.g., *Keller et al.*, 1991]. The circles and solid line show 1984; dashed lines 1987-91.

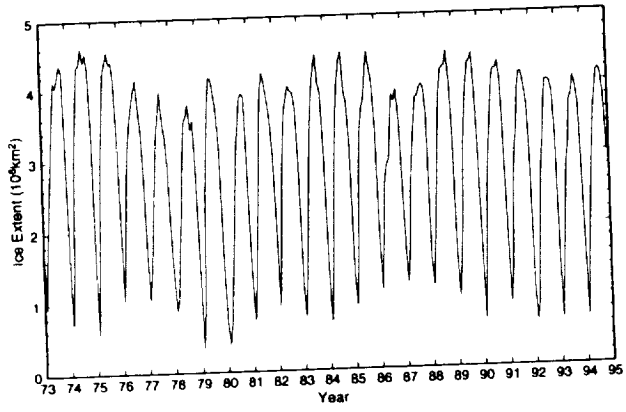

Fig. 8. Sea ice extent in the Ross Sea (160-230°E), derived mainly from monthly average satellite passive microwave observations processed with the NASA 'bootstrap' algorithm [*Comiso et al.*, 1997]. Gaps in the microwave observations were filled from tabular data in *Naval Oceanography Command* [1985], with December 1994 an average of prior Decembers. The summer minimum month has always been in February in this sector; the winter maximum has occurred from July - October over this 1973-94 period.

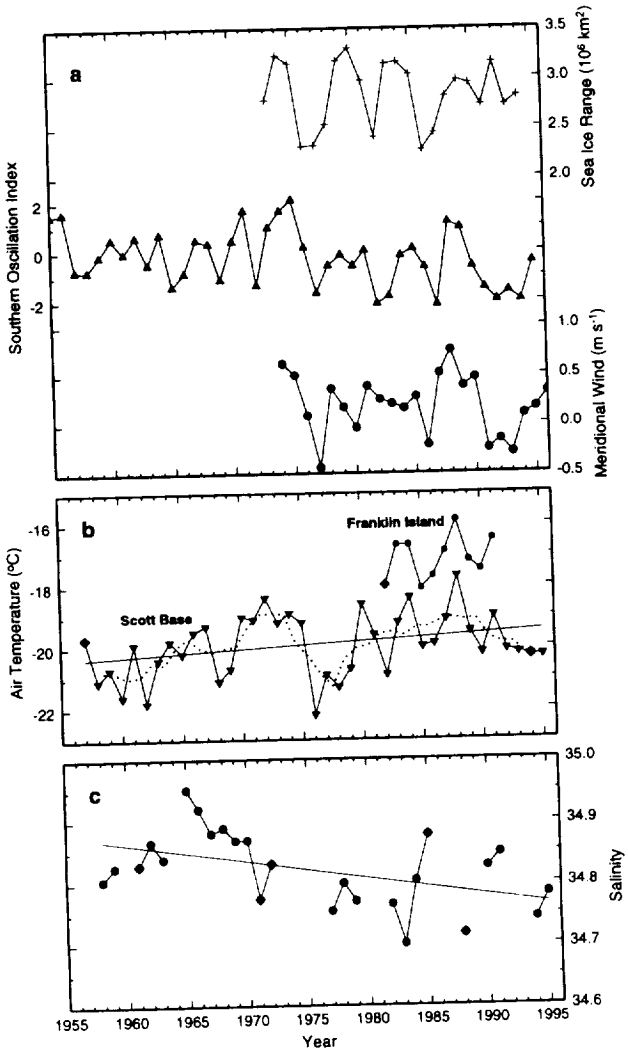

Fig. 9. (a) Annual range in sea ice extent in the Ross Sea, calculated from the winter maximum minus the previous summer minimum, both 3-month averages; Annual average Southern Oscillation Index; Annual average northward wind speed. (b) Annual average air temperature at the automatic weather station on Franklin Island and at Scott Base on Ross Island (Figure 1). A 4-year running mean (dotted line) and best fit linear regression are also shown for Scott Base. Diamonds include 1-2 months of data averaged from other years. (c) Average shelf water salinity between 450 and 550 m, from summer (DJF, using the JF year) ocean stations west of 180° in Figure 1, plus linear regression. Diamonds indicate years with data in only one 10° meridional band, adjusted for the mean zonal gradient.

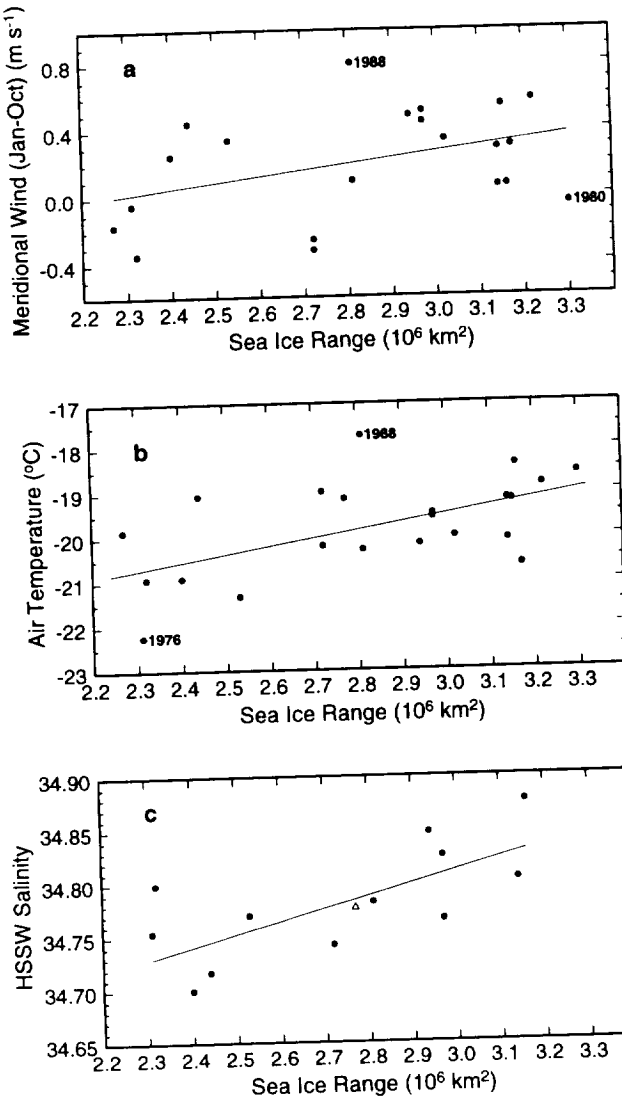

Fig. 10. (a) Sector average 1000 mbar meridional wind speed (positive northward, m s^{-1}) vs. sea ice range as in Figure 9a. Winds have been averaged over the January-October period to approximate the seasonal limits of the sea ice range. (b) Annual average air temperature at Scott Base (Figure 9b) vs. sea ice range the same year. (c) HSSW salinity, 450-550 m average, all data from 160-180°E (Figure 9c) vs. sea ice range the previous year. Summer (DJF) salinity data, except for the open triangle (October).

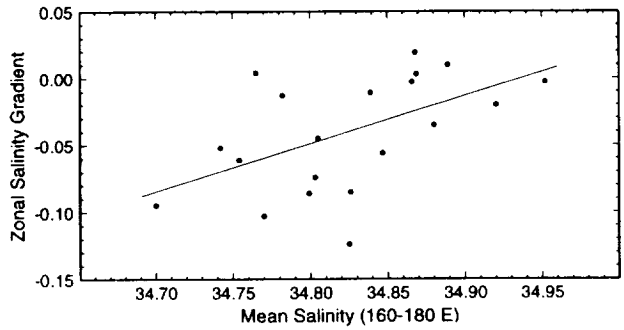

Fig. 11. Zonal (east to west) salinity gradient between the average shelf water salinity, 450-550 m, 170-180°E, minus that same average in the 160-170°E band. This is plotted against the mean salinity over both 10° meridional bands for each year with valid data, 1958-1995.